CALIFORNIA INSTITUTE OF TECHNOLOGY

EARTHQUAKE ENGINEERING RESEARCH LABORATORY

PARAMETER STUDY OF THE RESPONSE OF MOMENT-RESISTING STEEL FRAME BUILDINGS TO NEAR-SOURCE GROUND MOTIONS

BY

JOHN F. HALL

REPORT NO. EERL 95-08

A REPORT ON RESEARCH CONDUCTED UNDER A SUBCONTRACT FROM SAC JOINT VENTURE

FUNDED BY
THE FEDERAL EMERGENCY MANAGEMENT AGENCY (FEMA)

PASADENA, CALIFORNIA
DECEMBER 1995

Parameter Study of the Response of Moment-Resisting Steel Frame Buildings to Near-Source Ground Motions

by

John F. Hall

Report No. EERL 95-08

A Report on Research Conducted Under a Subcontract
from SAC Joint Venture

SAC Joint Venture: A partnership of
the Structural Engineers Association,
the Applied Technology Council, and
the California Universities for Research in
Earthquake Engineering

Funded by
the Federal Emergency Management Agency (FEMA)

California Institute of Technology
Pasadena, California
December 1995

This report covers research conducted under a subcontract with the SAC Joint Venture which was funded by the Federal Emergency Management Agency (FEMA).

The SAC Joint Venture entered into a contract with the Federal Emergency Management Agency (FEMA) to furnish all professional, technical and clerical personnel, services, materials, equipment and facilities to conduct a "Program to Reduce Earthquake Hazards in Steel Moment Frame Structures." This publication reports on the research conducted under a subcontract between this Joint Venture and Professor John F. Hall of the California Institute of Technology.

Parameter Study of the Response of Moment-Resisting Steel Frame Buildings to Near-Source Ground Motions

John F. Hall
CALIFORNIA INSTITUTE OF TECHNOLOGY

SUMMARY

A parameter study is performed to investigate the effects of strong near-source ground motions from moderate-size earthquakes ($M_W \approx 7$) on moment-resisting steel frame buildings. Two buildings, one 6 stories and the other 20 stories, are subjected to the Olive View Hospital free-field record from the Northridge earthquake and other ground motions from three earthquake simulations (Northridge earthquake, a hypothetical M_W7.1 Elysian Park blind-thrust earthquake, and another blind-thrust earthquake of M_W7.0). Parameters examined for the buildings include material yielding, weld fracture, presence of slab, accumulation of damage from a second earthquake, and vertical ground motion.

A significant fraction of the ground motions cause excessive amounts of deformations in the buildings, especially the 6-story one, even for the case where all welds are assumed to be perfect. These ground motions exceed the earthquake representation in the code, and, since they appear to be reasonable motions that should be considered in design, the implication is that the code design force levels need to be raised for locations in near-fault regions. Including weld fracture increases the displacements of the building and the potential for severe damage or collapse from column failure or excessive lateral sway. The buildings collapsed in several of the analyses. Including the floor slab increased the amount of column yielding and did not improve the behavior. A second earthquake such as a strong aftershock or subsequent main shock is a concern, especially if many welds are cracked from the initial event. However, a limited study of vertical ground motion showed it to be of minor importance. Strongly nonlinear building behavior is sensitive to many assumptions about features which are poorly understood, both structure and ground motion, and so the results need to be carefully interpreted.

INTRODUCTION

Although the Northridge earthquake caused much damage to steel frame buildings in the form of fractured welds, no such buildings collapsed, and thus the life-safety objective of the building code was met. However, the Northridge earthquake was smaller than the "code earthquake," and the most damaging ground motions occurred to the north of the fault where there were few buildings. Therefore, one can not argue that current steel construction is not deficient. Indeed, given the fracture-prone nature of existing welds, the steel building stock falls far short of the code's required levels of ductility. All of this raises an important question. Given our seismic environment and the newfound knowledge of how steel frame buildings behave, is the risk of possible collapse during future shaking that is more intense than delivered by the Northridge earthquake acceptable? To answer this question, the level and type of ground motion capable of collapsing steel buildings, as well as its likelihood of occurrence, must be determined. The posed question pertains to those steel buildings which are in a damaged state from a previous earthquake and those which haven't been shaken hard enough yet to receive damage. Once the collapse-level earthquake is quantified, then issues of repair and retrofit can be rationally addressed.

In this report, 6-story and 20-story steel frame buildings with a variety of different assumptions about possible structural behavior are analyzed under strong earthquake ground motions. Some analyses employ a double earthquake sequence to investigate accumulation of damage. The results provide an indication of the level and type of ground motion necessary to produce severe damage or collapse. Used here are ground motions thought to be typical of those close to earthquakes of magnitude $M_W \approx 7$. Such motions have a few strong pulses, but not long durations. Effects of long duration shaking from large earthquakes should also be studied. Concern about near-source ground motions has also been expressed in earlier studies: Bertero, et al. (1978), Anderson and Bertero (1987), and Roeder, et al. (1993).

MODELLING ASSUMPTIONS

The basic structural model is a planar frame of beams and columns. More than one frame can be linked together single-file with equal floor displacements imposed at each floor level. This method is appropriate for buildings constructed of orthogonal frames connected by rigid floor diaphragms and loaded by forces and ground motions in the plane parallel to one of the two sets of orthogonal frames, which is the set that is modelled. Thus, the ground motion can consist of one horizontal component and the vertical component. In addition, because of symmetry or other reasons, the building must not twist. The only interaction between the frames is through horizontal forces in the floor diaphragms; other interactive forces such as vertical shear in beams of the perpendicular frames are neglected.

Usually, only some of the frames are moment resisting; others have simple beam-to-column connections and are designed to support only gravity loads. These simply-connected frames still provide some lateral support through column deformations and incidental connection stiffness, but if this contribution is small, they may be omitted. In this case, their horizontal tributary masses should be assigned to the moment-resisting frames, and lateral forces should be applied to these frames to simulate $P-\Delta$ effects of vertical loads on the omitted frames acting through the horizontal displacements. In addition, proper accounting of symmetry allows some of the moment-resisting frames to be eliminated.

Beams and columns are modelled by the fiber method whereby they are divided along their lengths into subelements, and each subelement is divided within its cross-section into axial fibers (**Figure 1.1**). Realistic axial stress-strain behavior including residual stress, strain hardening and hysteresis is used for each fiber (**Figure 1.2**). Shear forces in the subelements are computed elastically. Panel zones are modelled as shear elements with realistic shear stress-strain behavior including strain hardening and hysteresis (**Figure 1.2**). Actual dimensions of the joints are used, and geometric nonlinearity ($P-\Delta$ effects and member moment amplification) is accounted for by updating the nodal coordinates at each time step.

Approximate representation of composite floor slab action is accomplished through an additional fiber located an appropriate distance above the top of a beam. This fiber cracks when the tensile strength σ_{rc} is reached and yields plastically at the compressive strength σ_{yc}. Hysteretic behavior is shown in **Figure 1.3**.

Strength and stiffness of nonstructural elements is approximately included through shear springs that connect adjacent floors. These inter-story shear springs are elastic-perfectly plastic (**Figure 1.3**) and provide a shear strength F_{yi} in story i equal to the story shear produced by lateral forces distributed to the floors according to the code formula and totaling a fraction γ of the building weight. The stiffness k_i of the shear spring in story i is computed as $F_{yi} / 0.0025\, h_i$, where h_i is the height of story i.

Foundation interaction is modelled with axial spring supports, one horizontal and one vertical, at the base of each column. An elastic-plastic with strain hardening relation is used for these springs (**Figure 1.3**). Parameters of this relation are initial stiffness k_f, ratio of secondary to primary stiffness α_f, tension yield strength F_{yf}^{ten} and compression yield strength F_{yf}^{comp}.

Viscous damping is added as two stiffness proportional terms. The first is the total linear stiffness matrix multiplied by the factor $2\xi' T_1 / 2\pi$ where ξ' is specified and T_1 is the fundamental period of the elastic building. As this term is used to control numerical "noise," ξ' is chosen to be small (say, $\xi' = 0.005$). The second term consists of dampers in parallel with the inter-story shear springs, with damping value in story i equal to an equivalent shear building story stiffness $\dfrac{\frac{V}{W} \cdot \frac{1.7}{1.33} + \gamma}{\gamma} k_i$ multiplied by the factor $2\xi'' T_1 / 2\pi$, where ξ'' is specified and $\frac{V}{W}$ is the code lateral force design coefficient. A limit is placed on the forces carried by the story dampers.

This cap on damping forces is necessary because high inter-story velocities that occur during yielding of the building otherwise can cause unrealistically high damping forces. A reasonable value of ξ'' is 0.05 which corresponds to damping at 5% of critical when the building is vibrating in the elastic range.

In order to include weld fracture in the beam-to-column connections and in the column splices, certain fibers are given the property of fracturing (loss of tensile capability) when the fiber axial stress reaches some critical value. This property is assigned only to fibers at weld locations: beam subelements 1 and 8 for beam-to-column welds and column subelement 4 just below mid-height for those columns containing splices. (See **Figure 1.1** for subelement numbering.) The fracture stress is generally set to the yield stress, but where partial penetration welds are used, such as at splices of interior columns, then a lower fracture stress may be appropriate to account for the reduced section area at the weld. Some welds can also be classified as perfect; in which case, the fibers involved behave in the regular manner. Capability to transmit shear force is retained in a beam even after all fibers at an end segment fracture. However, when every fiber at a column splice has fractured, all load carrying capability, including compression, is permanently lost. This latter assumption is based on the likelihood that the column will become misaligned across the broken splice, owing to story offsets and residual deformations in the column.

The solution process uses two levels of iterative solutions: at the frame level in each time step and at the member level for each frame iteration. Each frame iteration produces displacements of the frame degrees of freedom, i.e., those associated with the nodes at the beam and column junctions. These displacements define the end displacements of the members, and each member solution produces displacements at the interior nodes of the member. Mass and gravity loads are only associated with the frame degrees of freedom, and therefore each member solution is static with only end displacements applied. If a beam in the frame being modelled supports a floor beam spanning in the perpendicular direction, say, a single one at mid-span, then two members connected by a "frame node" at mid-span can be used. More details of the solution procedure can be found in Challa and Hall (1994).

Of interest in this report are assessments of the potential for severe damage or collapse of steel buildings when subjected to strong near-source earthquake ground motions, and many of the above modelling details bear importantly on this task. Details and limitations of the model should be appreciated so that the results can be properly interpreted.

20-STORY BUILDING

The building considered is 20 stories tall with a rectangular plan and two axes of symmetry (**Figure 1.4**). Moment-resisting frames exist on the perimeter only, and all interior connections are simple. Design meets the 1994 Uniform Building Code for gravity loads [floor live load = 3.8 kPa (80 psf), floor dead load = 4.5 kPa (95 psf), roof dead load = 3.8 kPa (80 psf), exterior cladding load = 1.7 kPa (35 psf)], wind [basic wind speed = 113 kph, urban exposure (B)] and earthquake [Zone 4, deep stiff soil (Type S_2)]. For seismic design, the resulting code base-shear coefficient $\frac{V}{W}$ = 0.03. Steel grade is A36. Where necessary, the panel zones are strengthened with doubler plates so that the panel zone yield moment equals 0.8 times the sum of the plastic moment capacity of the connecting beams. This building has been strengthened compared to the original one considered in previous analytical studies (Tsai and Popov, 1988; Challa and Hall, 1994; Heaton, et al., 1995) in order to reduce the wind drift in the lower stories from about 0.0030 to 0.0025. This drift is accomplished without the inter-story shear springs and slab mentioned in the previous section.

The direction of interest is the short direction of the building for which there are five parallel frames. Because of the symmetry and the three interior frames being simply connected, only the one exterior moment-resisting frame is modelled explicitly. Actual steel strengths are σ_y = 290 MPa (42 ksi) yield and σ_u = 448 Mpa (65 ksi) ultimate. At beam-to-column welds, the fracture stress σ_r is taken as the yield stress σ_y. At column splices, $\sigma_r = \sigma_y$ for exterior columns (lines A and D), and $\sigma_r = \frac{2}{3}\sigma_y$ for interior columns (lines B and C) where partial penetration welds are assumed to be present. Column splices are located in stories 1, 3, 5, ... and 19. Areas of web fibers at beam-to-column and column-splice welds are reduced by half to better represent conditions of bolted web plates.

Contributions to strength and stiffness from the nonstructural elements as well as from the 1½ interior frames are represented by the inter-story shear springs which are sized for strength using $\gamma = \frac{1}{3}\frac{V}{W} = 0.01$ and for stiffness as indicated in the previous section. Parameters of the foundation springs are selected as k_f = 5254 kN/cm (3000 kips/in), α_f = 0.10, F_{yf}^{ten} = 6.67 MN (1500 kips) and F_{yf}^{comp} = 13.3 MN (3000 kips). Very stiff panel elements are used in the basement story to simulate the presence of basement walls.

Half the mass of the building (including live load of 0.48 kPa) is distributed to the horizontal degrees of freedom of the exterior frame. Masses and gravity loads for the vertical degrees of freedom of this frame (including live load of 0.72 kPa) are from a ½-bay tributary width. The $P-\Delta$ contribution from the interior frames is from a 1½-bay tributary width. The fundamental period of the elastic building is 3.49 seconds (with shear springs, $P-\Delta$, and flexible foundation; without slab). Parameters of the damping are ξ' = 0.005 and ξ'' = 0.05, and the force cap on the damper in story i is the inter-story shear spring strength F_{yi}.

6-STORY BUILDING

As in the previous case, this building also has a rectangular plan, two axes of symmetry, and moment-resisting frames on the exterior only, but the number of stories is six and there is no basement (**Figure 1.5**). This building was studied by Tsai and Popov (1988) and meets the 1994

Uniform Building Code requirements. Distributed floor and cladding loads are the same as for the 20-story building, and the direction of interest is again the short direction. Steel is A36 and panel zones are strengthened with doubler plates so that the panel zone yield moment equals 0.8 times the sum of the plastic moment capacity of the connecting beams. Design of the exterior frame (**Figure 1.5**) is governed by Zone 4 seismic loads (S_2 soil type). The coefficient $\frac{V}{W}$ equals 0.0437, resulting from a code-computed period of 1.22 seconds.

In the analysis, the beams, columns and slabs are modelled with fibers and the panel zones with shear elements, as with the 20-story building using the same strengths and fracture criteria at weld locations. Column splices are located in stories 3 and 5. The shear springs are sized using $\gamma = \frac{1}{3}\frac{V}{W} = .015$, and the foundation is taken to be rigid. The elastic building model gives a fundamental period of 1.36 seconds (with shear springs and $P-\Delta$; without slab). Damping is as for the 20-story building.

For most analyses with the 6-story building (as with all analyses of the 20-story building), each beam and column is composed of a single 8-segment member, which means that the frame nodes where mass and gravity loads are applied are at the junctions of the beams and columns. For other analyses, those where the effect of vertical ground motion is studied, an additional frame node is created at mid-span of each beam where gravity and mass loads are also applied. This node is created by using two 8-segment members for each beam.

STRUCTURAL CASES

Various modifications of the structure are examined for both the 6-story and 20-story buildings as detailed for the cases below. Weld fibers are classified as either perfect (never fracture prematurely) or bad (fracture according to the criteria given in previous sections). The designation [N_T, N_B, N_C] defines the weld condition for a case. N_T is the percent probability that a top fiber group at a beam-to-column weld is bad. N_B is similar but for a bottom fiber group. N_C is the percent probability that the fibers at a column splice are bad. Weld fibers within each beam top fiber group, beam bottom fiber group or column splice are either all perfect or all bad. A fiber group is defined in **Figure 1.1**.

The cases are as follows.

Case P:	nonlinear building and foundation; no composite slab action; all welds perfect [0,0,0]; no mid-span beam nodes
Case E:	same as P except building and foundation are elastic
Case PS:	same as P except composite slab action included
Case B:	same as P except most welds are bad [50,100,100]
Case I:	similar to B but fewer bad beam welds [25,100,100]
Case BS:	same as B except composite slab action included
Case C:	similar to B and I except only bad column-splice welds [0,0,100]

Case P′: same as P except mid-span beam nodes included.

Case C is used to investigate the situation where all beam-to-column welds have been retrofitted (perfectly), the column-splice welds being left in their original state. Case P′ is used only in studies of vertical ground motion with the 6-story building.

GROUND MOTIONS

The set of ground motions employed consists of the free-field records from Olive View Hospital during the 1994 M_W6.7 Northridge earthquake (SYLM), simulated motions of the Northridge earthquake at 21 stations along a linear array over the fault (NR01, NR02,...,NR21), simulated motions of a hypothetical M_W7.1 blind-thrust Elysian Park earthquake at 21 stations along a linear array over the fault (EP01, EP02,...,EP21), and one of the strongest ground motions (C05) from a simulated hypothetical M_W7.0 blind-thrust earthquake. The simulated Northridge and Elysian Park earthquake motions were supplied by Paul Somerville of Woodward-Clyde, while the C05 ground motion was provided by Tom Heaton and David Wald of the USGS.

The analyses in this study, being planar, use a single horizontal component of ground motion (denoted by a /H suffix) which is oriented to produce the largest difference between peak positive and negative ground velocities. The vertical component (denoted by a /V suffix) is combined with the horizontal component (denoted by /H+V) for some analyses of the 6-story building. In other analyses, the horizontal component is repeated to produce a double earthquake (denoted by /DH) in order to demonstrate accumulation of damage.

Table 1.1 lists parameters of the complete set of ground motions used. The peak displacement is 182 cm for C05/H, and the peak velocity is 207 cm/sec for EP14/H. Detailed results are presented for some of the ground motions: SYLM/H, SYLM/V, SYLM/DH, NR11/H, NR11/DH, EP14/H, EP17/H, EP17/V and C05/H. Time histories of these are plotted in **Figures 1.6** to **1.14**. Pseudo-acceleration response spectra (5% damping) are shown in **Figure 1.15** for SYLM/H, NR11/H, EP14/H, EP17/H and C05/H along with the UBC spectrum which has been scaled up by the load factor 1.7/1.33. The UBC spectrum is significantly exceeded over wide period ranges by the ground motion spectra.

RESULTS AND CONCLUSIONS

The sets of 21 ground motions from the simulated Northridge and Elysian Park earthquakes were used in Case E and P analyses of the 6-story and 20-story buildings (results in **Figures 1.16** to **1.19**). Based on these results, ground motions NR11/H for both buildings, EP17/H for the 6-story building and EP14/H for the 20-story building were selected for detailed studies using six structural cases (P, PS, B, I, BS and C), along with ground motions SYLM/H and C05/H. Double earthquake SYLM/DH was used in a Case I analysis of the 6-story building, and

NR11/DH was used in a Case I analysis of the 20-story building. Finally, Case P′ of the 6-story building was subjected to SYLM/H, SYLM/H+V, EP17/H and EP17/H+V to investigate effects of vertical ground motion. In all, 54 detailed studies were made, and results for all but Case C are presented in **Figures 1.20** to **1.65**. A summary of these as well as those from Case E appears in **Tables 1.2** and **1.3**. Results for Case C are identical to those of Case P.

Figures 1.20 to **1.65** contain four types of plots: floor displacement time histories, deflected shapes at selected times, ductility demands, and time histories of beam moment and plastic hinge rotation. The floor displacement histories are plotted along with the ground displacements and are total displacements (i.e., not relative to the ground). The deflected shapes are shown at times of maximum left and right roof displacements (relative to ground) and at the end of the simulation. The shapes are scaled so that the maximum plotted displacement is the same from one figure to another; the scaling (AMP) is stated. Vertical dashed lines in the floor displacement time history plots mark the times at which the deflected shapes are plotted. Included in the deflected shape plots are small triangles which designate locations where flange welds have fractured. Possible locations of these triangles are at the ends of the beams, top and bottom, and at mid-height of the columns, left side and right. Ductility demand plots include inelastic shear rotations in panel zones and plastic hinge rotations in beams and columns throughout the building height. Dashed lines refer to exterior column lines (A and D), while solid lines refer to interior column lines (B and C). These ductility plots are omitted if the building collapses. Time histories of beam moment and plastic hinge rotation are shown only for the analyses performed for the vertical ground motion study, and are the only results shown for these analyses.

In reviewing the results presented below, it should be kept in mind that engineers view story drifts and plastic hinge rotations above 2% as excessive because they cause considerable structural deterioration such as local flange buckling, and only deterioration from weld fracture is included here. This omission of important mechanisms of structural deterioration underestimates the building response and the likelihood of serious damage and possible collapse.

CASES WITH PERFECT WELDS

These cases include the inelastic ones without slabs (P) and with slabs (PS). No collapses occurred in any of these analyses.

Peak responses (story drift, roof displacement and beam plastic hinge rotation) for Case P for the complete sets of ground motions from the simulated Northridge and Elysian Park earthquakes appear in Figures 1.16 to 1.19. Details of the responses for Case P for the selected ground motions from the simulated Northridge and Elysian Park earthquakes, as well as from SYLM and C05, are shown in the figures as follows:

Figure 1.20: 6-story building, Case P, SYLM/H
Figure 1.21: 6-story building, Case P, NR11/H

Figure 1.22:	6-story building, Case P, EP17/H
Figure 1.23:	6-story building, Case P, C05/H
Figure 1.24:	20-story building, Case P, SYLM/H
Figure 1.25:	20-story building, Case P, NR11/H
Figure 1.26:	20-story building, Case P, EP14/H
Figure 1.27:	20-story building, Case P, C05/H

The ground motions with the largest displacements produce greater yielding and permanent displacement in the building. Inelastic action occurs mainly in the beams, but appreciable amounts of yielding also occur in the columns. Responses are larger for the 6-story building and exceed 2% story drift and beam plastic hinge rotation for SYLM/H, 6% for NR11/H and a few of the Elysian Park ground motions (maximum for EP17/H), and 7% for C05/H. For the 20-story building, this value is 1% for SYLM/H, 3% for NR11/H, 4% for several of the Elysian Park motions (maximum for EP14/H), and 5% for C05/H. Such large story drifts and plastic hinge rotations for these ground motions that have reasonable likelihood of occurring suggest that code design force levels are too low.

Including the floor slab (case PS) increases the beam strength relative to the column strength and results in more column yielding. This occurs mostly in the first story causing more drift there, which is evident from the Case PS results shown in **Tables 1.2** and **1.3** and in the figures:

Figure 1.28:	6-story building, Case PS, SYLM/H
Figure 1.29:	6-story building, Case PS, NR11/H
Figure 1.30:	6-story building, Case PS, EP17/H
Figure 1.31:	6-story building, Case PS, C05/H
Figure 1.32:	20-story building, Case PS, SYLM/H
Figure 1.33:	20-story building, Case PS, NR11/H
Figure 1.34:	20-story building, Case PS, EP14/H
Figure 1.35:	20-story building, Case PS, C05/H

Although modelling composite slab action in the floor slab is very crude, the increase in column yielding, which is undesirable, is probably real. Thus, omitting floor slabs in mathematical models may not be conservative regarding prediction of collapse potential.

CASES WITH FRACTURING WELDS

These cases include three without floor slabs (B, I and C) and one with floor slabs (Case BS). The analyses show the effect of weld fracture on the response and stability of steel buildings.

Results for Case B appear in the figures as follows:

Figure 1.36:	6-story building, Case B, SYLM/H
Figure 1.37:	6-story building, Case B, NR11/H

Figure 1.38:	6-story building, Case B, EP17/H
Figure 1.39:	6-story building, Case B, C05/H
Figure 1.40:	20-story building, Case B, SYLM/H
Figure 1.41:	20-story building, Case B, NR11/H
Figure 1.42:	20-story building, Case B, EP14/H
Figure 1.43:	20-story building, Case B, C05/H

The 6-story building collapses for all four ground motions. Collapse to the C05/H ground motion owes to excessive lateral sway while the others involve loss of axial capacity in columns. The assumption that a column no longer carries compression when its splice completely fractures plays an important role here. The 20-story building remains stable under the SYLM/H and NR11/H ground motions but collapses under excessive lateral sway for EP14/H and C05/H. In no case does a column splice in the 20-story building fracture. These results indicate that the susceptibility of welds to fracture as revealed by the Northridge earthquake is a serious problem and that some collapses of steel buildings during the Northridge earthquake could have occurred if more had been located to the north of the epicenter in the region of the strongest ground pulses. Of course, such a statement must be qualified by the many assumptions made in the analysis. Also, the term "collapse" may mean only a partial collapse in many instances.

In Case I the percentage of bad welds in the top fiber group of the beams is reduced from the 50% in Case B to 25%. Results appear in

Figure 1.44:	6-story building, Case I, SYLM/H
Figure 1.45:	6-story building, Case I, NR11/H
Figure 1.46:	6-story building, Case I, EP17/H
Figure 1.47:	6-story building, Case I, C05/H
Figure 1.48:	20-story building, Case I, SYLM/H
Figure 1.49:	20-story building, Case I, NR11/H
Figure 1.50:	20-story building, Case I, EP14/H
Figure 1.51:	20-story building, Case I, C05/H

For the 6-story building, collapse only occurs for the NR11/H ground motion, but a column has failed for EP17/H and the stability after C05/H is marginal due to the very large displacements (12% story drift, 9% beam plastic hinge rotation). Likewise, the 20-story building only collapses for one ground motion (C05/H). For SYLM/H and NR11/H, which did not produce collapse in the 20-story building in Case B, the responses are reduced, but they are still greater than what occurred for Case P. For EP14, the response is significantly greater than for Case P (7% story drift, 5% beam plastic hinge rotation), but not enough to precipitate the collapse which occurred for Case B. Thus, whereas weld fracture greatly increases the potential for collapse, the amount is sensitive to characteristics of the fracturing. For this reason, it is important to understand the conditions under which welds fracture.

The presence of floor slabs, which is examined by adding slabs to Case B to make Case BS, reduces the force carried by the top beam flange and should reduce the number of weld fractures there. However, the expected benefit does not occur as seen in the results of

Figure 1.52:	6-story building, Case BS, SYLM/H
Figure 1.53:	6-story building, Case BS, NR11/H
Figure 1.54:	6-story building, Case BS, EP17/H
Figure 1.55:	6-story building, Case BS, C05/H
Figure 1.56:	20-story building, Case BS, SYLM/H
Figure 1.57:	20-story building, Case BS, NR11/H
Figure 1.58:	20-story building, Case BS, EP14/H
Figure 1.59:	20-story building, Case BS, C05/H

Collapse occurs in 5 out of the 8 analyses, the same as for Case B except that collapse does not occur in Case BS for the 6-story building subjected to C05/H. However, the building is left in a precarious position (15% story drift, 12% beam plastic hinge rotation). The reason for the ineffectiveness of the slab in preventing top flange fractures is that the ground motions are strong enough to crack the slab, after which it carries no tension. Perhaps a more realistic model would show greater benefit, although the undesirable effect of increased column yielding would still be present.

Case C results are identical to those of Case P because no breakage of column splices occurred when the beam-to-column welds were assumed to be perfect. This result depends on the assumed fracture strength of the column splice welds and whether they are full or partial penetration. Slightly less conservative assumptions than made here would have resulted in splice breakages, and this deserves further study.

ACCUMULATION OF DAMAGE

Results of the two analyses using double earthquakes appear in

Figure 1.60:	6-story building, Case I, SYLM/DH
Figure 1.61:	20-story building, Case I, NR11/DH

After the first earthquake, both buildings were left with many weld fractures, and the 20-story building also had a significant lean. In both analyses, collapse occurred during the second earthquake. These results demonstrate the obvious fact that weakened buildings are at greater risk in subsequent earthquakes. Accurately quantifying this risk would take more study.

VERTICAL GROUND MOTION

Importance of vertical ground motion is investigated with Case P′ of the 6-story building using two sets of horizontal only and horizontal plus vertical ground motions (SYLM and EP17). Little effect was seen by the addition of vertical ground motion, and the responses are similar to those shown in **Figure 1.20** (Case P, SYLM/H, 6-story building) and **Figure 1.22** (Case P, EP17/H, 6-story building). To better show the insignificance of this effect, time histories of beam moment and plastic hinge rotation at three joints of the 6-story building (one each on the 2nd, 4th and 6th floors) are plotted in

Figure 1.62:	6-story building, Case P´, SYLM/H
Figure 1.63:	6-story building, Case P´, SYLM/H+V
Figure 1.64:	6-story building, Case P´, EP17/H
Figure 1.65:	6-story building, Case P´, EP17/H+V

Differences between the horizontal only and horizontal plus vertical analyses are very slight. Since the design of the beams is controlled by seismic loads, they are much stiffer and stronger than if designed only for gravity. With a typical natural frequency of about 20 Hz, they experience little dynamic amplification, and so the vertical ground acceleration, being considerably less than 1g, produces stresses less than even the small gravity load stresses. These observations should also hold for the 20-story building.

LOAD HISTORY OF BEAMS

The time histories of beam moment and plastic hinge rotation in **Figures 1.62** to **1.65** demonstrate typical loading histories for beams. The frequency of these loading cycles is the same as the response frequency of the building (compare with **Figures 1.20** and **1.22**). The number of cycles into the nonlinear range is small, and the histories for the EP17 ground motion are dominated by a single large excursion in which the plastic hinge rotation changes by 0.10 radians in about a second (**Figure 1.64** or **1.65**, 2nd floor joint). Such information is useful for determining load histories to be used on specimens in laboratory tests. Load histories for large earthquakes with long durations should also be defined.

TOPICS FOR FUTURE STUDY

Results of the present study, although they indicate plenty of cause for concern, must be viewed as preliminary because of the many simplifying assumptions made. In order to be able to adequately assess potential for severe damage or collapse of steel buildings under strong earthquake ground motions, future work is needed in the following areas.

- Full accounting of 3-dimensional effects. This will mean devising more efficient beam and column elements because computational requirements grow greatly when considering buildings as true 3-dimensional structures.

- Better understanding of weld fracture processes and formulation of realistic rules governing weld fracture.

- Consideration of structural deterioration mechanisms other than weld fracture, such as local flange buckling.

- Quantification of contributions from nonstructural components and from frames with simple beam-to-column connections.
- Improved representation of effects of floor slabs.
- Better modelling of the foundation and its nonlinearity.
- Examination of long-duration earthquakes with many load cycles.
- Studies of braced frames.

TABLE 1.1: SUMMARY OF GROUND MOTION PARAMETERS.

Ground Motion	Displacement (cm)	Velocity (cm/s)	Acceleration (cm/s/s)	Angle (deg E of N)	Figure
SYLM/H	31.	131.	818.	10.	1.6
SYLM/V	10.	19.	525.		1.7
SYLM/DH	31.	131.	830.	10.	1.8
NR01/H	21.	61.	481.	21.	
NR02/H	22.	52.	576.	10.	
NR03/H	21.	53.	500.	8.	
NR04/H	18.	51.	364.	-22.	
NR05/H	20.	91.	646.	-22.	
NR06/H	29.	73.	546.	10.	
NR07H	30.	95.	663.	-12.	
NR08H	45.	141.	865.	5.	
NR09/H	44.	117.	989.	-27.	
NR10/H	67.	153.	910.	27.	
NR11/H	72.	168.	917.	27.	1.9
NR11/DH	80.	168.	918.	27.	1.10
NR12/H	58.	153.	1184.	36.	
NR13/H	53.	152.	1407.	34.	
NR14/H	37.	179.	1296.	21.	
NR15/H	36.	156.	912.	29.	
NR16/H	33.	137.	890.	32.	
NR17/H	30.	79.	584.	21.	
NR18/H	29.	79.	382.	30.	
NR19/H	27.	66.	350.	24.	
NR20/H	22.	67.	294.	27.	
NR21/H	20.	65.	264.	25.	
EP01/H	31.	54.	989.	18.	
EP02/H	34.	82.	815.	13.	
EO03/H	34.	124.	1166.	37.	

TABLE 1.1: SUMMARY OF GROUND MOTION PARAMETERS (CONT'D.)

EO04/H	32.	82.	792.	-2.	
EP05/H	35.	199.	1685.	23.	
EP06/H	50.	190.	1507.	30.	
EP07/H	51.	203.	1518.	28.	
EP08/H	55.	174.	1178.	25.	
EP09/H	65.	142.	1040.	26.	
EP10/H	91.	100.	1152.	29.	
EP11/H	110.	133.	727.	28.	
EP12/H	124.	153.	1026.	25.	
EP13/H	128.	180.	745.	25.	
EP14/H	117.	207.	936.	29.	1.11
EP15/H	108.	173.	1227.	22.	
EP16/H	91.	171.	957.	31.	
EP17/H	82.	174.	1007.	21.	1.12
EP17/V	52.	62.	386.		1.13
EP18/H	71.	159.	870.	27.	
EP19/H	63.	142.	1068.	31.	
EP20/H	48.	137.	798.	31.	
EP21/H	40.	138.	864.	29.	
C05/H	182.	139.	391.	36.	1.14

TABLE 1.2. SUMMARY OF RESULTS FOR THE 6-STORY BUILDING TO SELECTED GROUND MOTIONS (PEAK VALUES OF STORY DRIFT, ROOF DISPLACEMENT, BEAM HINGE ROTATION, AND COLUMN TENSION).

Case	Ground Motion	Collapse	1st Story Drift (%)	Upper Story Drift (%)	Roof Disp. (cm)	Beam Hinge Rot. (%)	Column Tension (MN)	Figure
E	SYLM/H	No	2.6	2.7	56.	0.0	4.5	
E	NR11/H	No	4.6	5.4	113.	0.0	7.5	
E	EP17/H	No	3.8	4.1	80.	0.0	6.8	
E	C05/H	No	1.8	1.9	40.	0.0	2.9	
P	SYLM/H	No	2.7	2.5	43.	2.0	1.2	1.20
P	NR11/H	No	6.7	6.0	90.	6.1	1.4	1.21
P	EP17/H	No	7.3	7.2	107.	7.3	1.1	1.22
P	C05/H	No	7.9	7.5	106.	7.5	1.2	1.23
PS	SYLM/H	No	1.9	3.2	43.	2.7	1.3	1.28
PS	NR11/H	No	6.9	5.1	81.	6.7	1.6	1.29
PS	EP17/H	No	8.8	7.7	112.	8.6	1.2	1.30
PS	C05/H	No	8.5	5.0	86.	4.9	1.3	1.31
B	SYLM/H	Yes						1.36
B	NR11/H	Yes						1.37
B	EP17/H	Yes						1.38
B	C05/H	Yes						1.39
I	SYLM/H	No	1.7	3.0	48.	2.0	0.2	1.44
I	NR11/H	Yes						1.45
I	EP17/H	No	5.5	5.7	92.	5.1	0.4	1.46
I	C05/H	No	11.7	12.4	207.	9.5	0.4	1.47
BS	SYLM/H	Yes						1.52
BS	NR11/H	Yes						1.53
BS	EP17/H	Yes						1.54
BS	C05/H	No	14.7	15.1	222.	12.1	0.3	1.55
I	SYLM/DH	Yes						1.60
P′	SYLM/H	No	2.9	2.6	45.	1.9	1.2	1.62
P′	SYLM/H+V	No	2.8	2.6	44.	1.9	1.5	1.63
P′	EP17/H	No	7.6	7.6	110.	7.4	1.2	1.64
P′	EP17/H+V	No	7.5	7.5	110.	7.3	1.3	1.65

TABLE 1.3. SUMMARY OF RESULTS FOR THE 20-STORY BUILDING TO SELECTED GROUND MOTIONS (PEAK VALUES OF STORY DRIFT, ROOF DISPLACEMENT, BEAM HINGE ROTATION, AND COLUMN TENSION).

Case	Ground Motion	Collapse	1st Story Drift (%)	Upper Story Drift (%)	Roof Disp. (cm)	Beam Hinge Rot. (%)	Column Tension (MN)	Figure
E	SYLM/H	No	1.0	1.3	84.	0.0	7.6	
E	NR11/H	No	1.5	2.7	139.	0.0	13.4	
E	EP14/H	No	2.1	2.8	170.	0.0	17.6	
E	C05/H	No	2.1	2.8	188.	0.0	20.3	
P	SYLM/H	No	1.4	1.5	77.	0.9	5.3	1.24
P	NR11/H	No	2.4	3.2	166.	2.4	8.8	1.25
P	EP14/H	No	4.2	4.3	184.	3.7	8.5	1.26
P	C05/H	No	3.7	5.9	273.	5.1	9.8	1.27
PS	SYLM/H	No	1.3	1.4	77.	0.8	6.1	1.32
PS	NR11/H	No	2.4	2.9	164.	1.8	10.3	1.33
PS	EP14/H	No	4.8	3.8	183.	3.0	9.7	1.34
PS	C05/H	No	5.1	4.9	263.	3.7	11.1	1.35
B	SYLM/H	No	1.2	2.3	73.	1.3	1.6	1.40
B	NR11/H	No	3.2	6.7	185.	4.7	3.1	1.41
B	EP14/H	Yes						1.42
B	C05/H	Yes						1.43
I	SYLM/H	No	1.3	2.0	74.	1.1	2.4	1.48
I	NR11/H	No	2.4	4.3	164.	3.6	4.0	1.49
I	EP14/H	No	5.7	6.9	197.	5.0	3.8	1.50
I	C05/H	Yes						1.51
BS	SYLM/H	No	1.2	2.1	73.	1.1	2.4	1.56
BS	NR11/H	No	2.6	4.8	162.	4.0	3.6	1.57
BS	EP14/H	Yes						1.58
BS	C05/H	Yes						1.59
I	NR11/DH	Yes						1.61

FIGURE 1.1: DETAILS OF BEAM-COLUMN MODELLING SHOWING LONGITUDINAL DISTRIBUTION OF SUBELEMENTS (TOP) AND ARRANGEMENT OF FIBERS WITHIN CROSS-SECTION (BOTTOM).

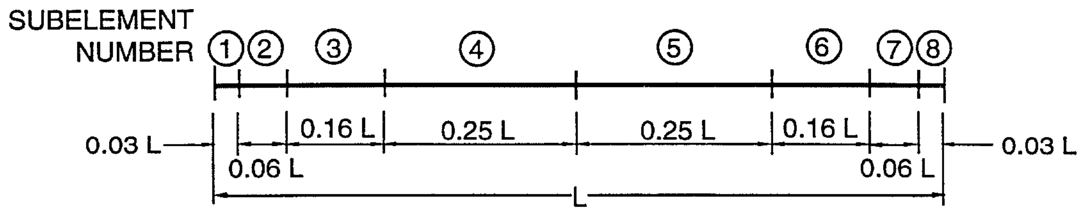

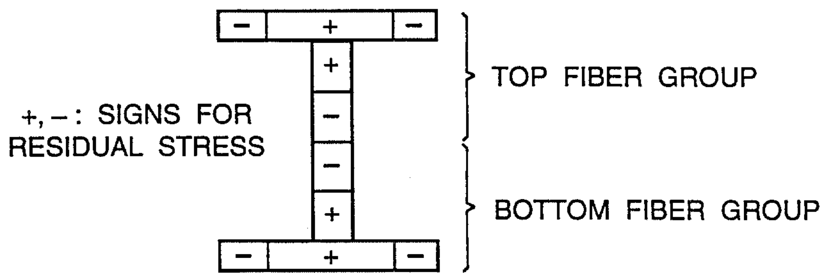

FIGURE 1.2: NONLINEAR MODELS FOR FIBERS AND PANEL ZONES: BACKBONE CURVE FOR AXIAL FIBER STRESS-STRAIN (TOP), BACKBONE CURVE FOR PANEL ZONE MOMENT-SHEAR STRAIN (MIDDLE), HYSTERETIC BEHAVIOR OF FIBER (BOTTOM).

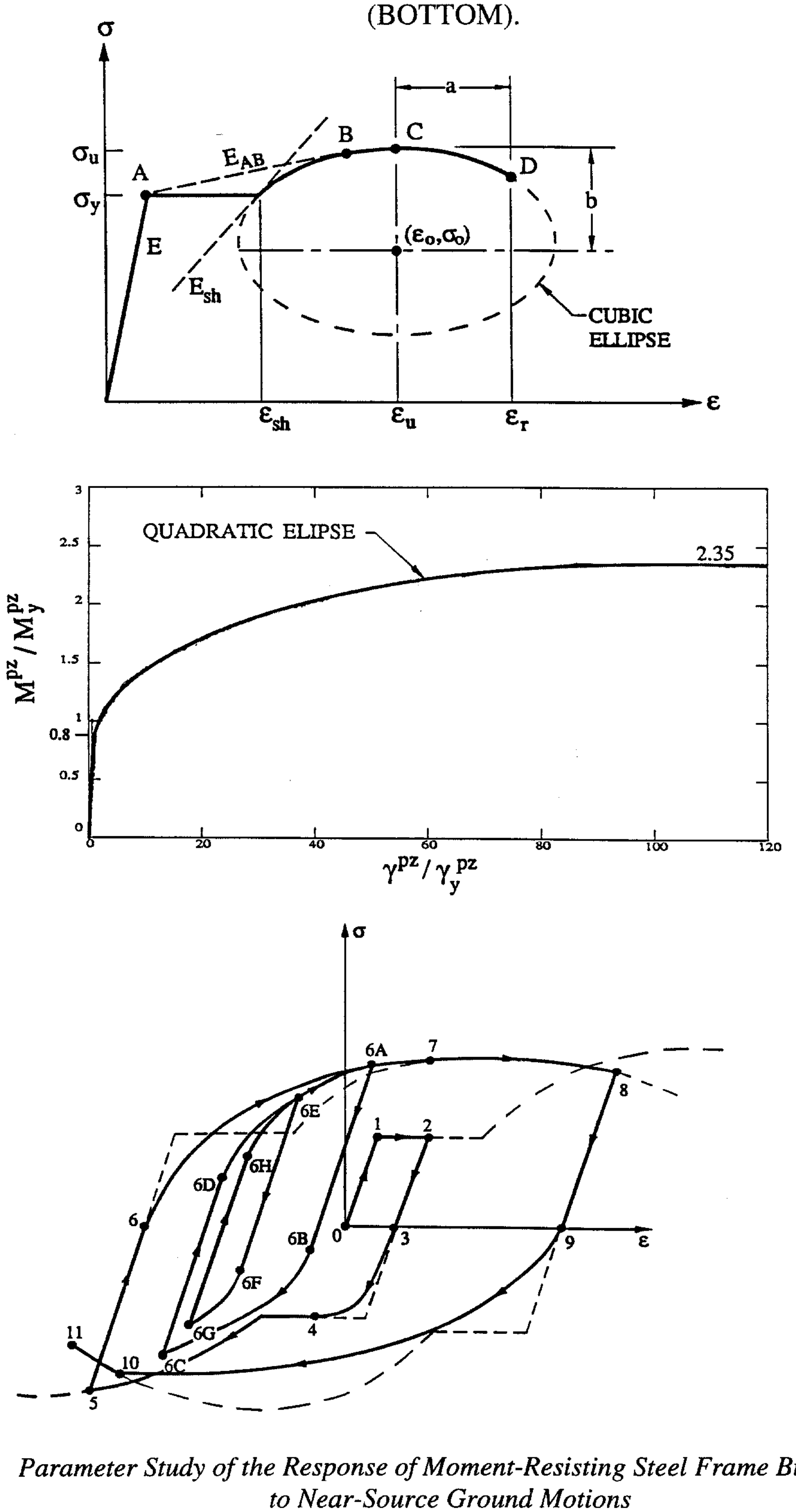

FIGURE 1.3: HYSTERETIC BEHAVIOR OF SLAB FIBER (TOP), SHEAR SPRING IN STORY *i* (MIDDLE), AND FOUNDATION SPRING (BOTTOM).

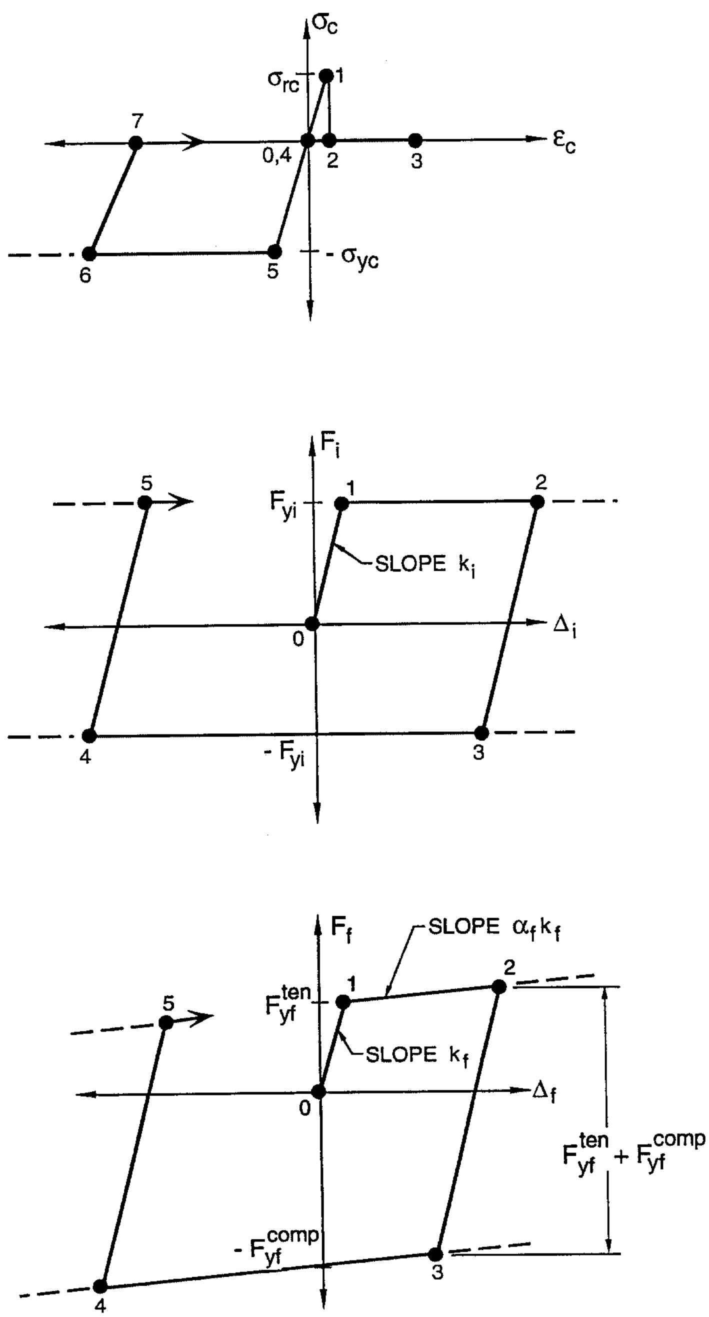

FIGURE 1.4: TWENTY-STORY STEEL FRAME BUILDING: PERSPECTIVE VIEW AND DETAILS OF END FRAME (NOT TO SCALE).

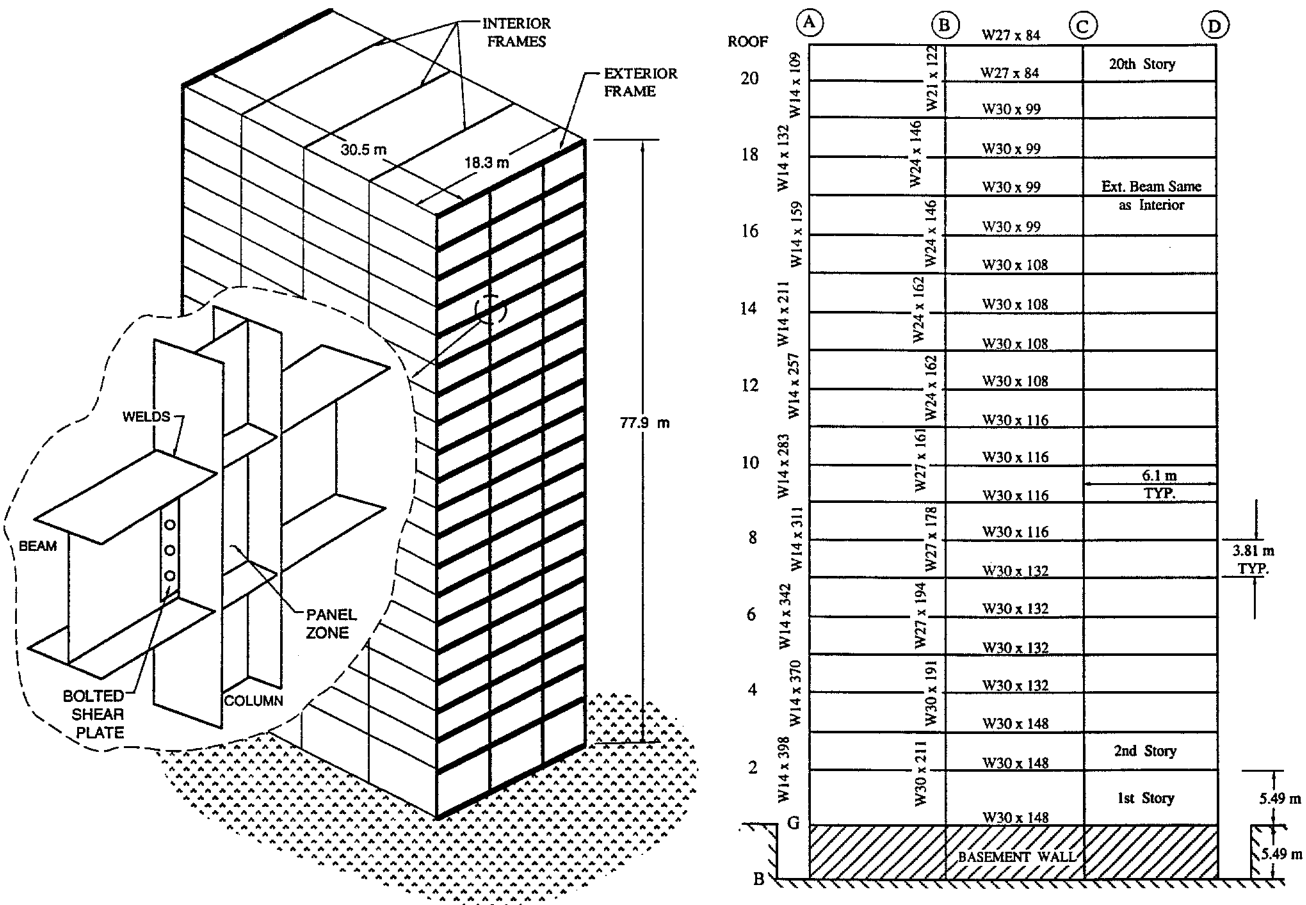

FIGURE 1.5: SIX-STORY STEEL FRAME BUILDING: PERSPECTIVE VIEW AND DETAILS OF END FRAME (NOT TO SCALE).

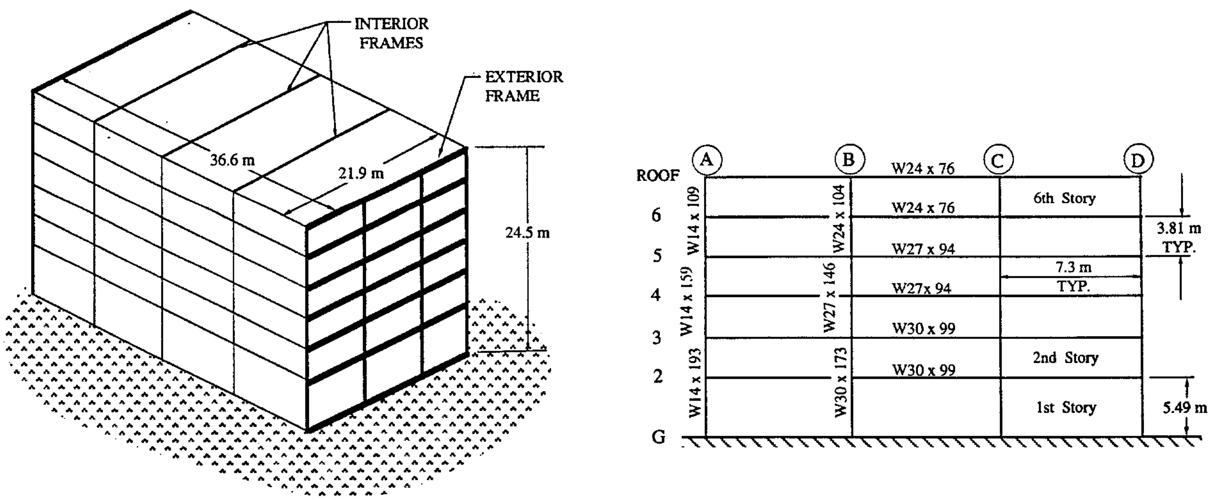

FIGURE 1.6: SYLM/H GROUND MOTION.

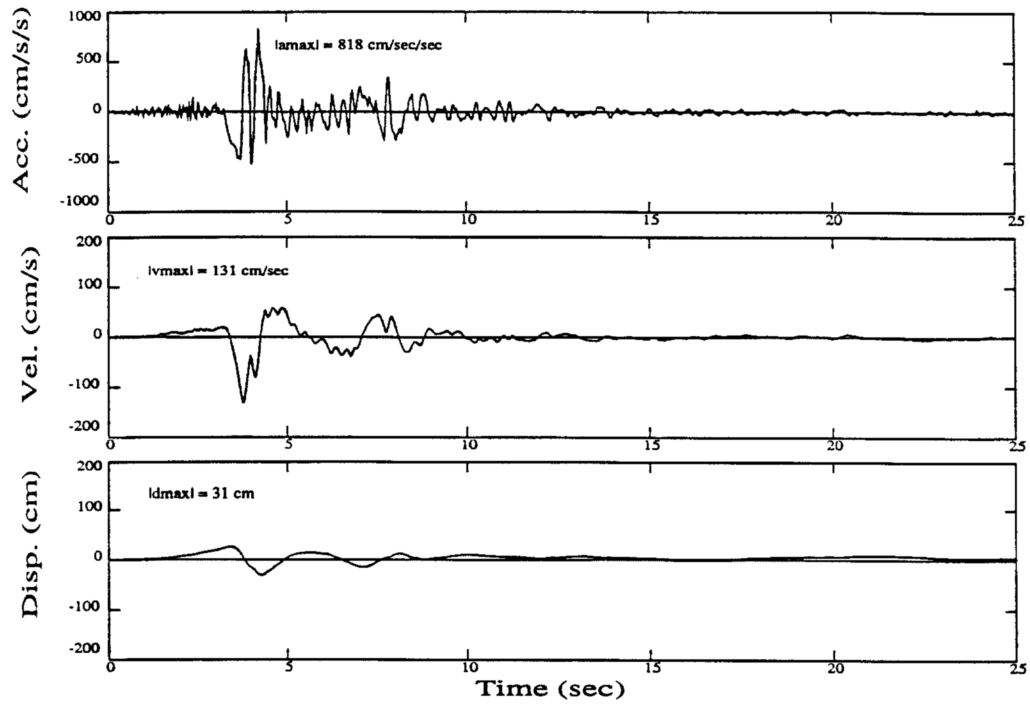

FIGURE 1.7: SYLM/V GROUND MOTION.

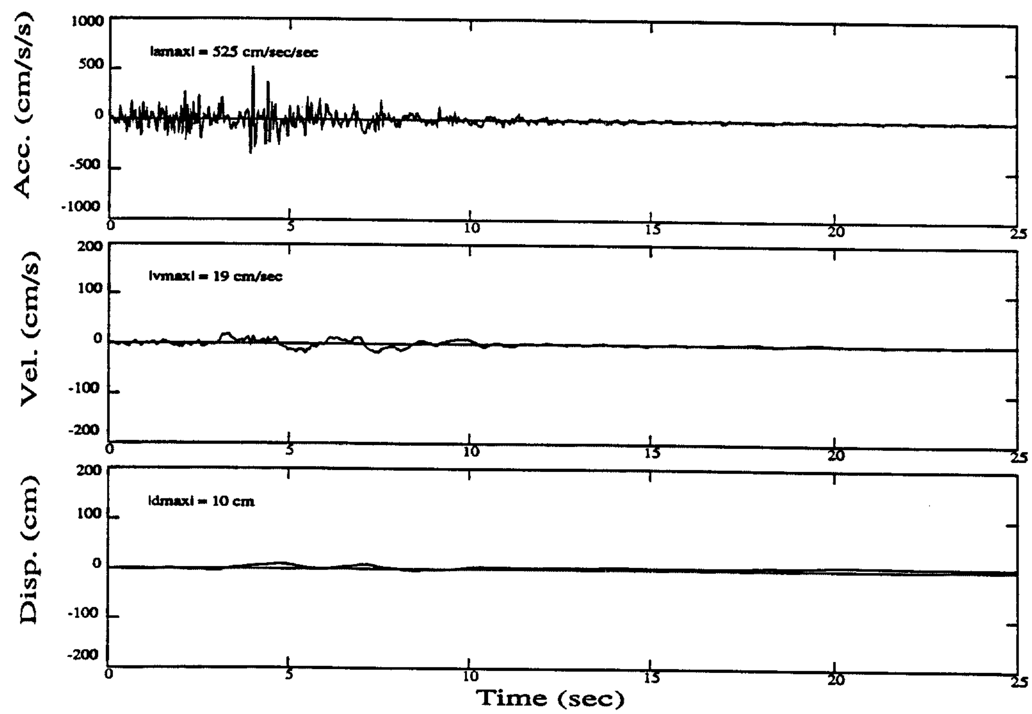

FIGURE 1.8: SYLM/DH GROUND MOTION

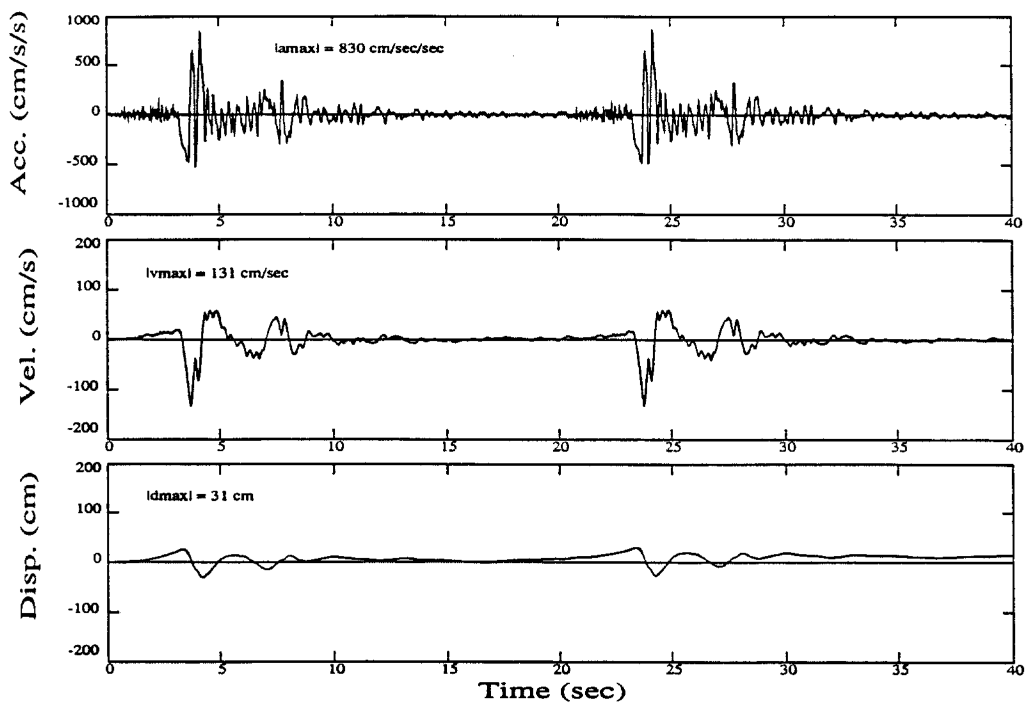

FIGURE 1.9: NR11/H GROUND MOTION.

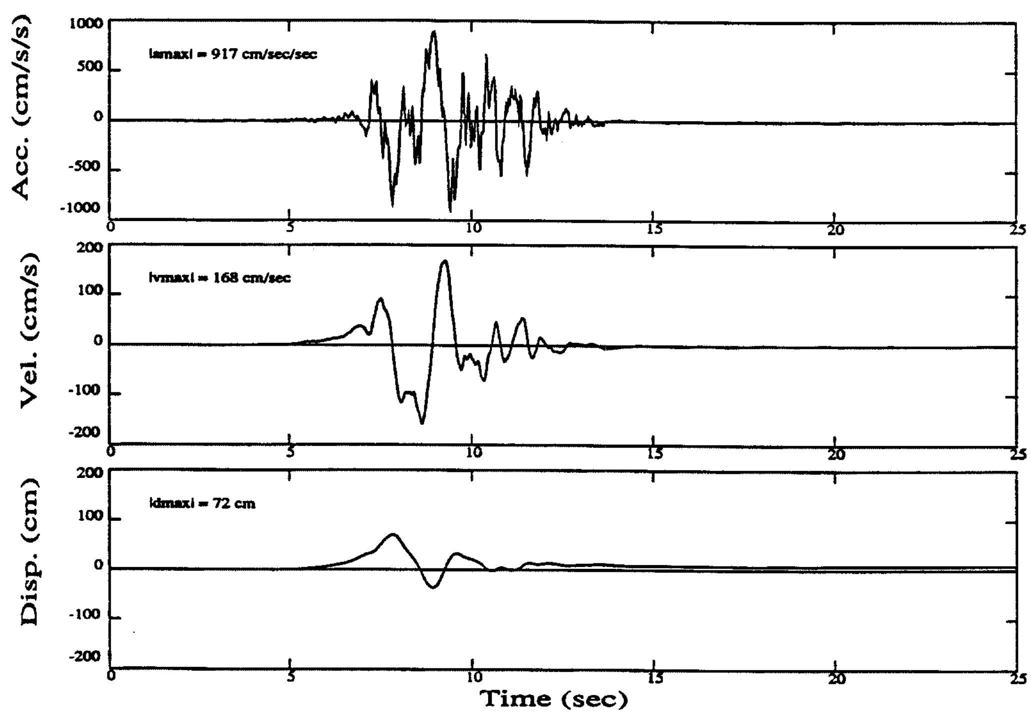

FIGURE 1.10: NR11/DH GROUND MOTION

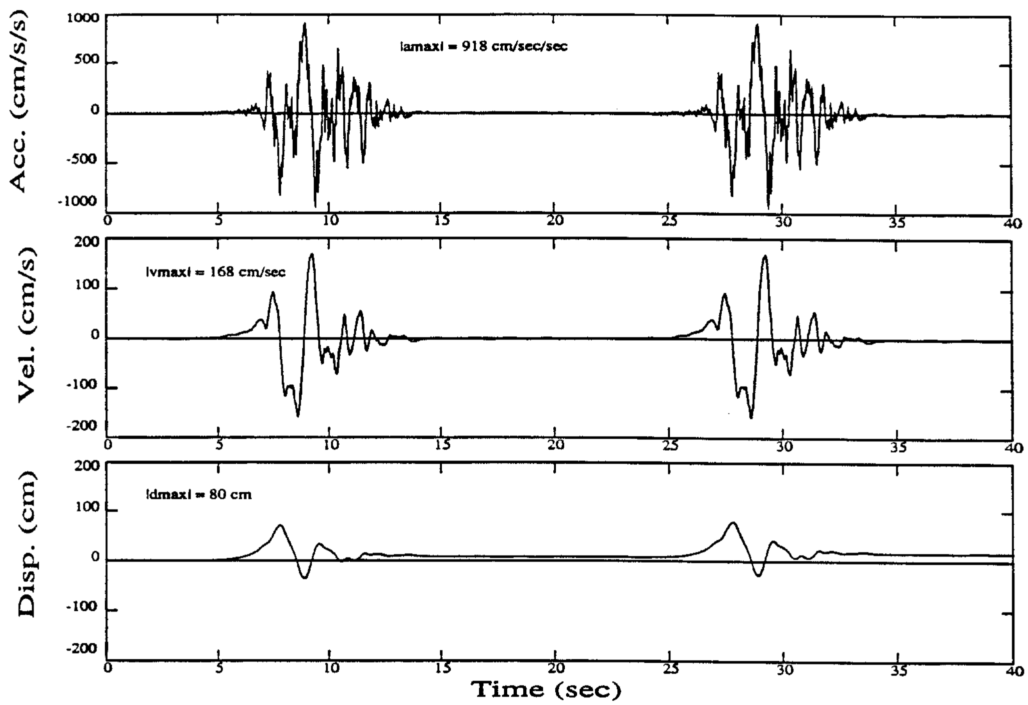

FIGURE 1.11: EP14/H GROUND MOTION.

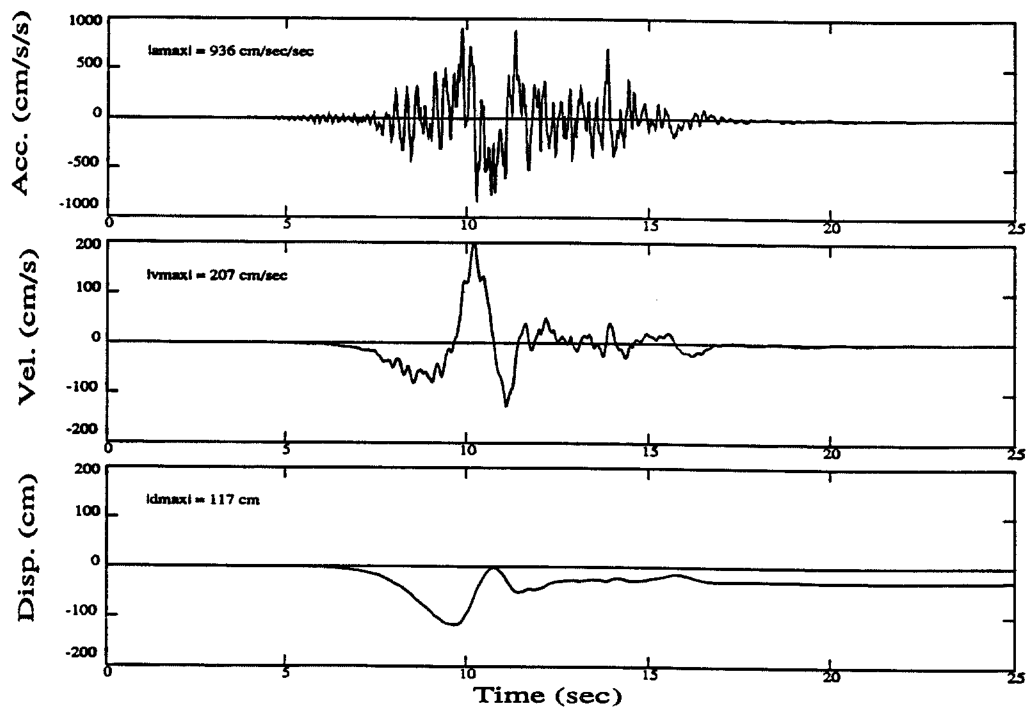

FIGURE 1.12: EP17/H GROUND MOTION.

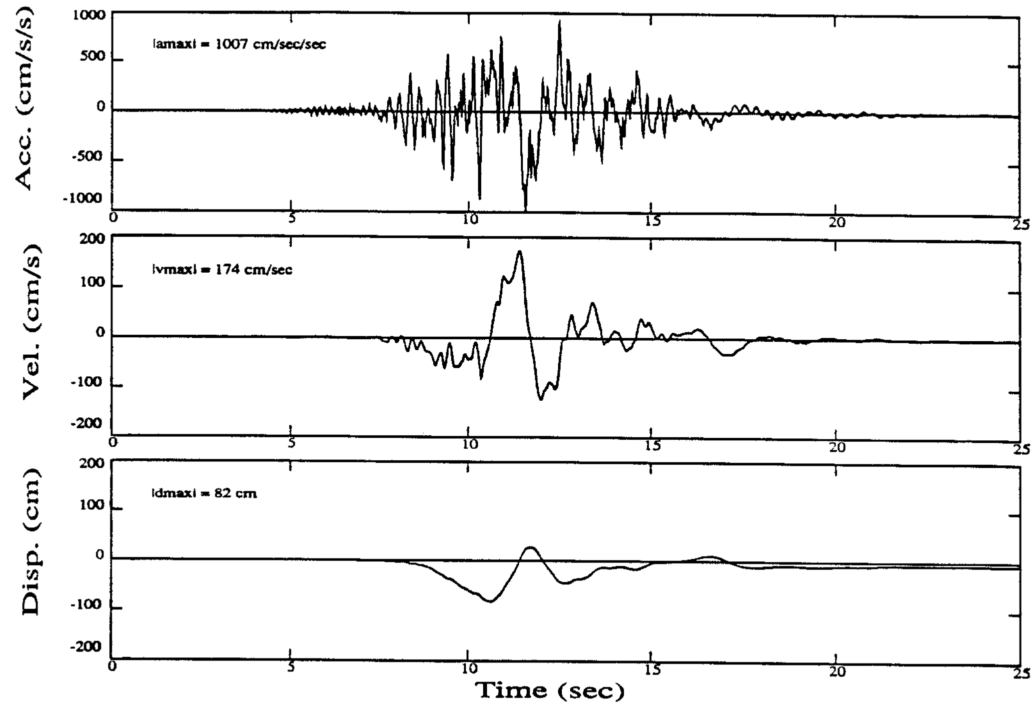

FIGURE 1.13: EP17/V GROUND MOTION.

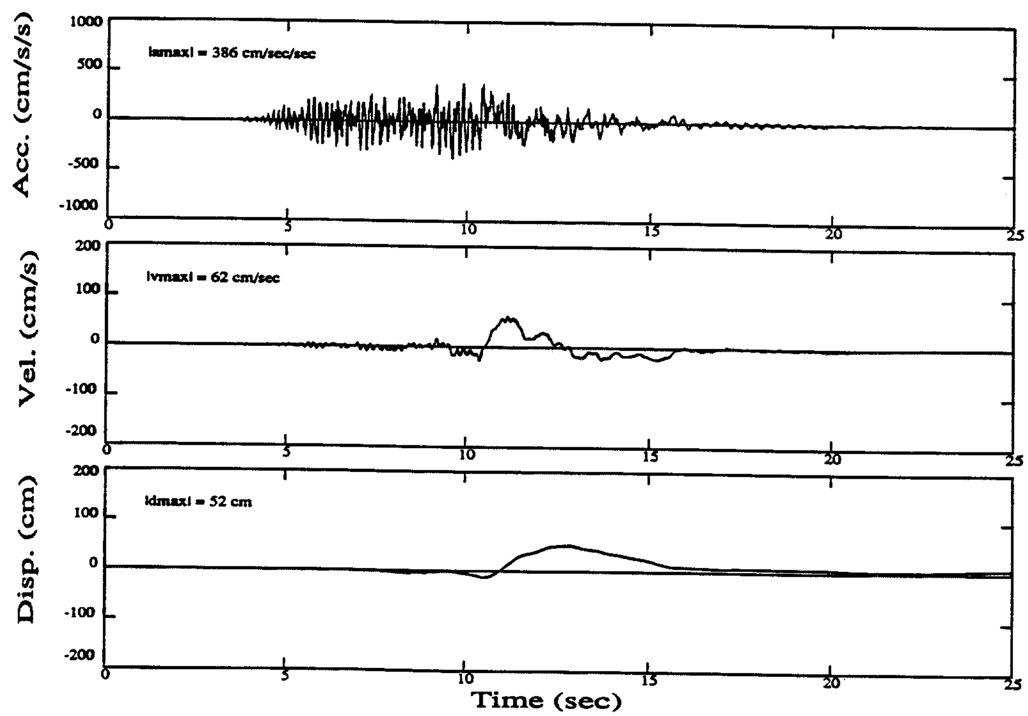

FIGURE 1.14: C05/H GROUND MOTION.

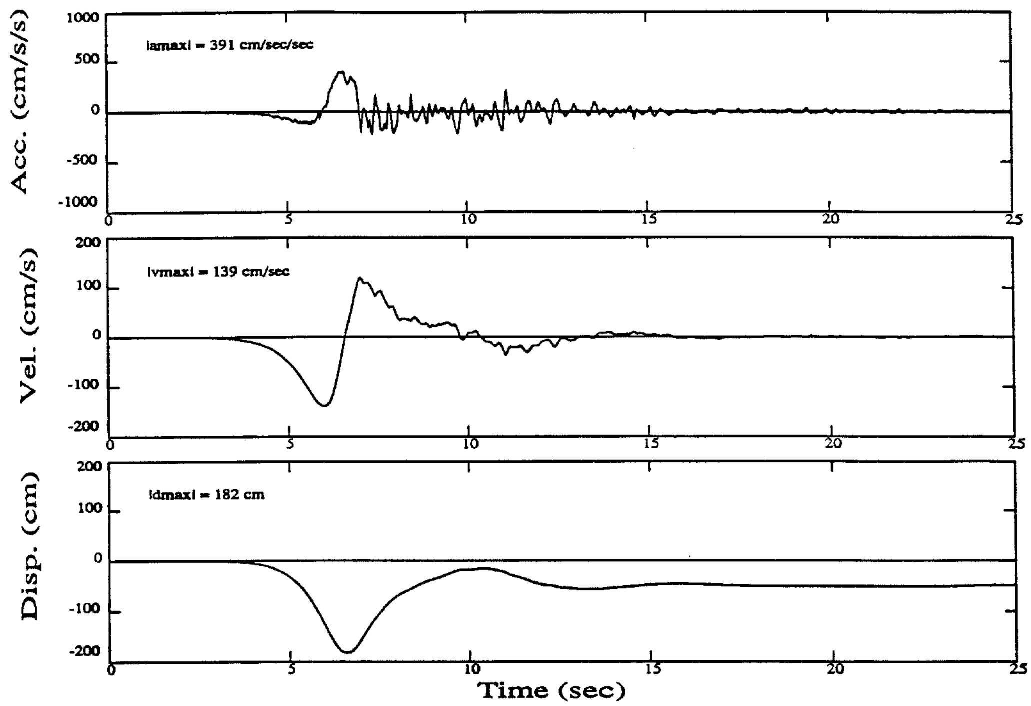

FIGURE 1.15: SPECTRA FOR SELECTED GROUND MOTIONS AND FOR THE EARTHQUAKE REPRESENTED IN THE UNIFORM BUILDING CODE.

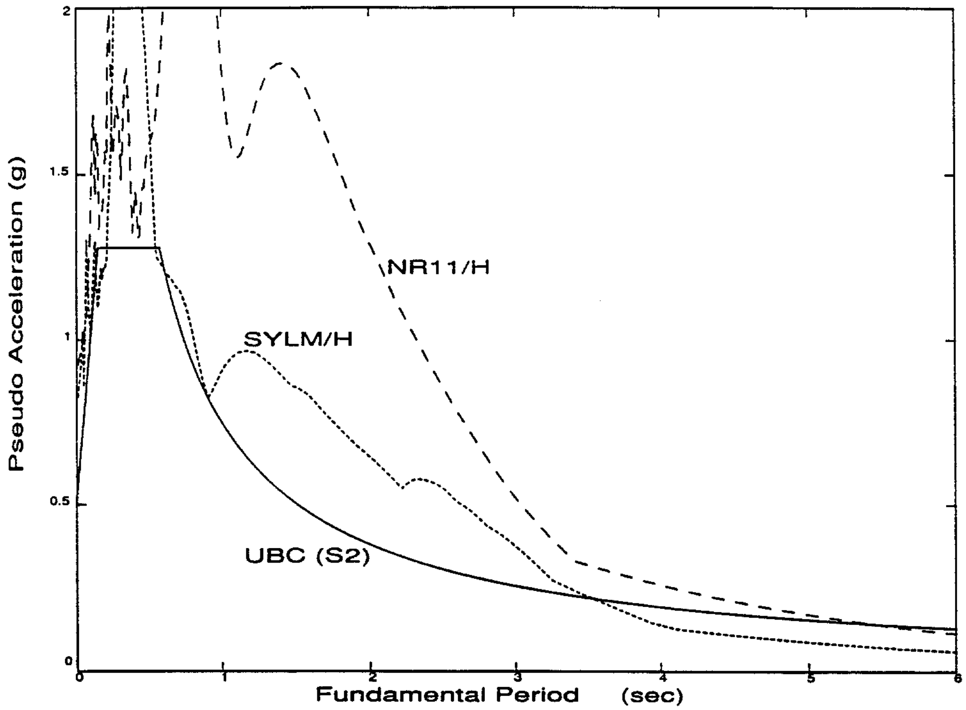

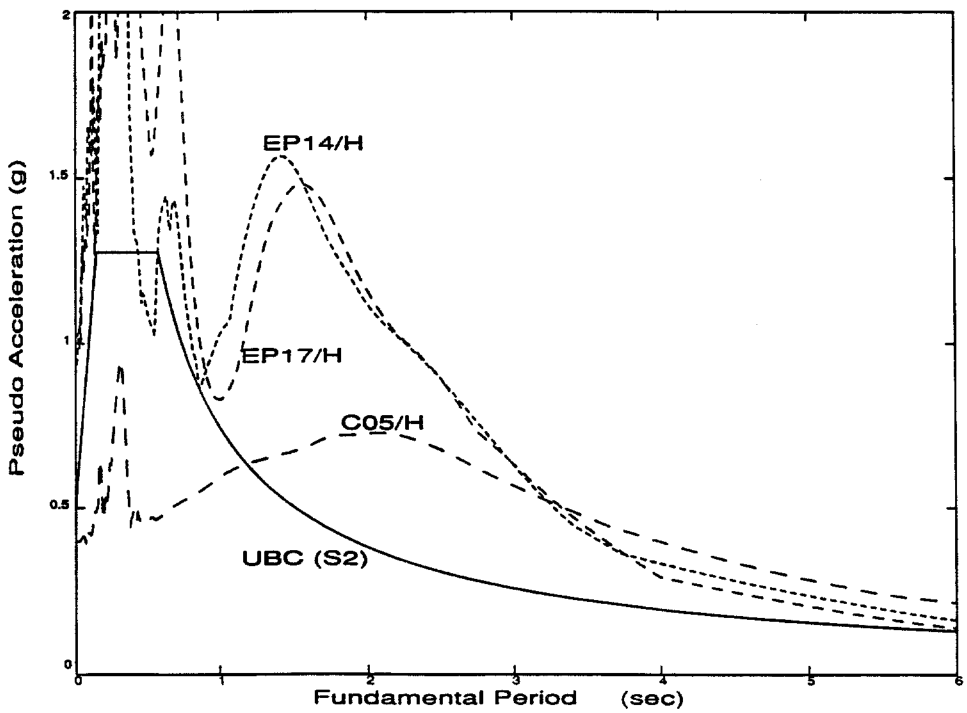

FIGURE 1.16: RESULTS FOR THE SIX-STORY BUILDING, CASES E AND P, SIMULATED NORTHRIDGE GROUND MOTIONS.

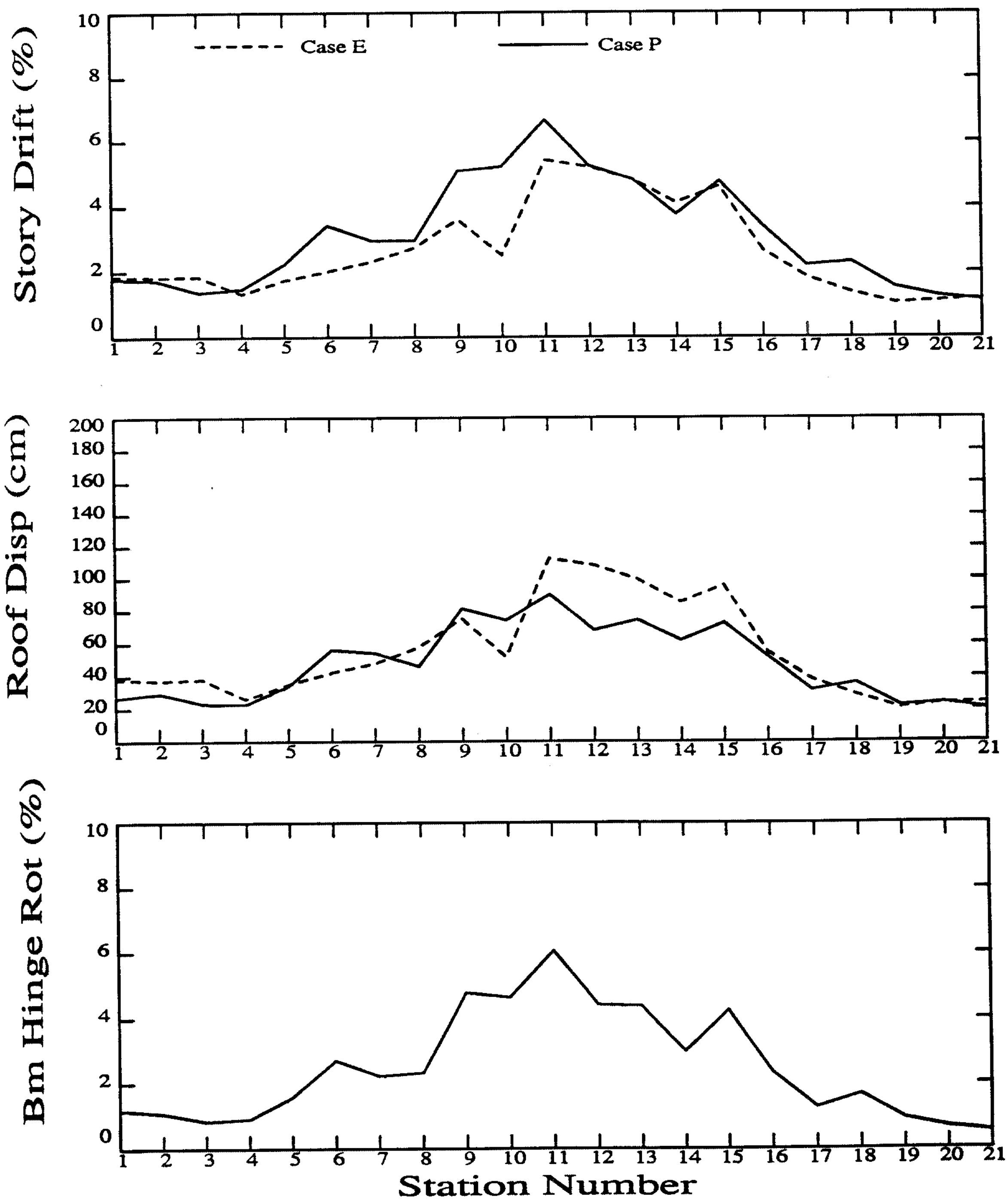

FIGURE 1.17: RESULTS FOR THE SIX-STORY BUILDING, CASES E AND P, SIMULATED ELYSIAN PARK GROUND MOTIONS.

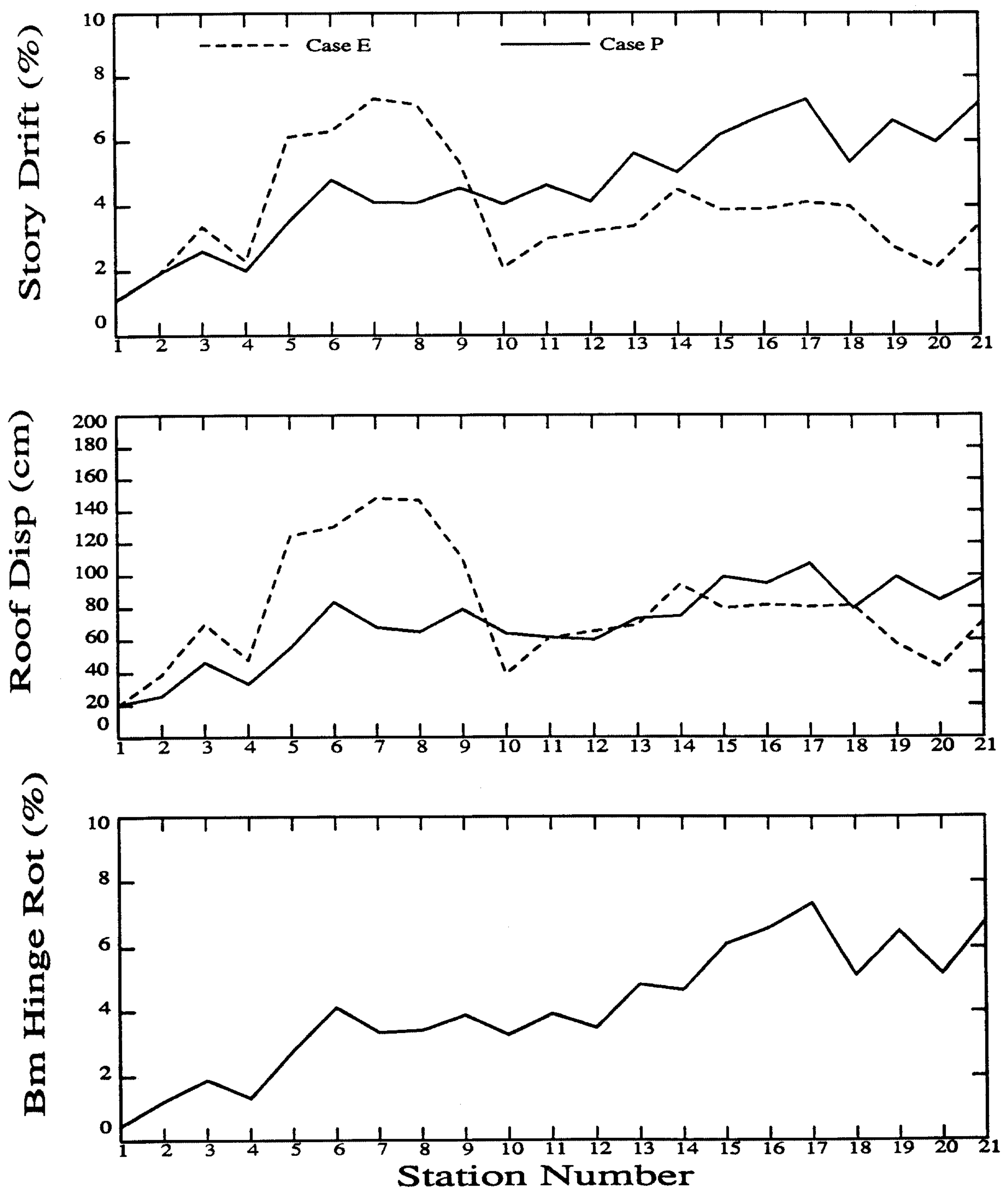

FIGURE 1.18: RESULTS FOR THE TWENTY-STORY BUILDING, CASES E AND P, SIMULATED NORTHRIDGE GROUND MOTIONS.

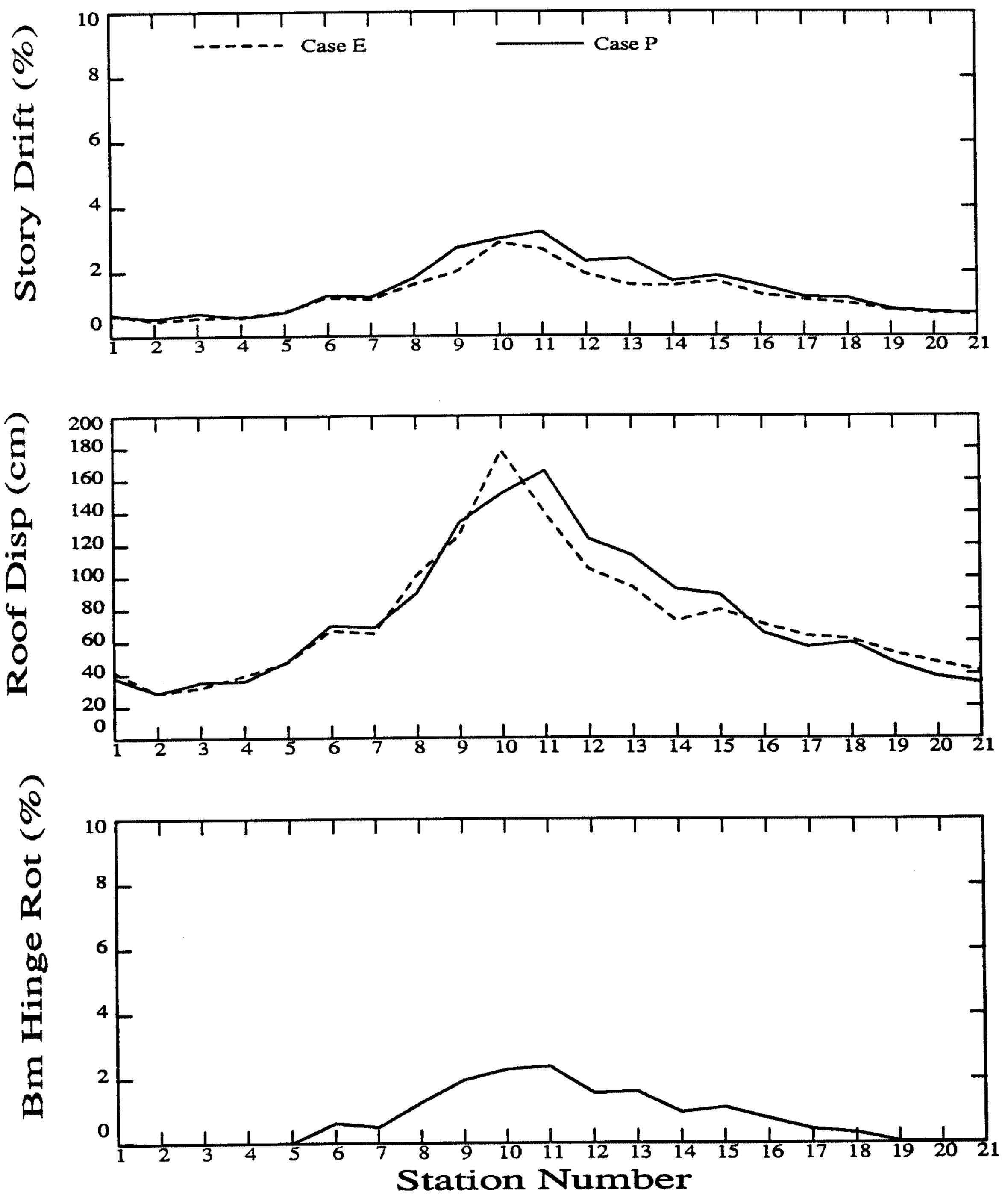

FIGURE 1.19: RESULTS FOR THE TWENTY-STORY BUILDING, CASES E AND P, SIMULATED ELYSIAN PARK GROUND MOTIONS.

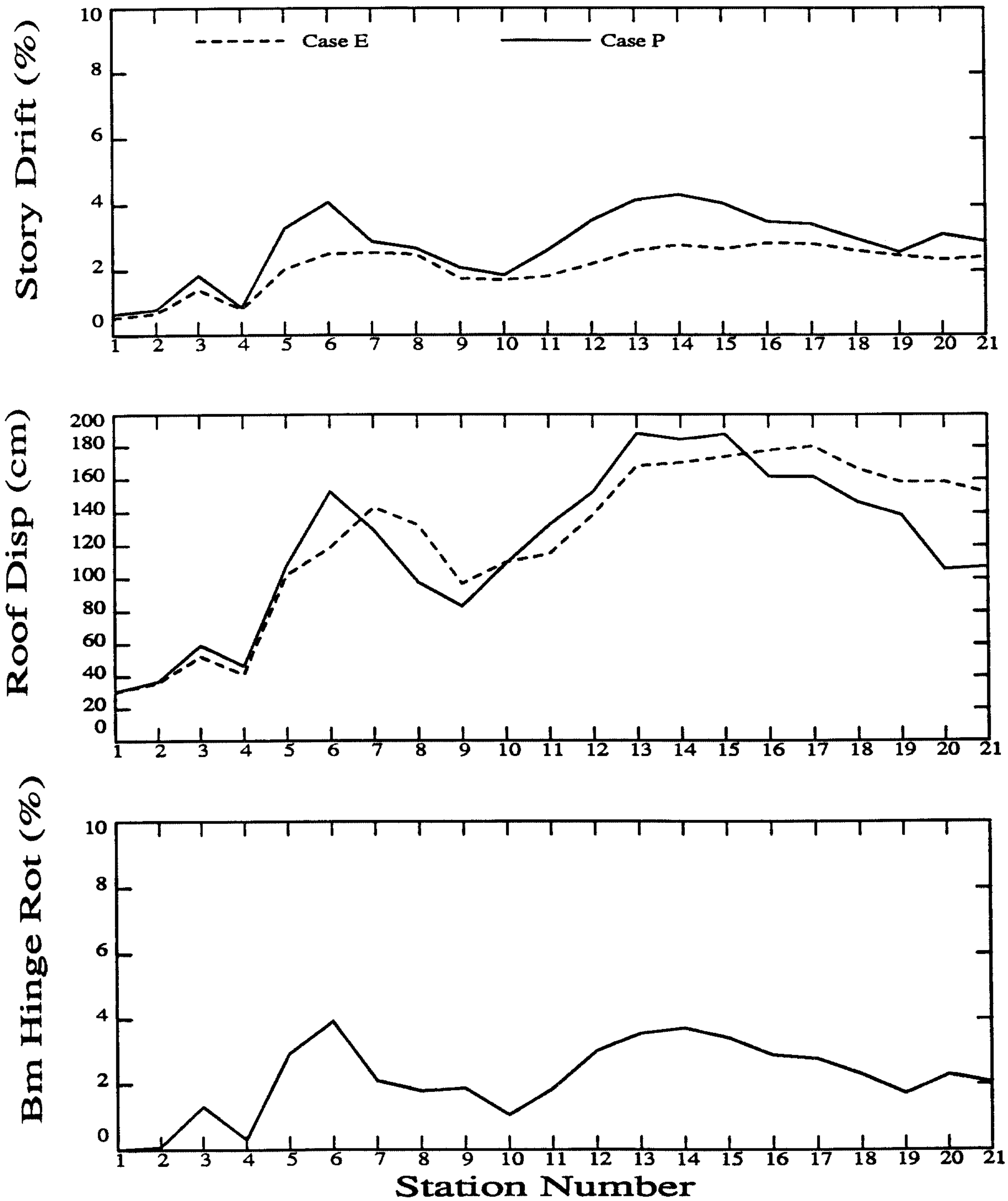

FIGURE 1.20: RESULTS FOR THE 6-STORY BUILDING, CASE P, SYLM/H GROUND MOTION.

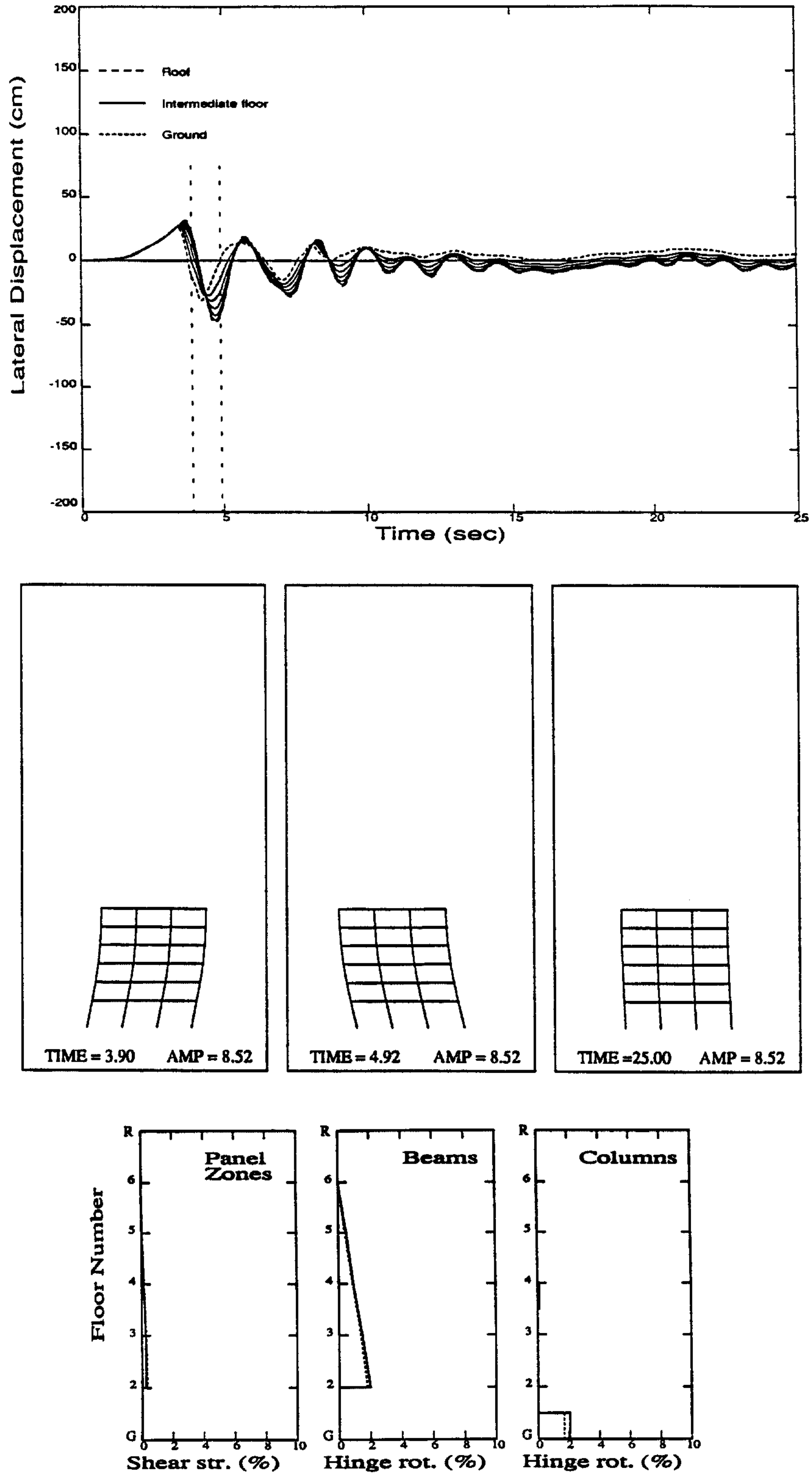

Parameter Study of the Response of Moment-Resisting Steel Frame Buildings to Near-Source Ground Motions

FIGURE 1.21: RESULTS FOR THE 6-STORY BUILDING, CASE P, NR11/H GROUND MOTION.

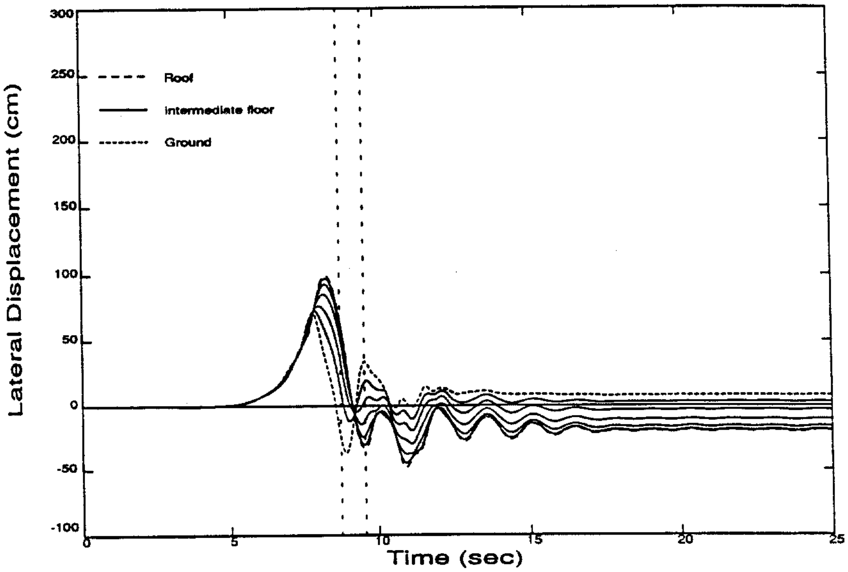

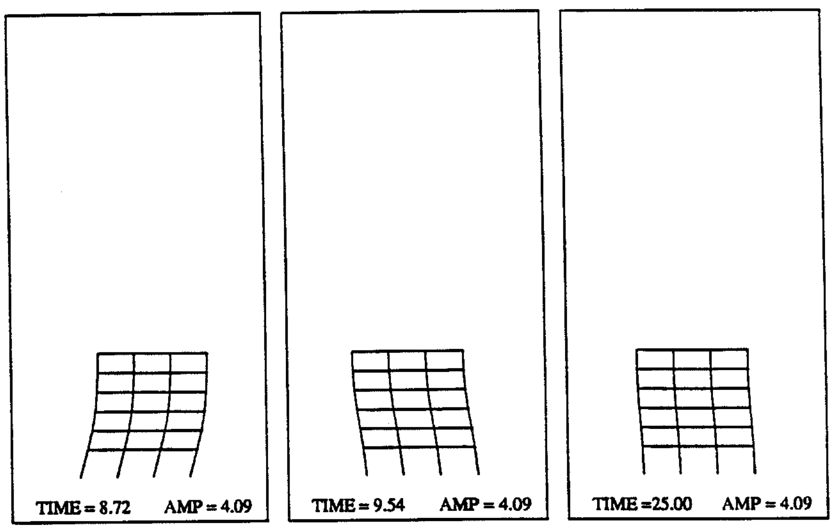

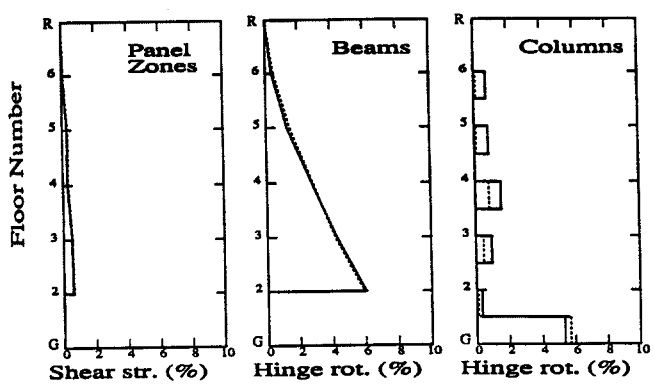

Parameter Study of the Response of Moment-Resisting Steel Frame Buildings to Near-Source Ground Motions

FIGURE 1.22: RESULTS FOR THE 6-STORY BUILDING,
CASE P, EP17/H GROUND MOTION.

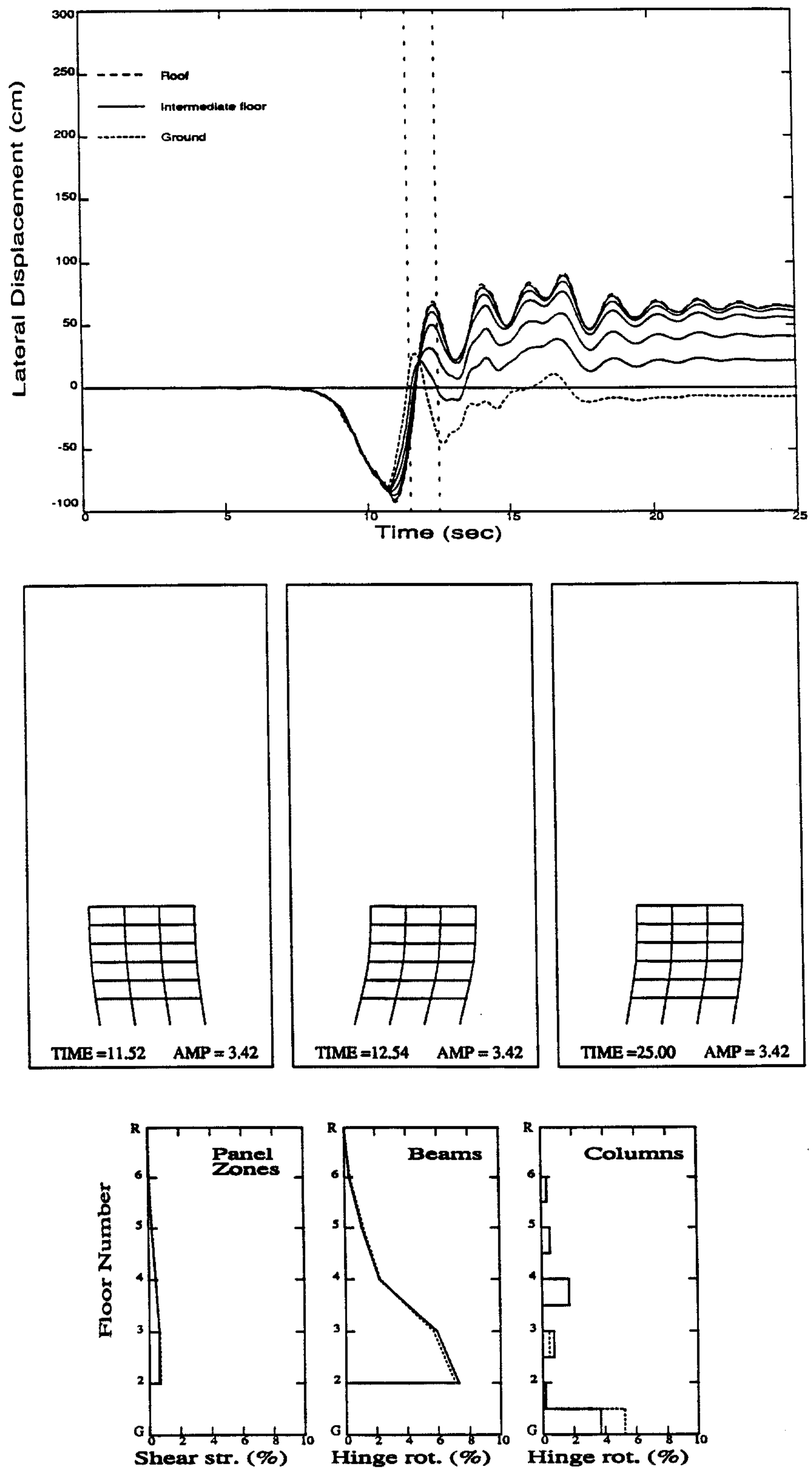

FIGURE 1.23: RESULTS FOR THE 6-STORY BUILDING,
CASE P, C05/H GROUND MOTION.

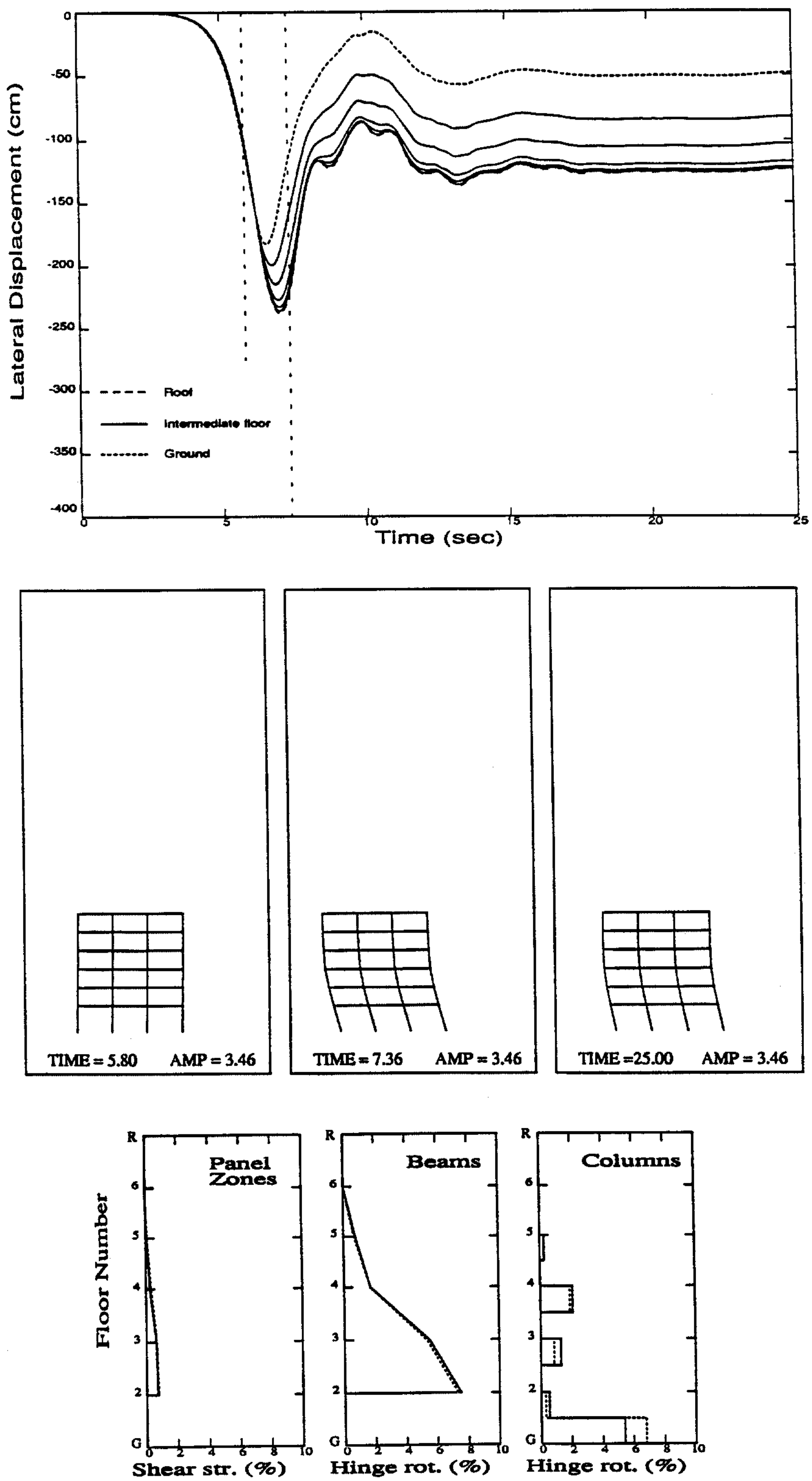

FIGURE 1.24: RESULTS FOR THE 20-STORY BUILDING, CASE P, SYLM/H GROUND MOTION.

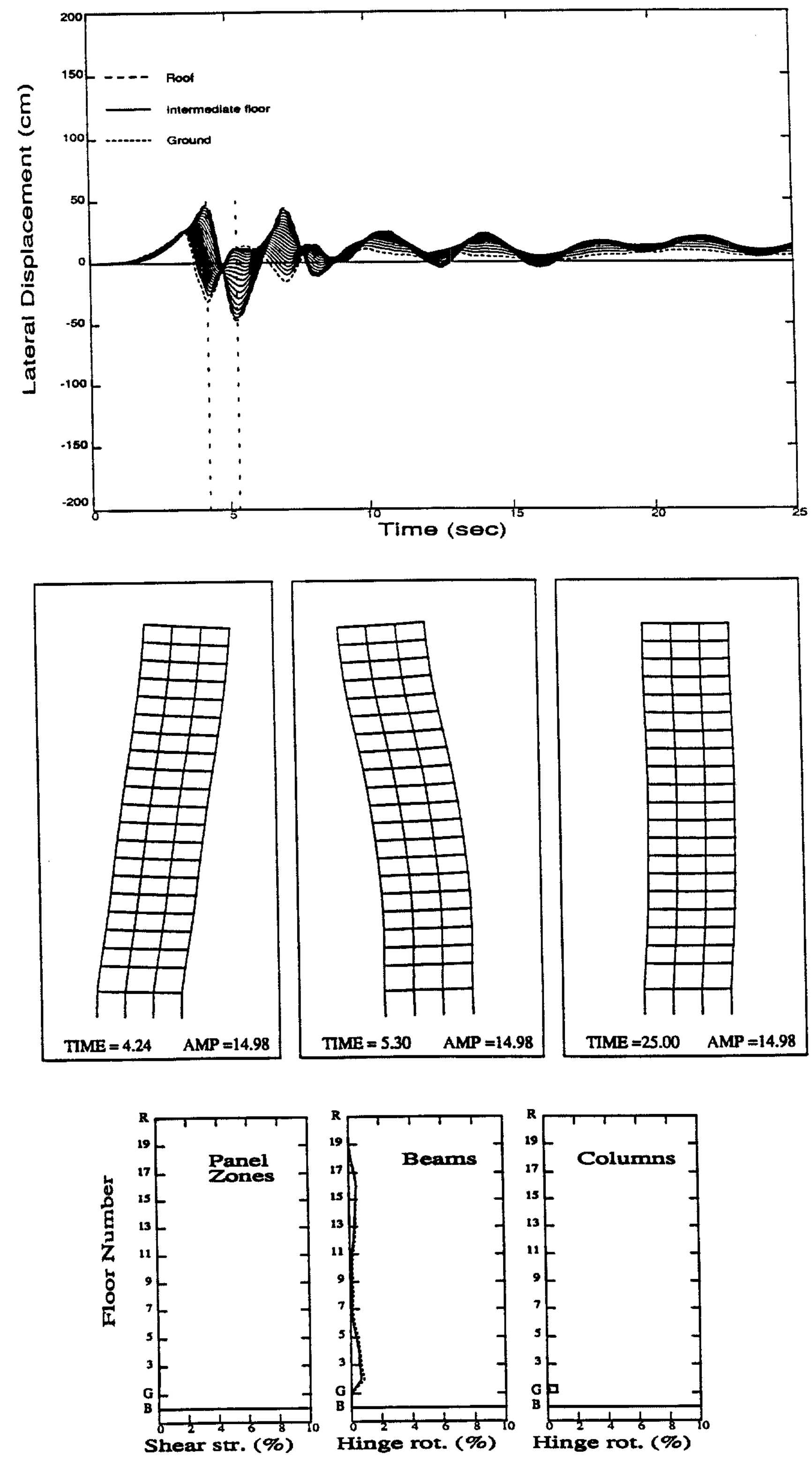

FIGURE 1.25: RESULTS FOR THE 20-STORY BUILDING, CASE P, NR11/H GROUND MOTION.

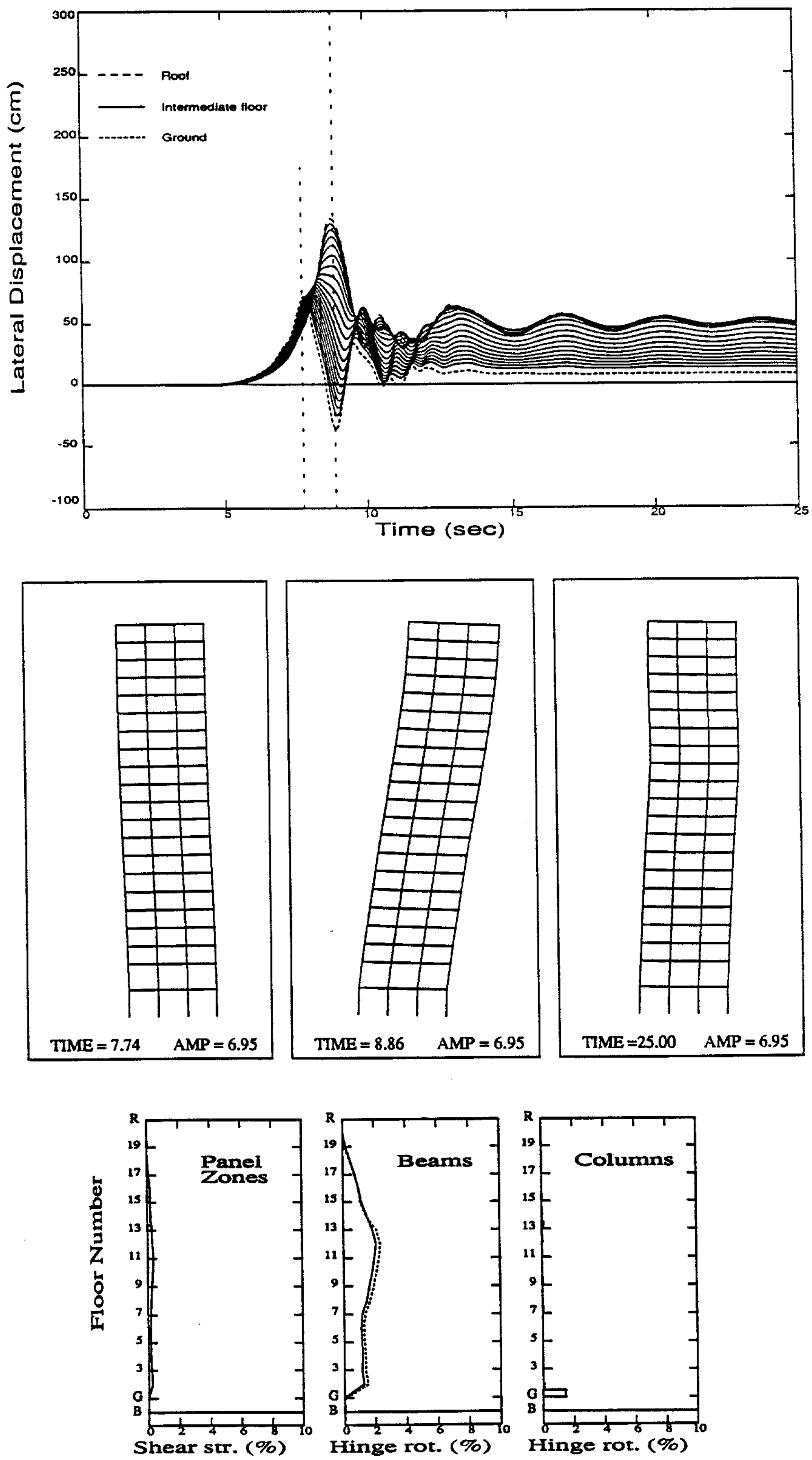

Parameter Study of the Response of Moment-Resisting Steel Frame Buildings to Near-Source Ground Motions

FIGURE 1.26: RESULTS FOR THE 20-STORY BUILDING, CASE P, EP14/H GROUND MOTION.

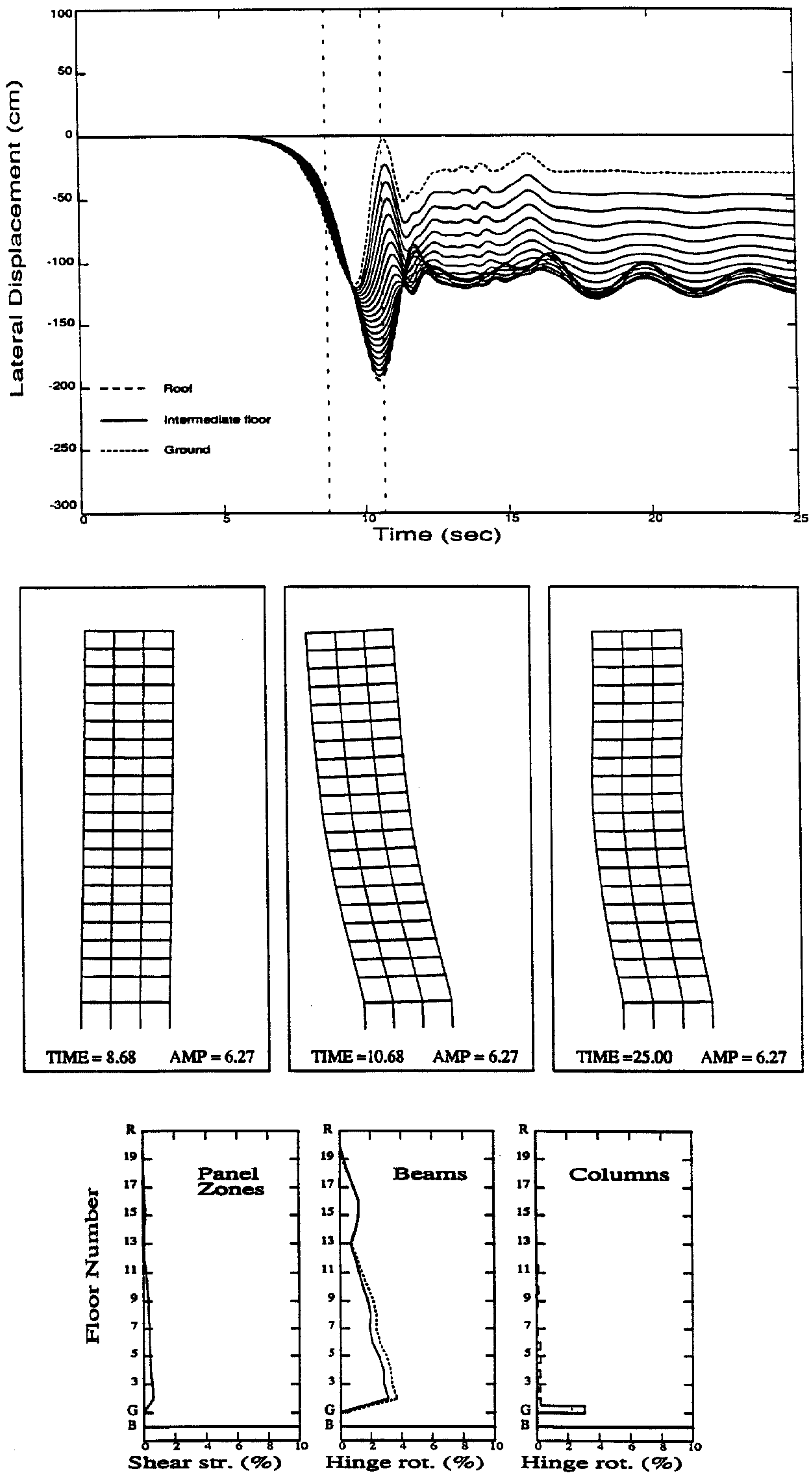

Parameter Study of the Response of Moment-Resisting Steel Frame Buildings to Near-Source Ground Motions

FIGURE 1.27: RESULTS FOR THE 20-STORY BUILDING, CASE P, C05/H GROUND MOTION.

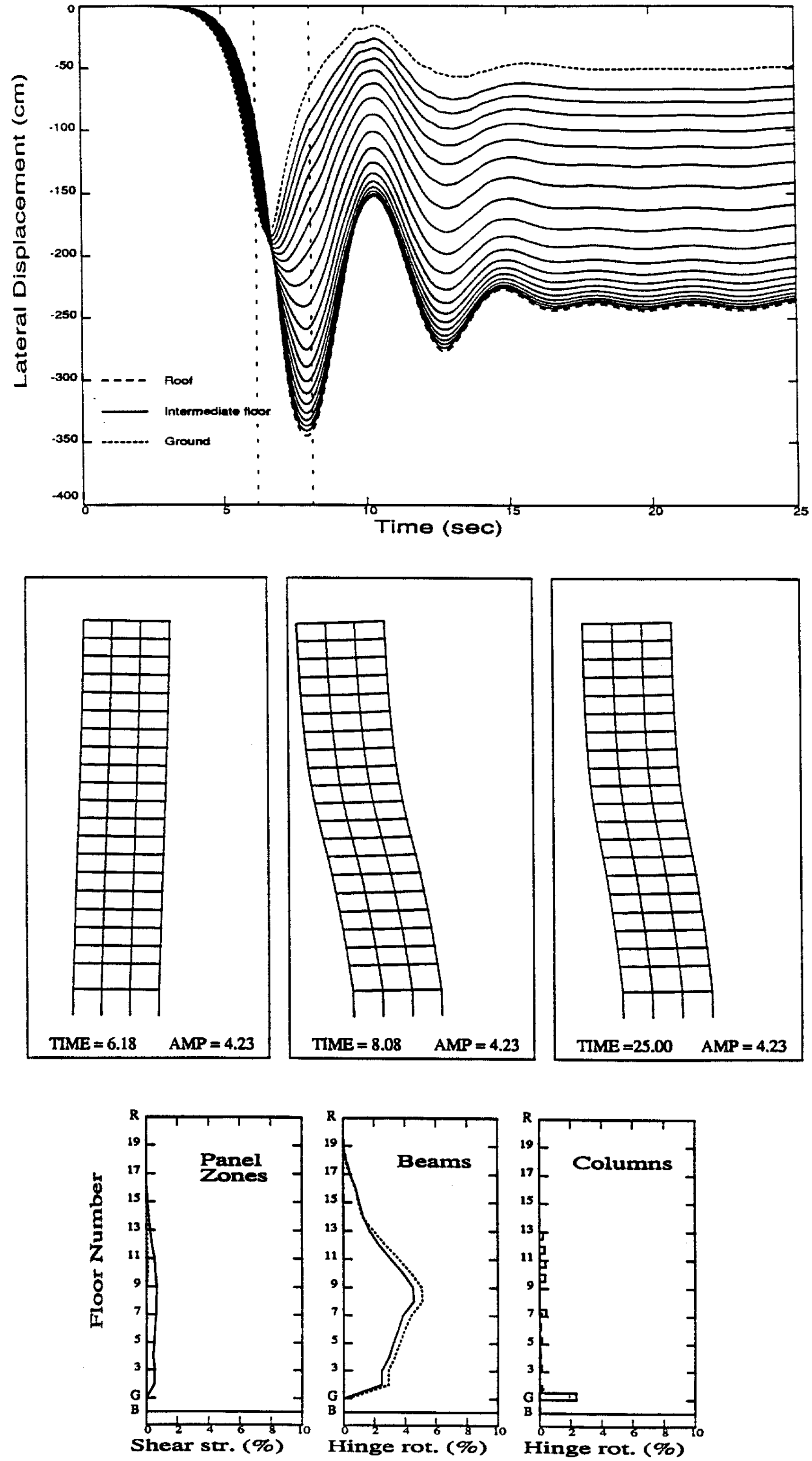

FIGURE 1.28: RESULTS FOR THE 6-STORY BUILDING, CASE PS, SYLM/H GROUND MOTION.

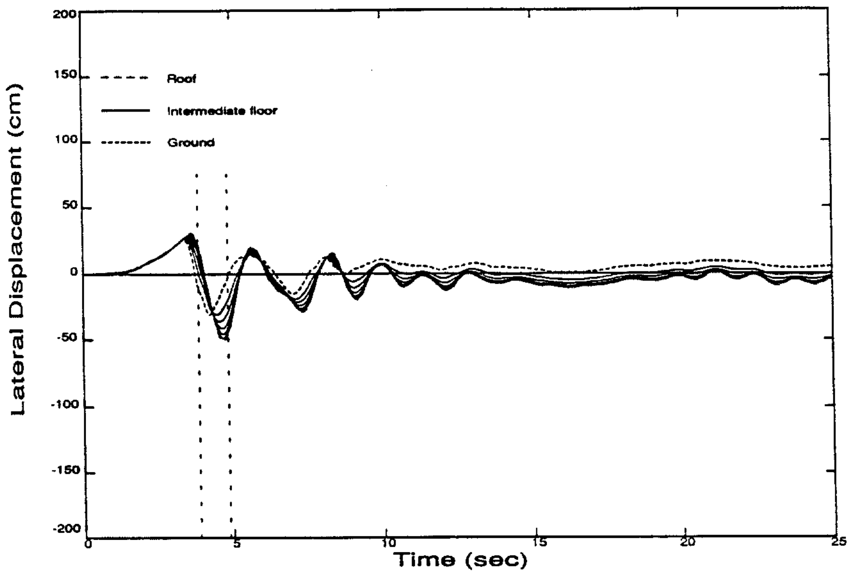

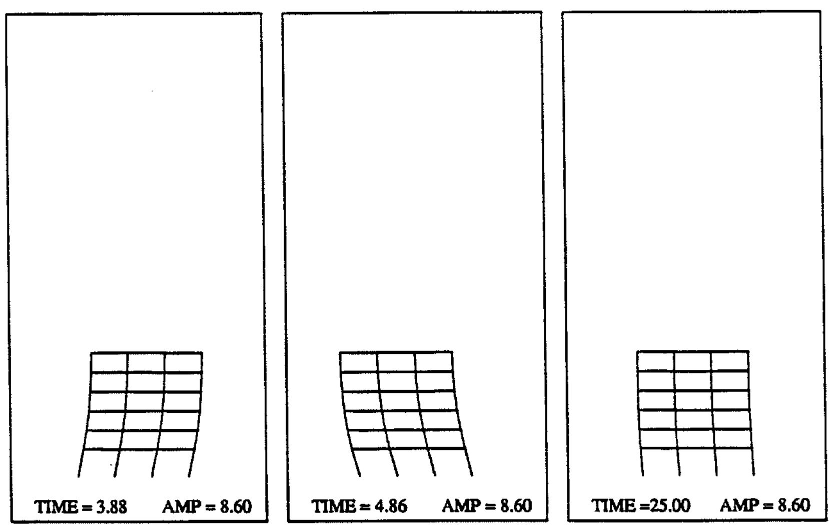

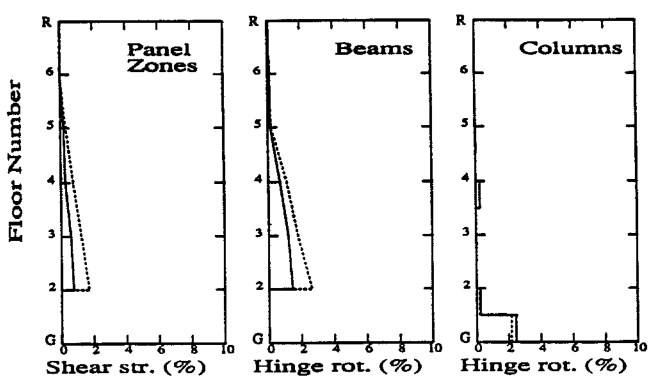

Parameter Study of the Response of Moment-Resisting Steel Frame Buildings to Near-Source Ground Motions

FIGURE 1.29: RESULTS FOR THE 6-STORY BUILDING, CASE PS, NR11/H GROUND MOTION.

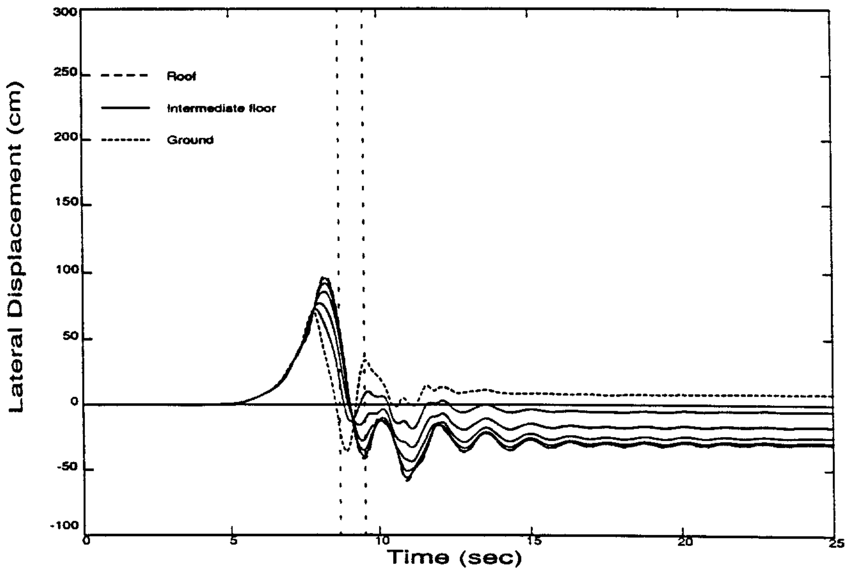

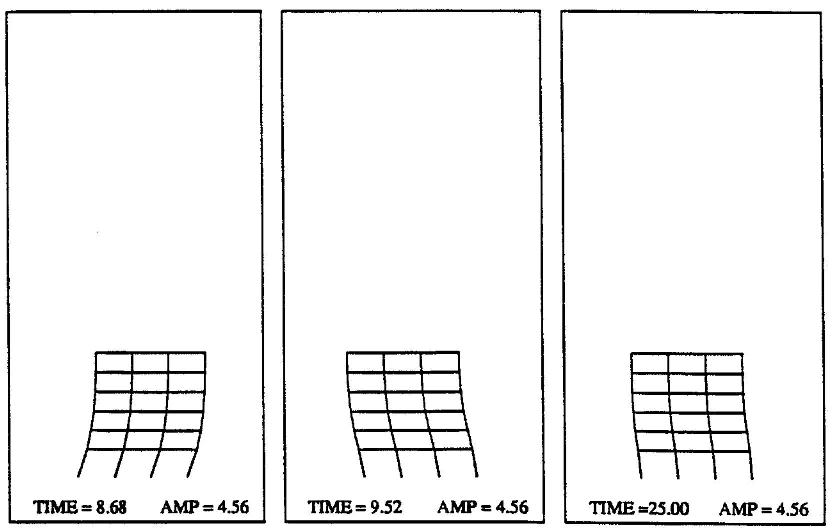

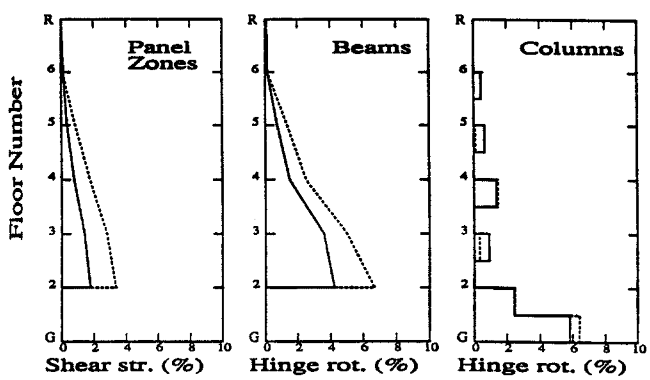

FIGURE 1.30: RESULTS FOR THE 6-STORY BUILDING, CASE PS, EP17/H GROUND MOTION.

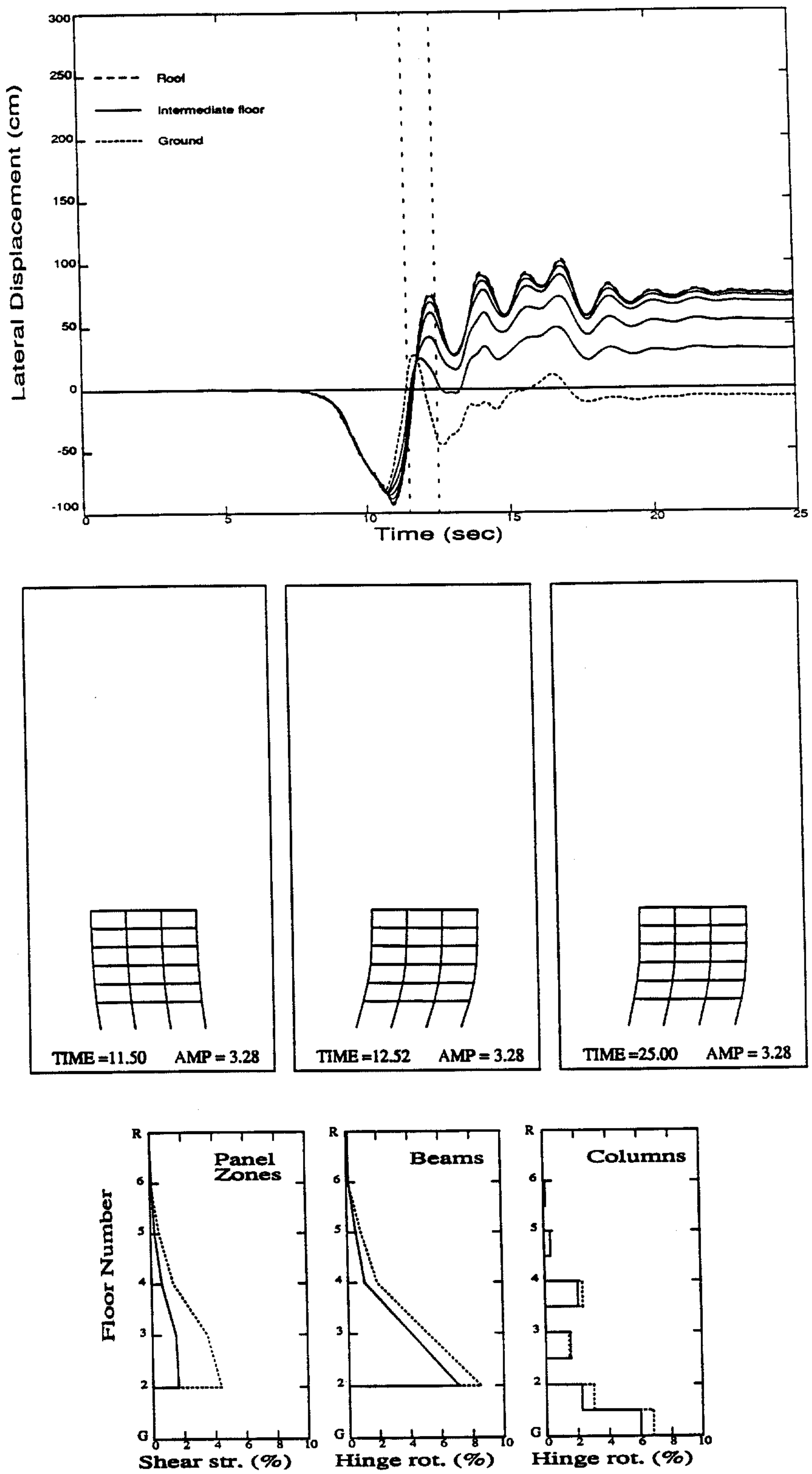

FIGURE 1.31: RESULTS FOR THE 6-STORY BUILDING, CASE PS, C05/H GROUND MOTION.

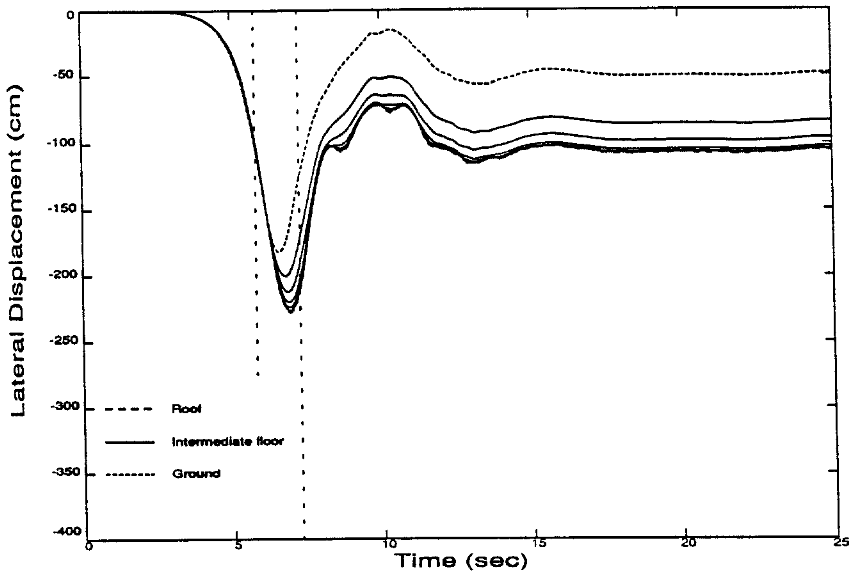

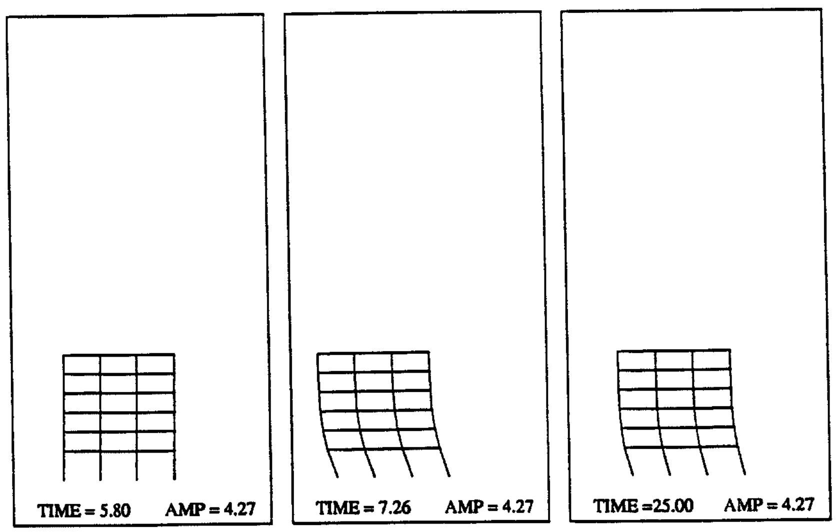

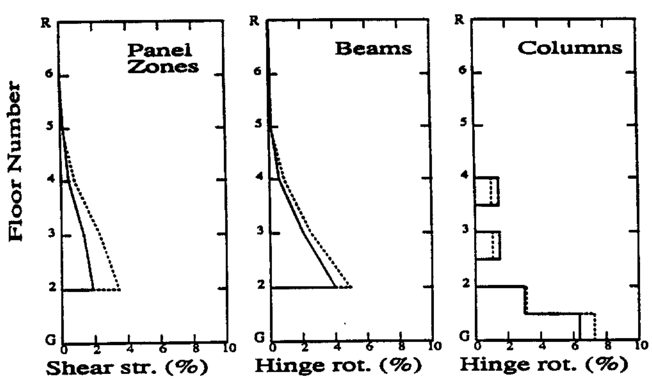

Parameter Study of the Response of Moment-Resisting Steel Frame Buildings to Near-Source Ground Motions

FIGURE 1.32: RESULTS FOR THE 20-STORY BUILDING, CASE PS, SYLM/H GROUND MOTION.

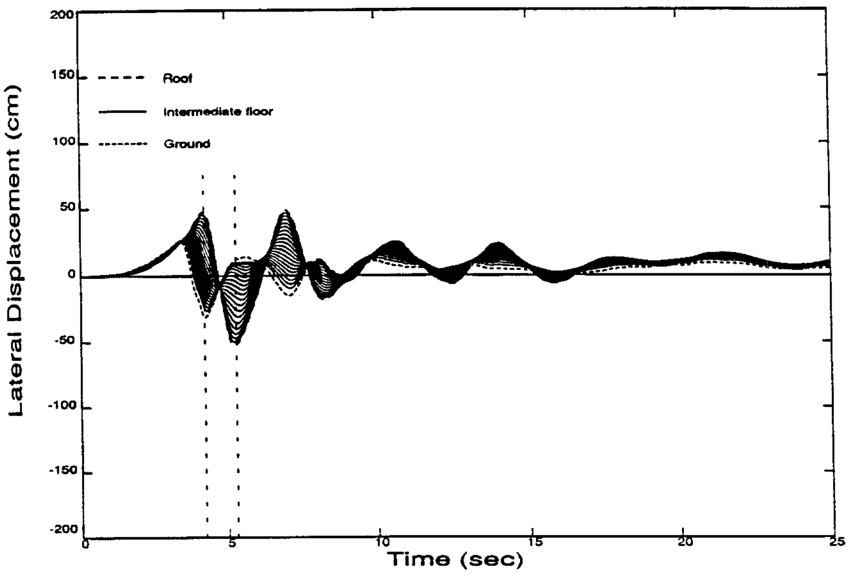

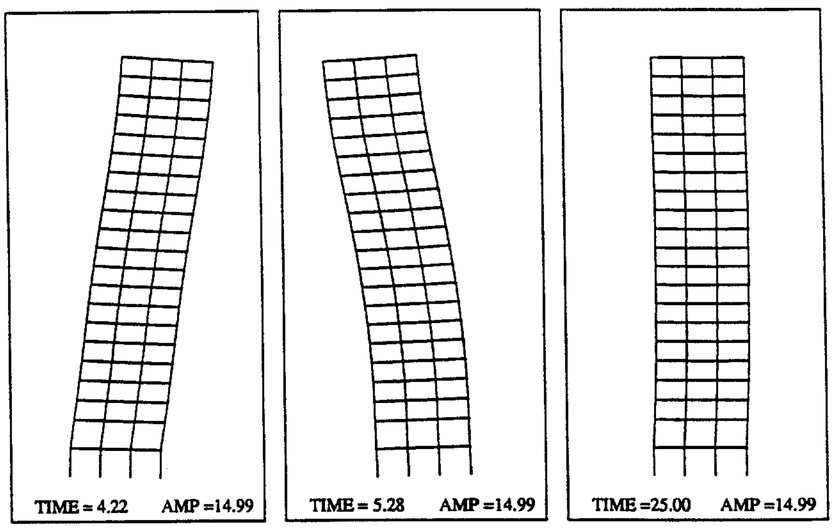

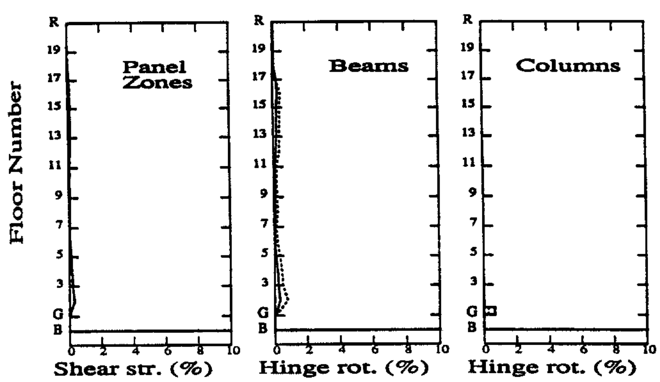

FIGURE 1.33: RESULTS FOR THE 20-STORY BUILDING, CASE PS, NR11/H GROUND MOTION.

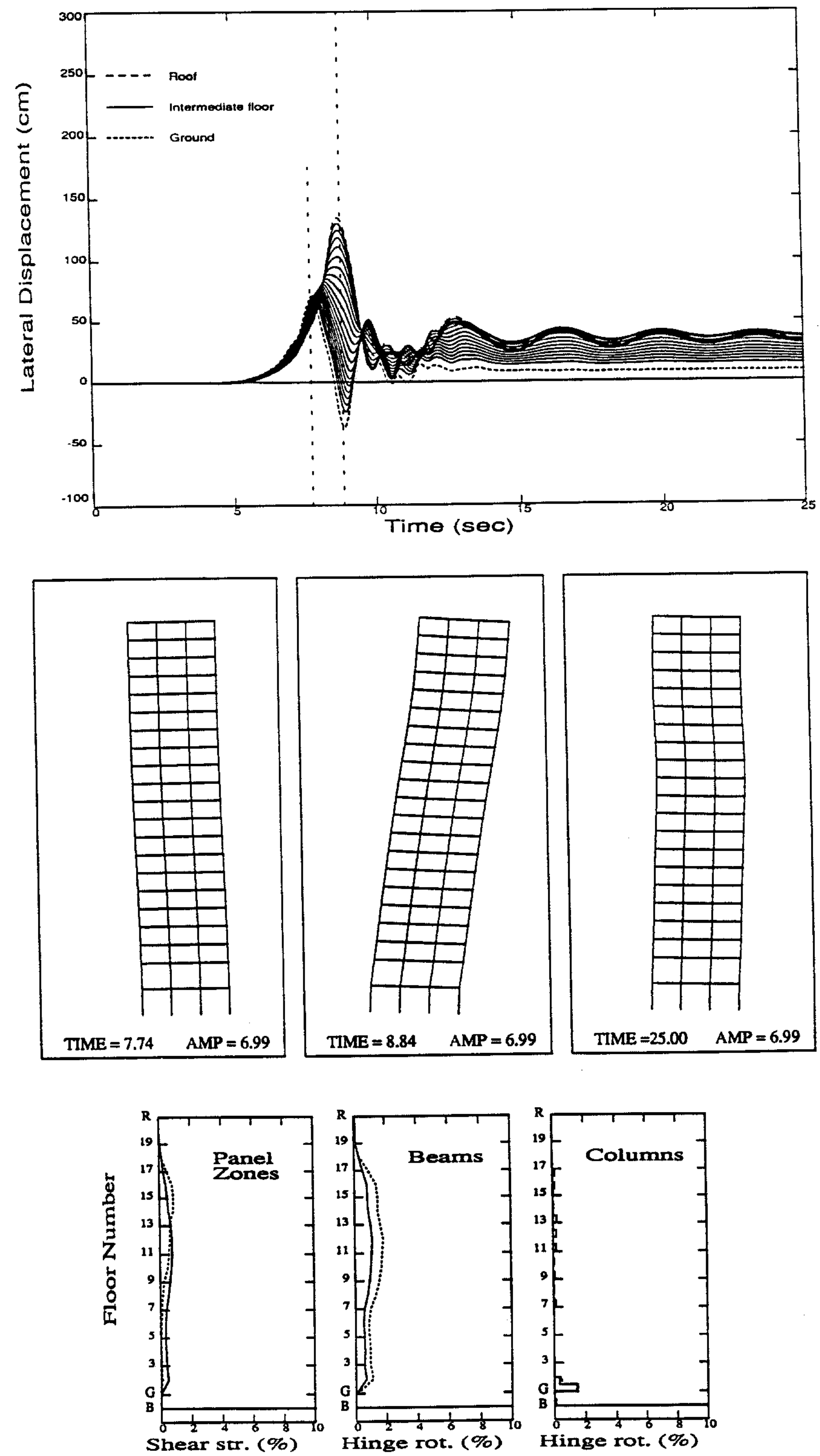

FIGURE 1.34: RESULTS FOR THE 20-STORY BUILDING, CASE PS, EP14/H GROUND MOTION.

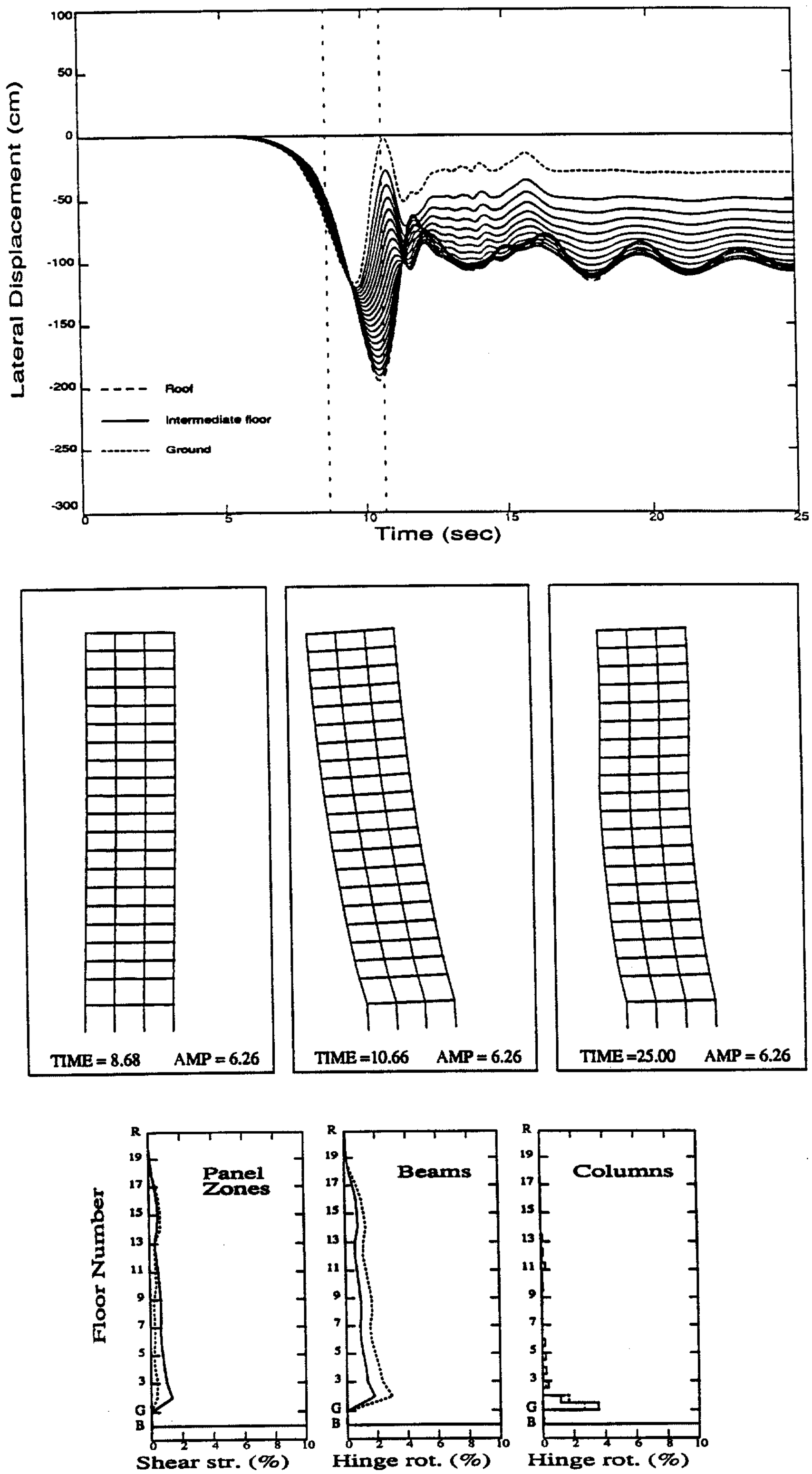

FIGURE 1.35: RESULTS FOR THE 20-STORY BUILDING,
CASE PS, C05/H GROUND MOTION.

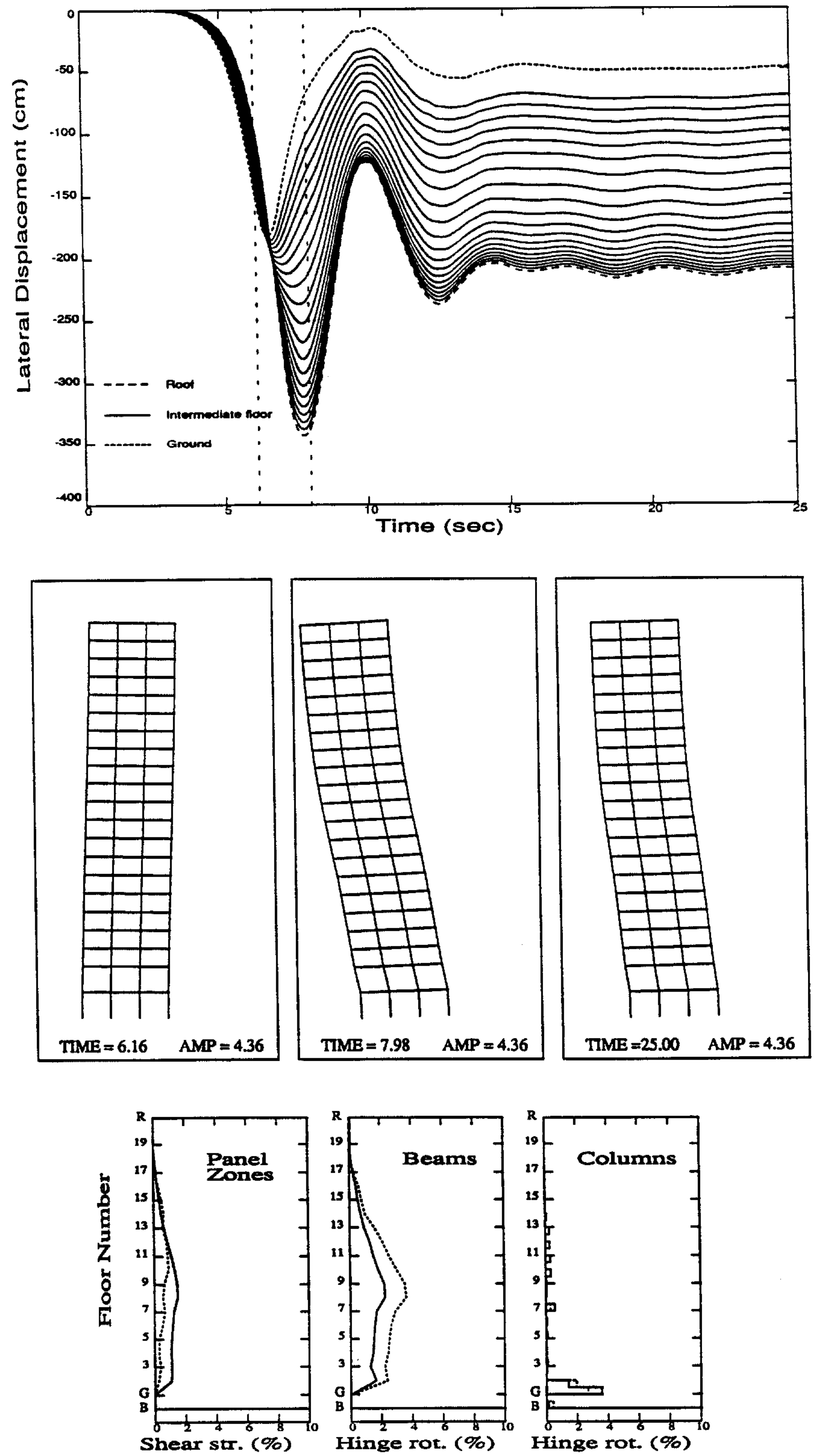

FIGURE 1.36: RESULTS FOR THE 6-STORY BUILDING, CASE B, SYLM/H GROUND MOTION.

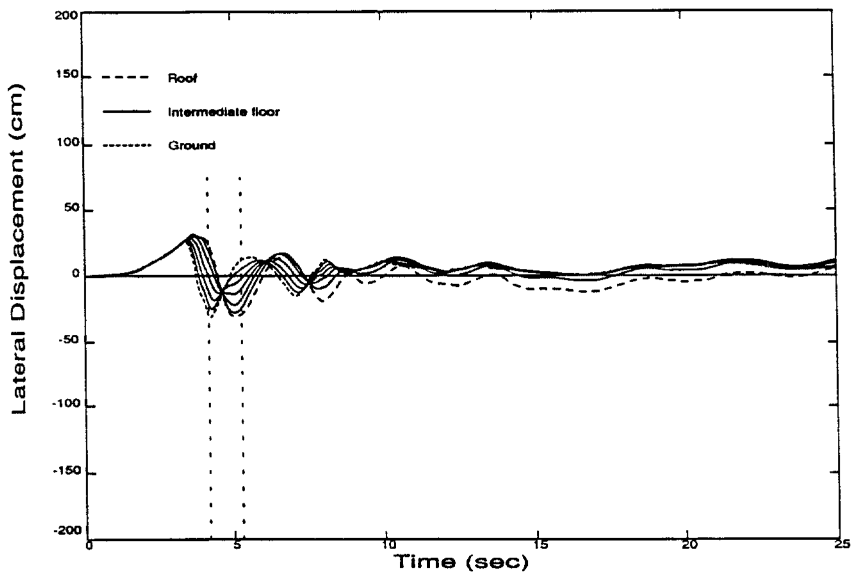

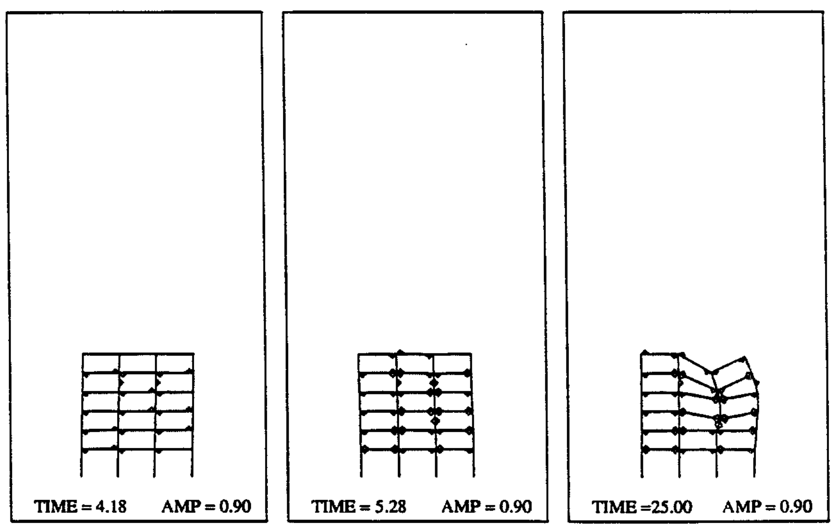

Parameter Study of the Response of Moment-Resisting Steel Frame Buildings to Near-Source Ground Motions

FIGURE 1.37: RESULTS FOR THE 6-STORY BUILDING,
CASE B, NR11/H GROUND MOTION.

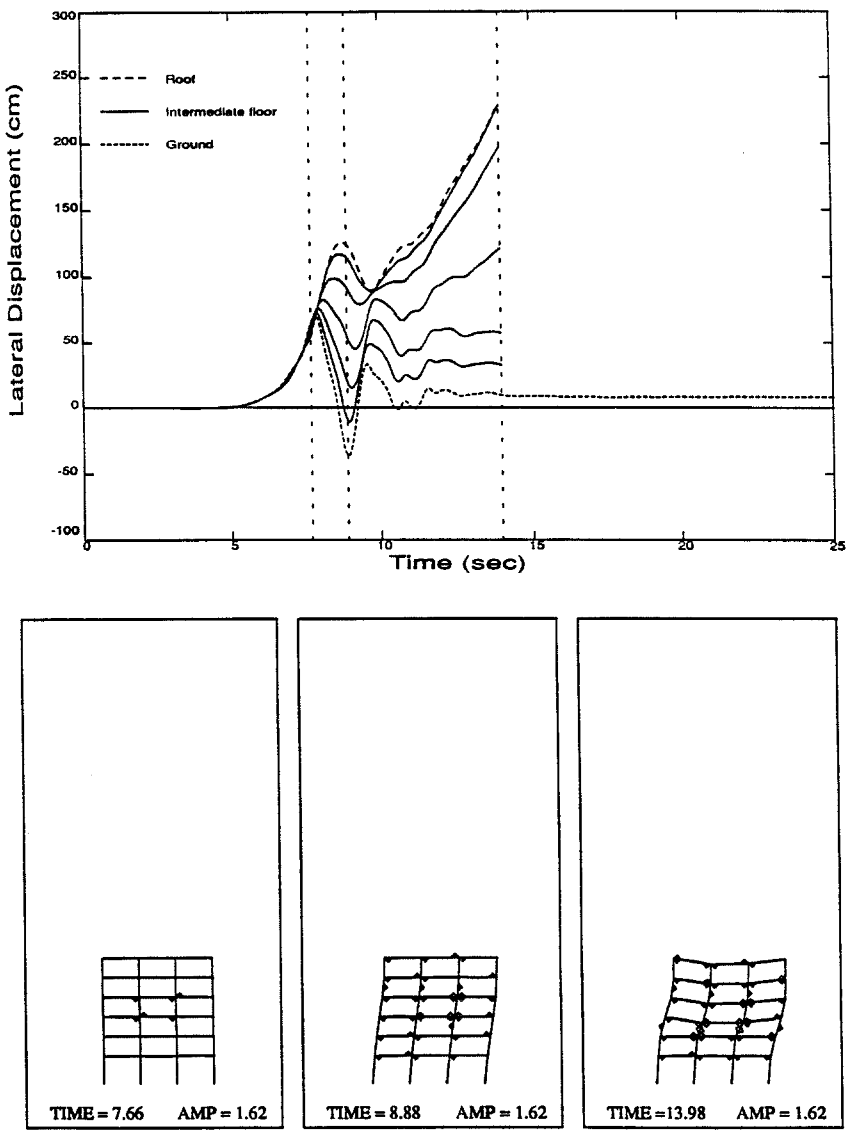

FIGURE 1.38: RESULTS FOR THE 6-STORY BUILDING, CASE B, EP17/H GROUND MOTION.

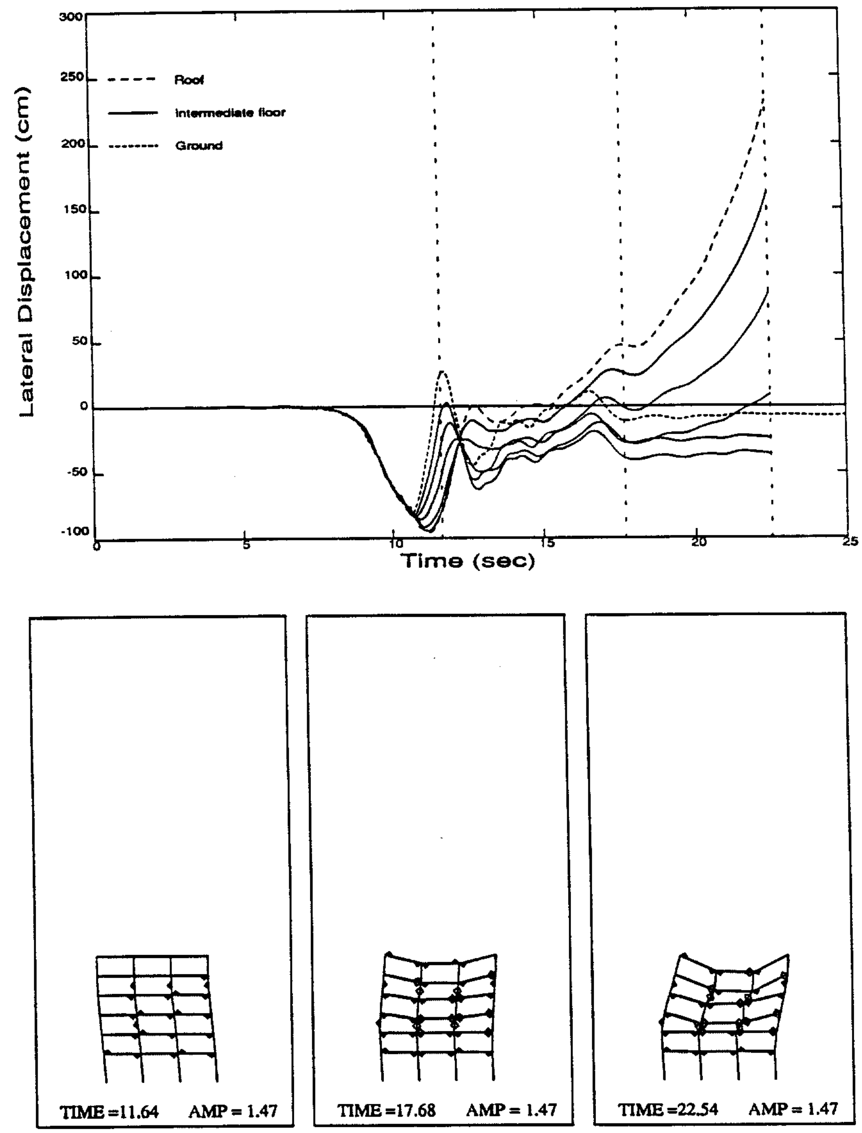

FIGURE 1.39: RESULTS FOR THE 6-STORY BUILDING, CASE B, C05/H GROUND MOTION.

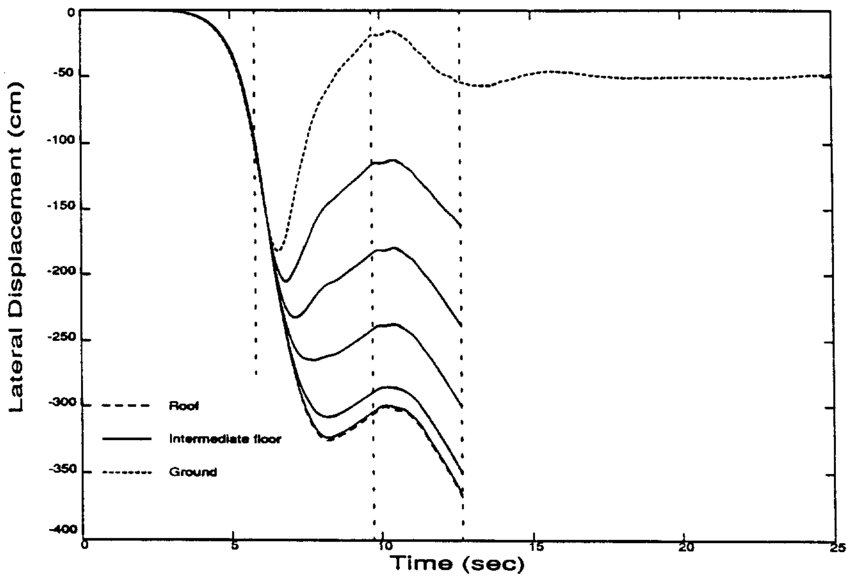

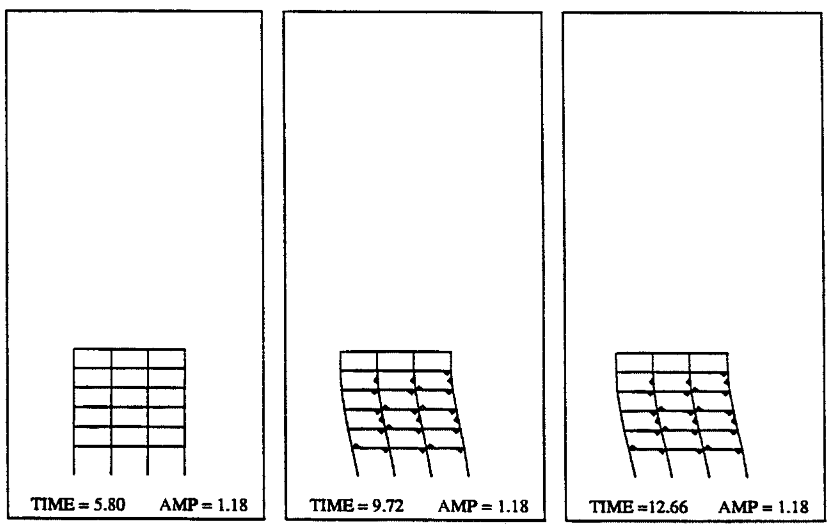

FIGURE 1.40: RESULTS FOR THE 20-STORY BUILDING, CASE B, SYLM/H GROUND MOTION.

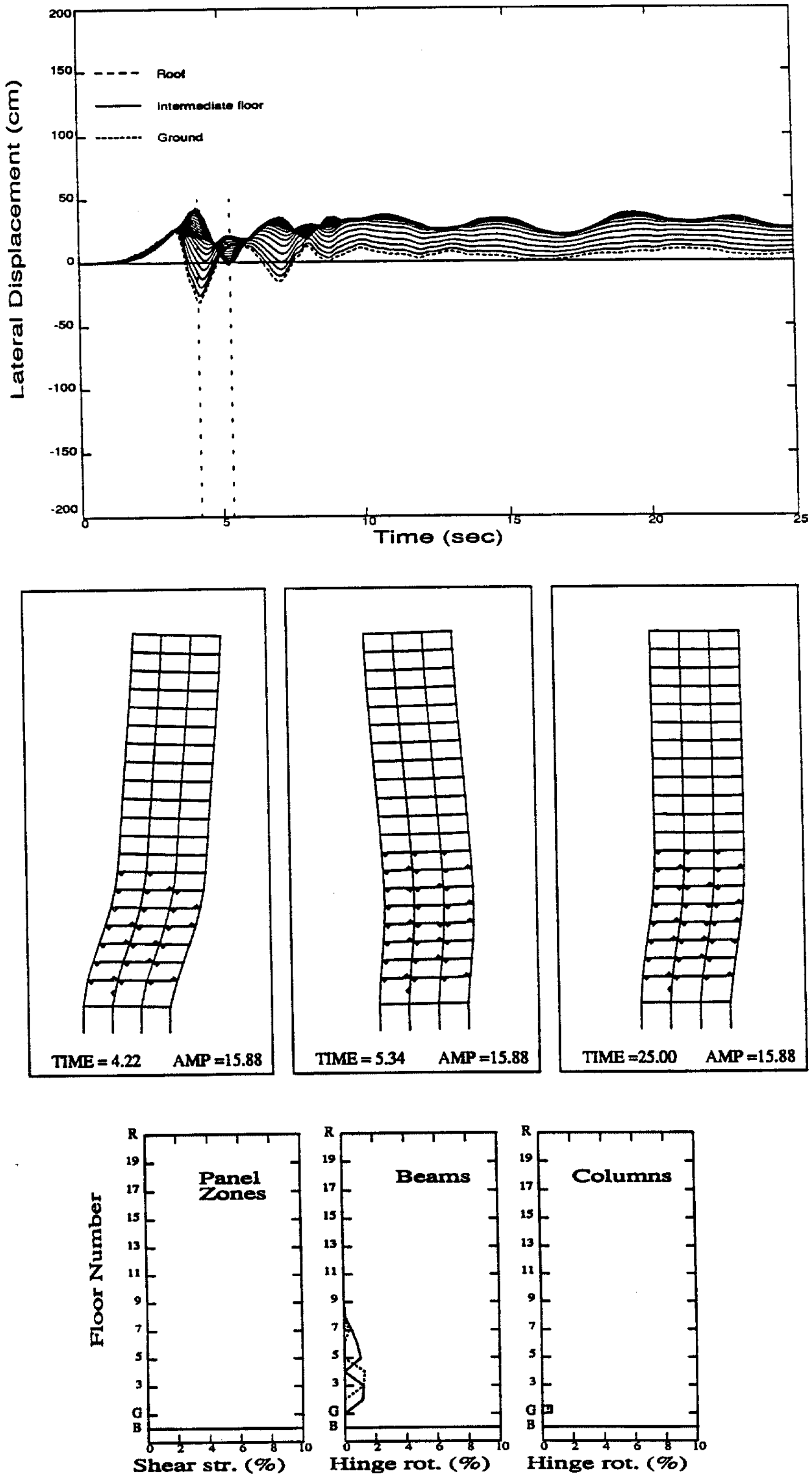

Parameter Study of the Response of Moment-Resisting Steel Frame Buildings to Near-Source Ground Motions

FIGURE 1.41: RESULTS FOR THE 20-STORY BUILDING, CASE B, NR11/H GROUND MOTION.

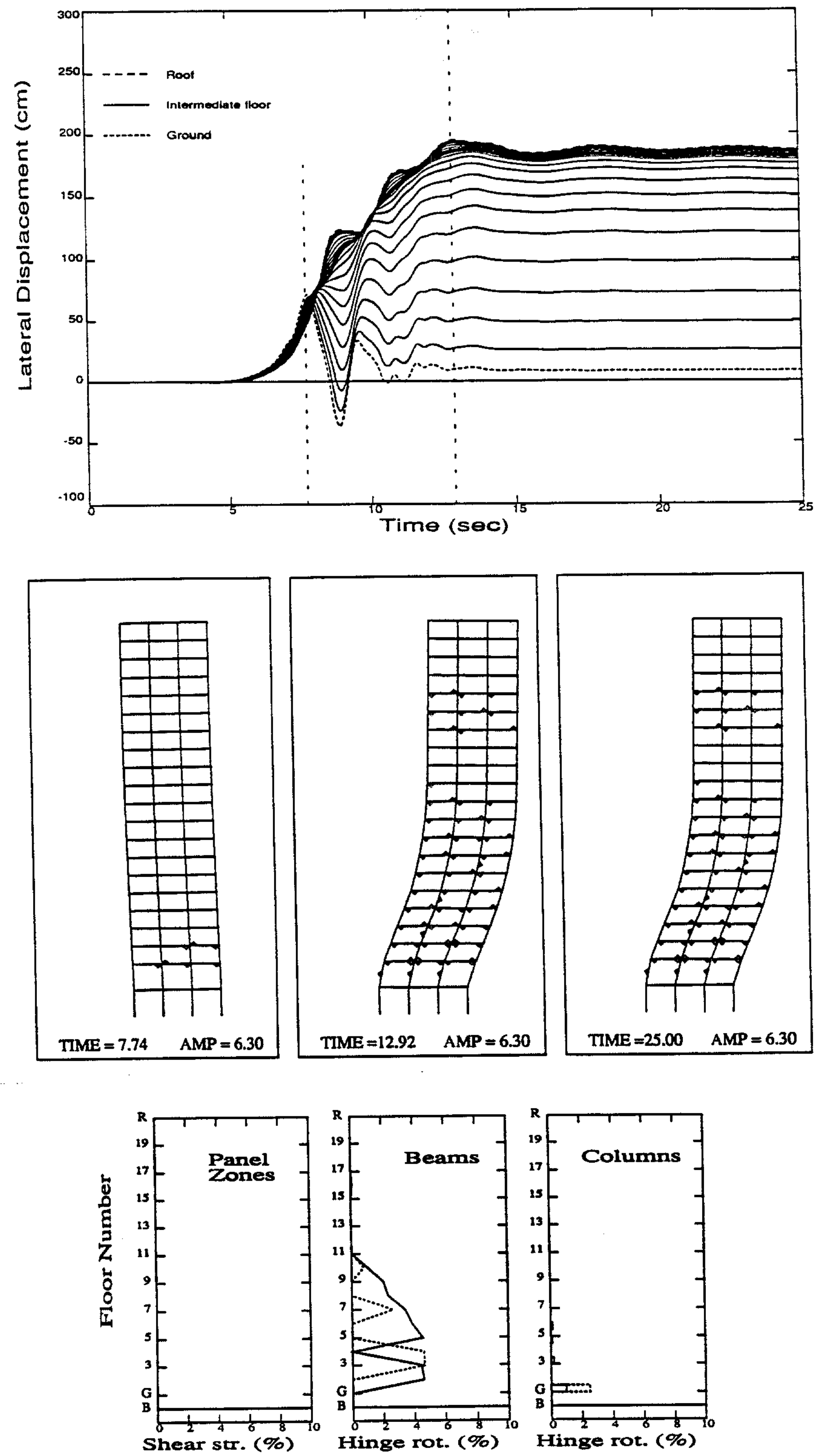

FIGURE 1.42: RESULTS FOR THE 20-STORY BUILDING, CASE B, EP14/H GROUND MOTION.

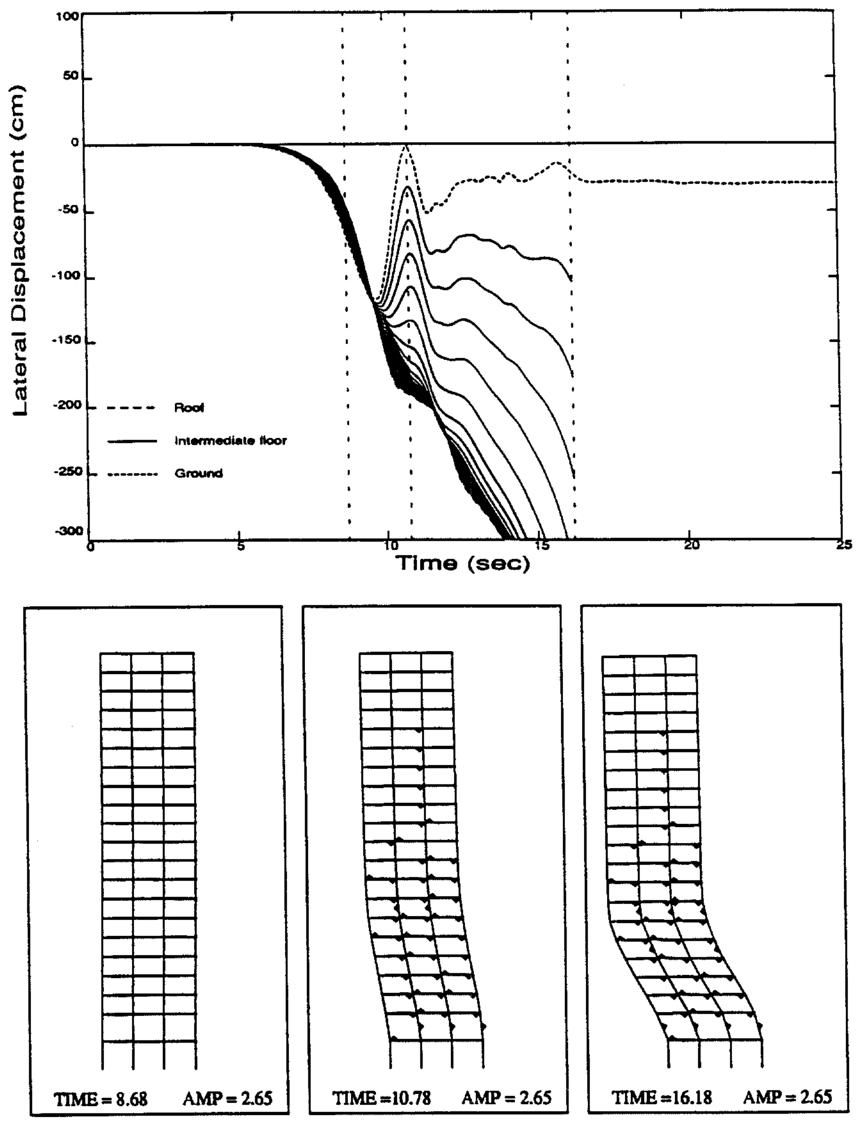

FIGURE 1.43: RESULTS FOR THE 20-STORY BUILDING,
CASE B, C05/H GROUND MOTION.

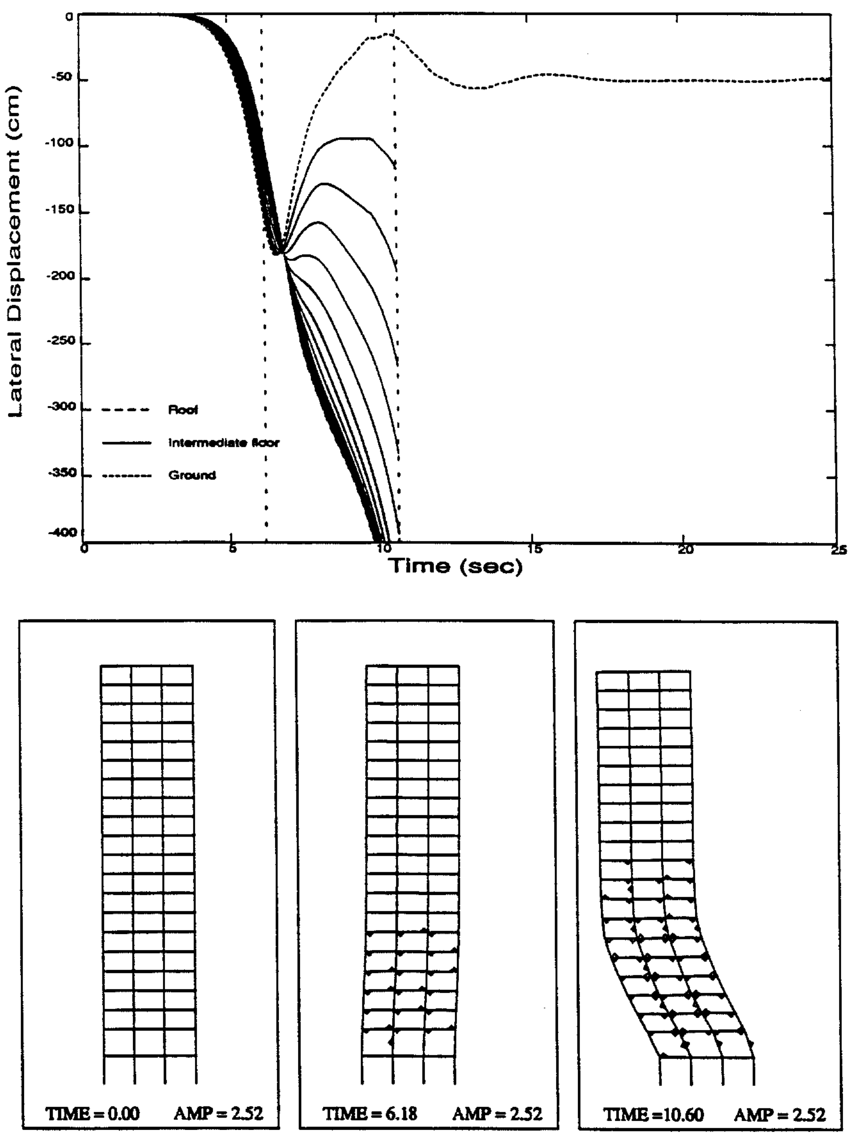

FIGURE 1.44: RESULTS FOR THE 6-STORY BUILDING, CASE I, SYLM/H GROUND MOTION.

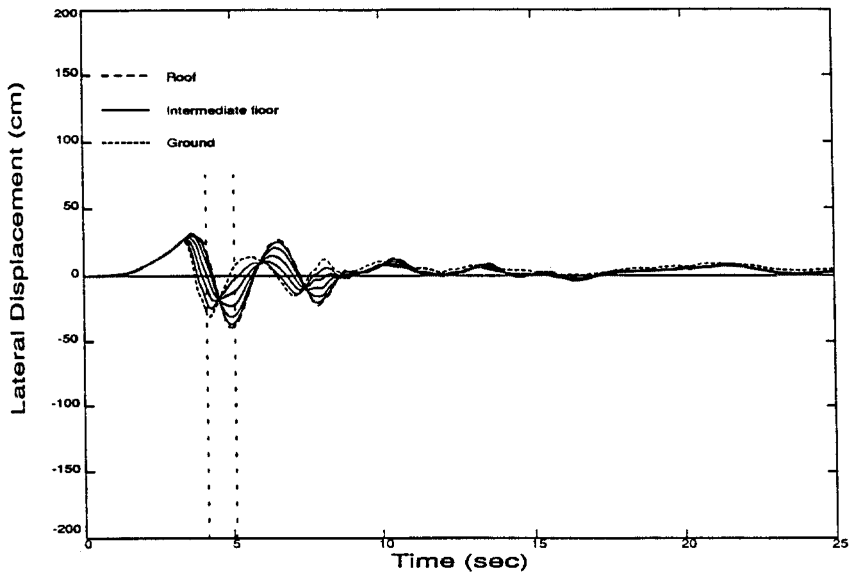

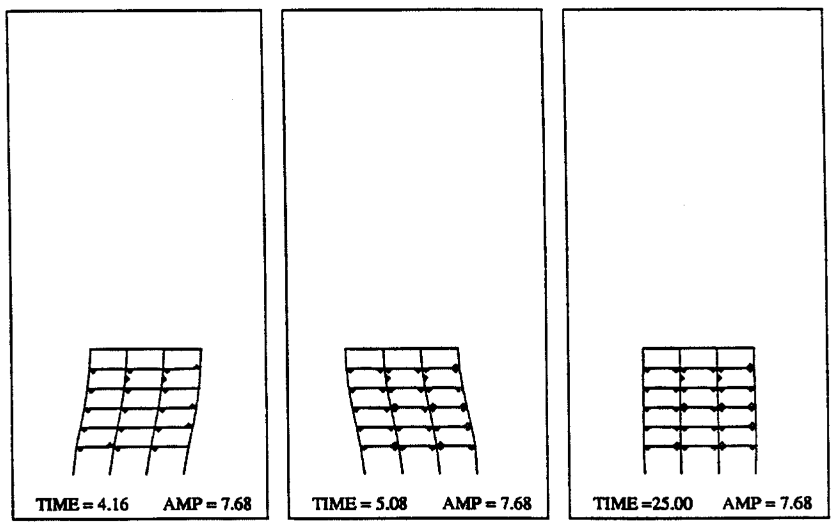

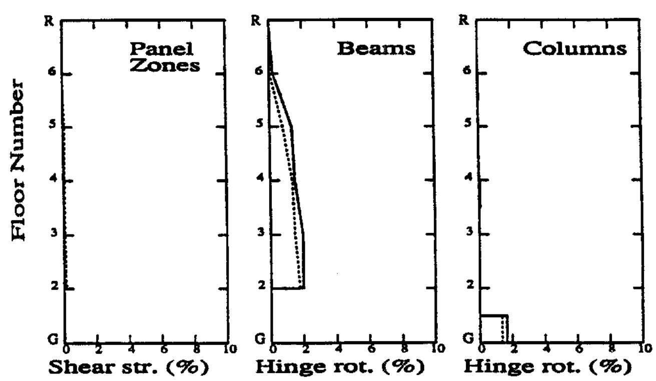

FIGURE 1.45: RESULTS FOR THE 6-STORY BUILDING,
CASE I, NR11/H GROUND MOTION.

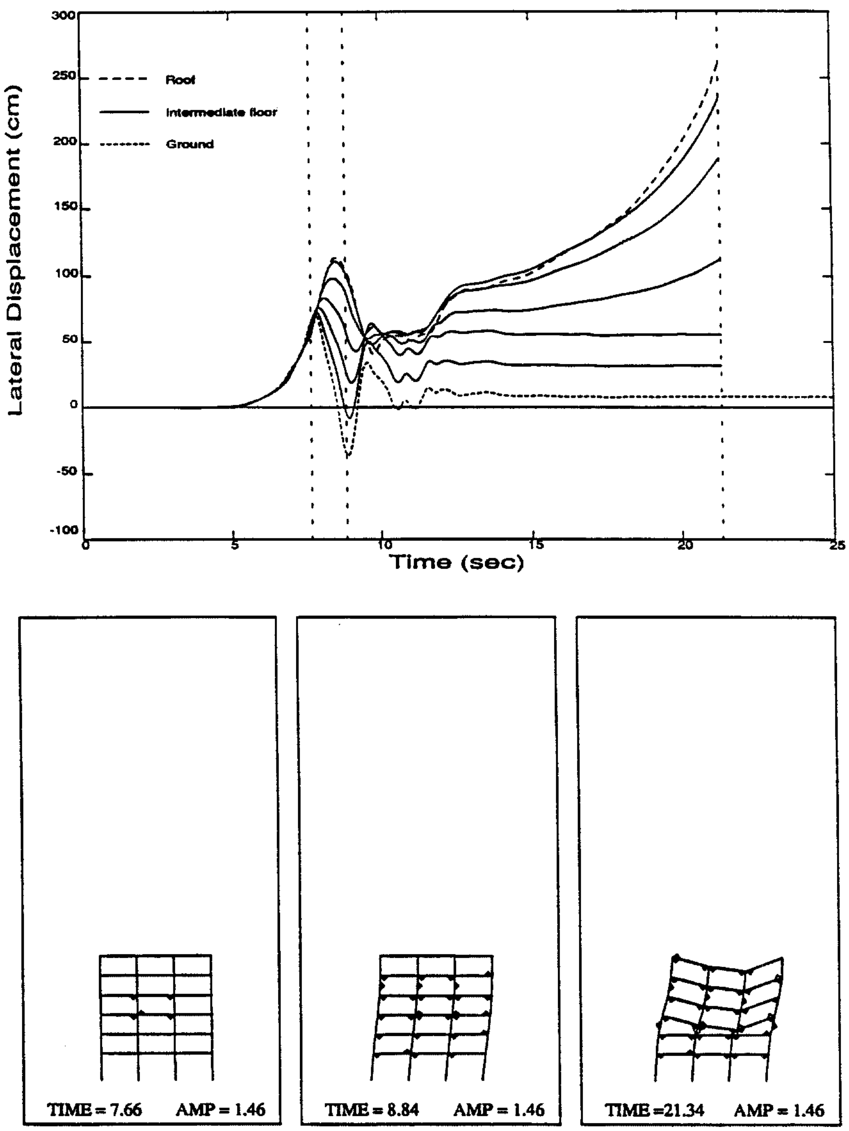

Parameter Study of the Response of Moment-Resisting Steel Frame Buildings to Near-Source Ground Motions

FIGURE 1.46: RESULTS FOR THE 6-STORY BUILDING,
CASE I, EP17/H GROUND MOTION.

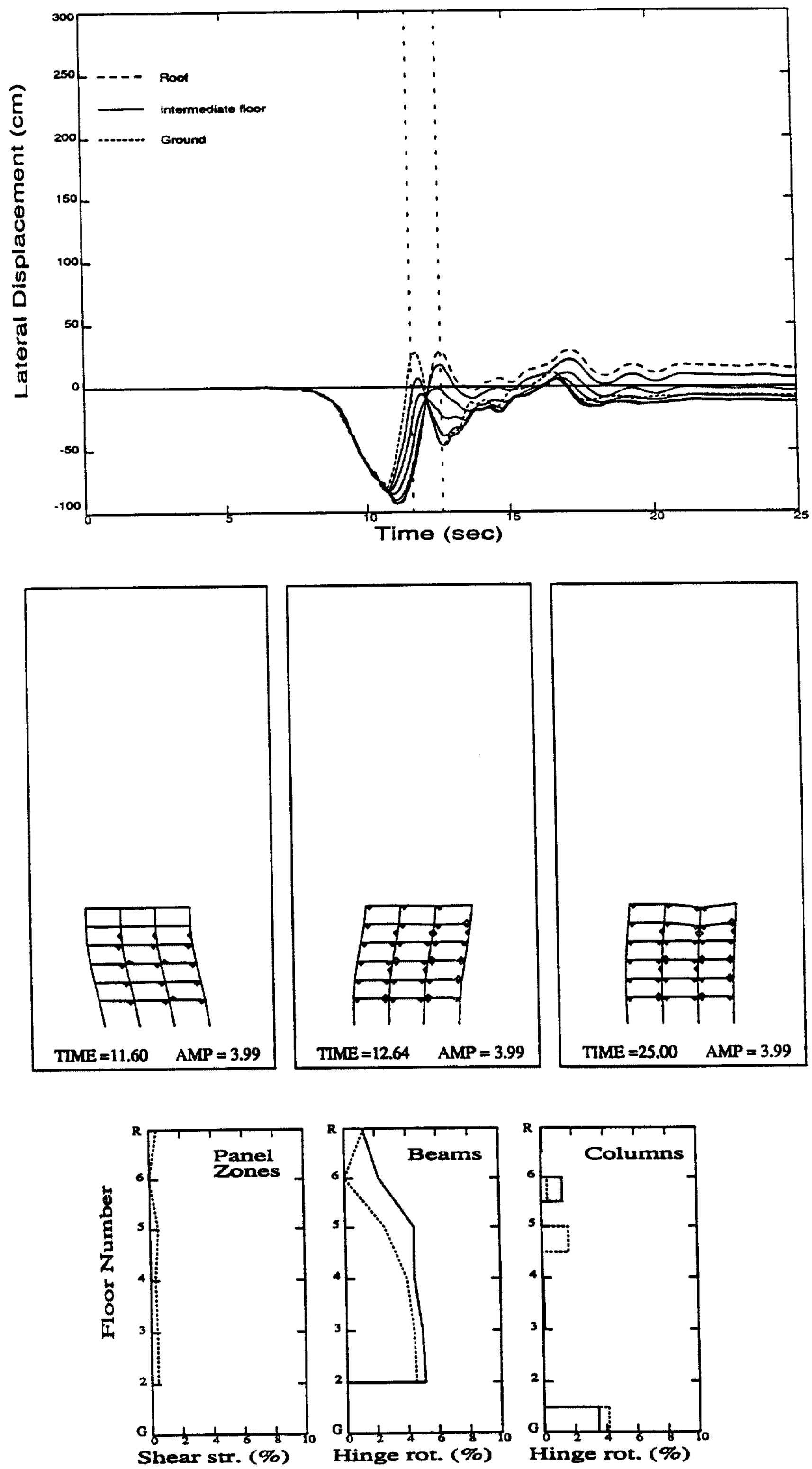

FIGURE 1.47: RESULTS FOR THE 6-STORY BUILDING, CASE I, C05/H GROUND MOTION.

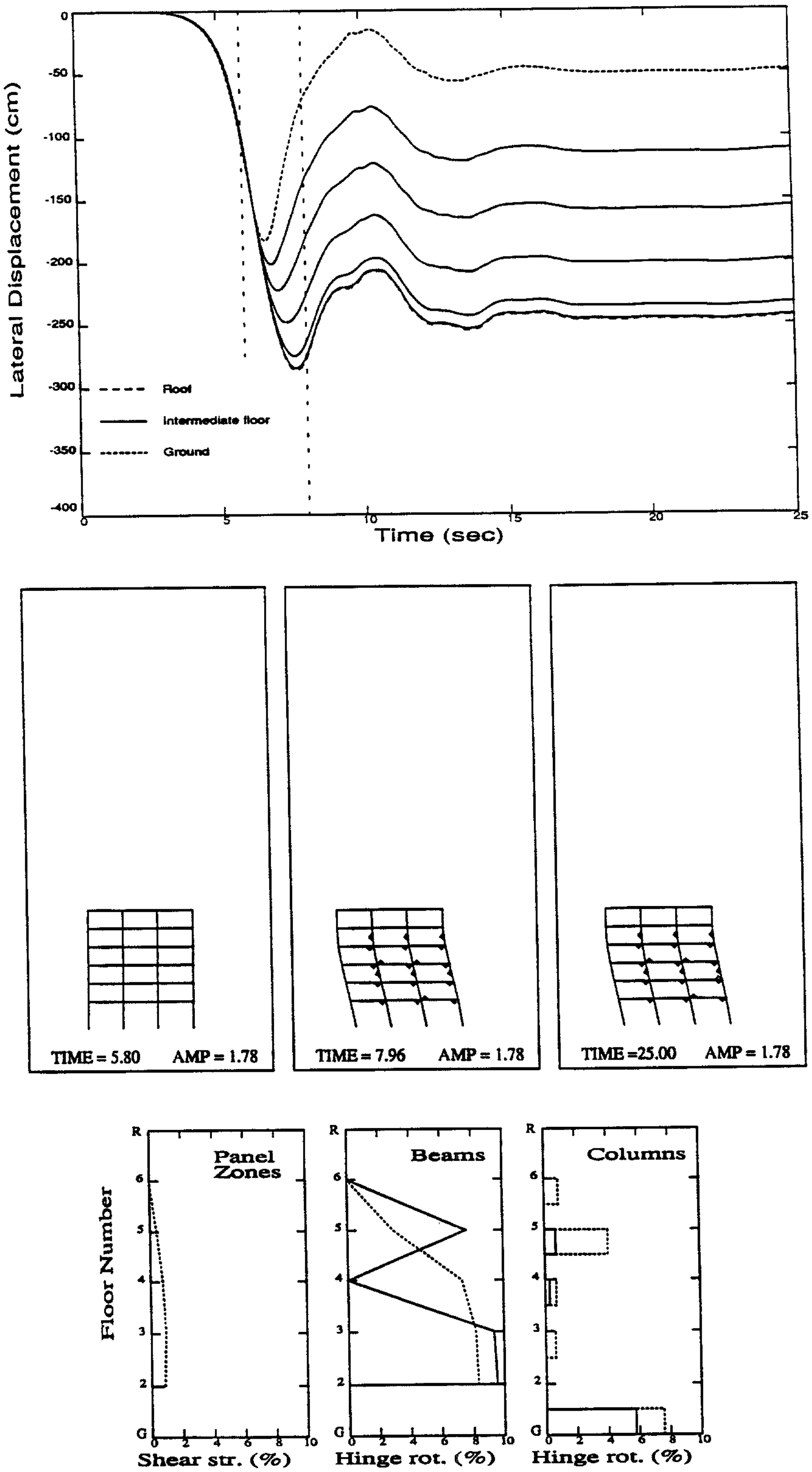

Parameter Study of the Response of Moment-Resisting Steel Frame Buildings to Near-Source Ground Motions

FIGURE 1.48: RESULTS FOR THE 20-STORY BUILDING, CASE I, SYLM/H GROUND MOTION.

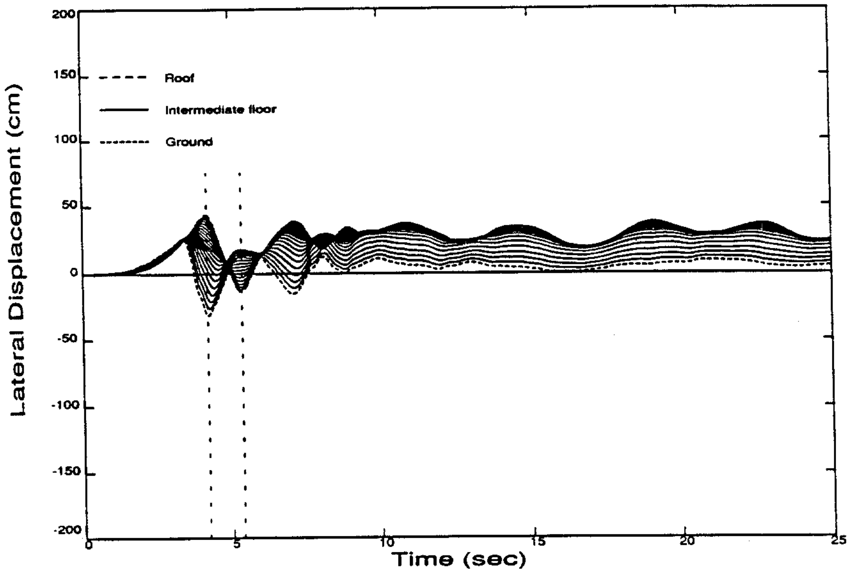

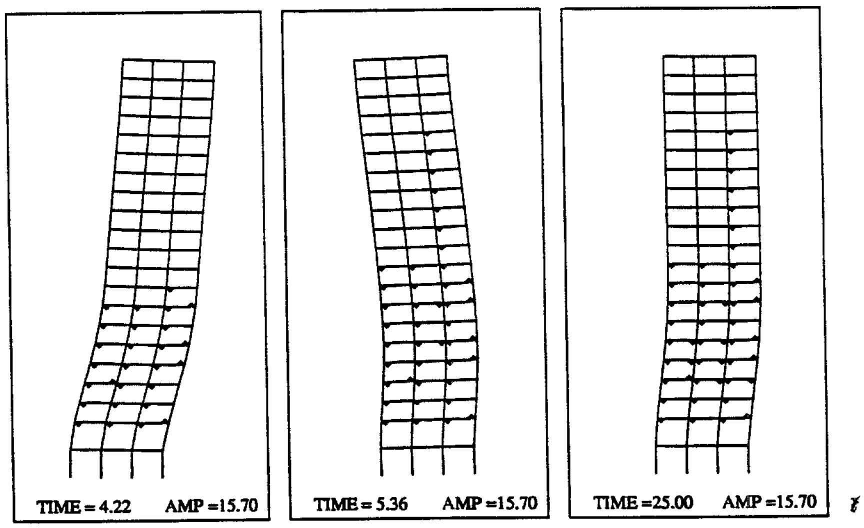

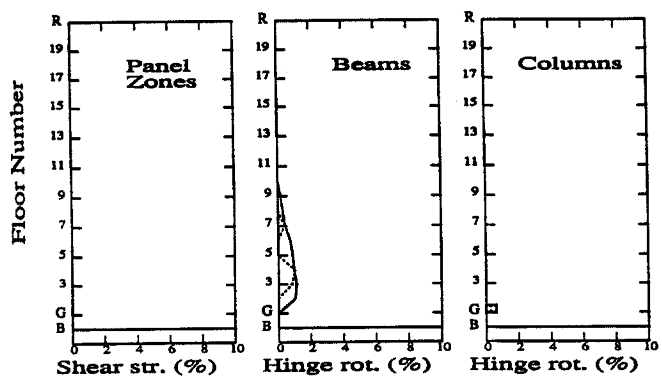

FIGURE 1.49: RESULTS FOR THE 20-STORY BUILDING,
CASE I, NR11/H GROUND MOTION.

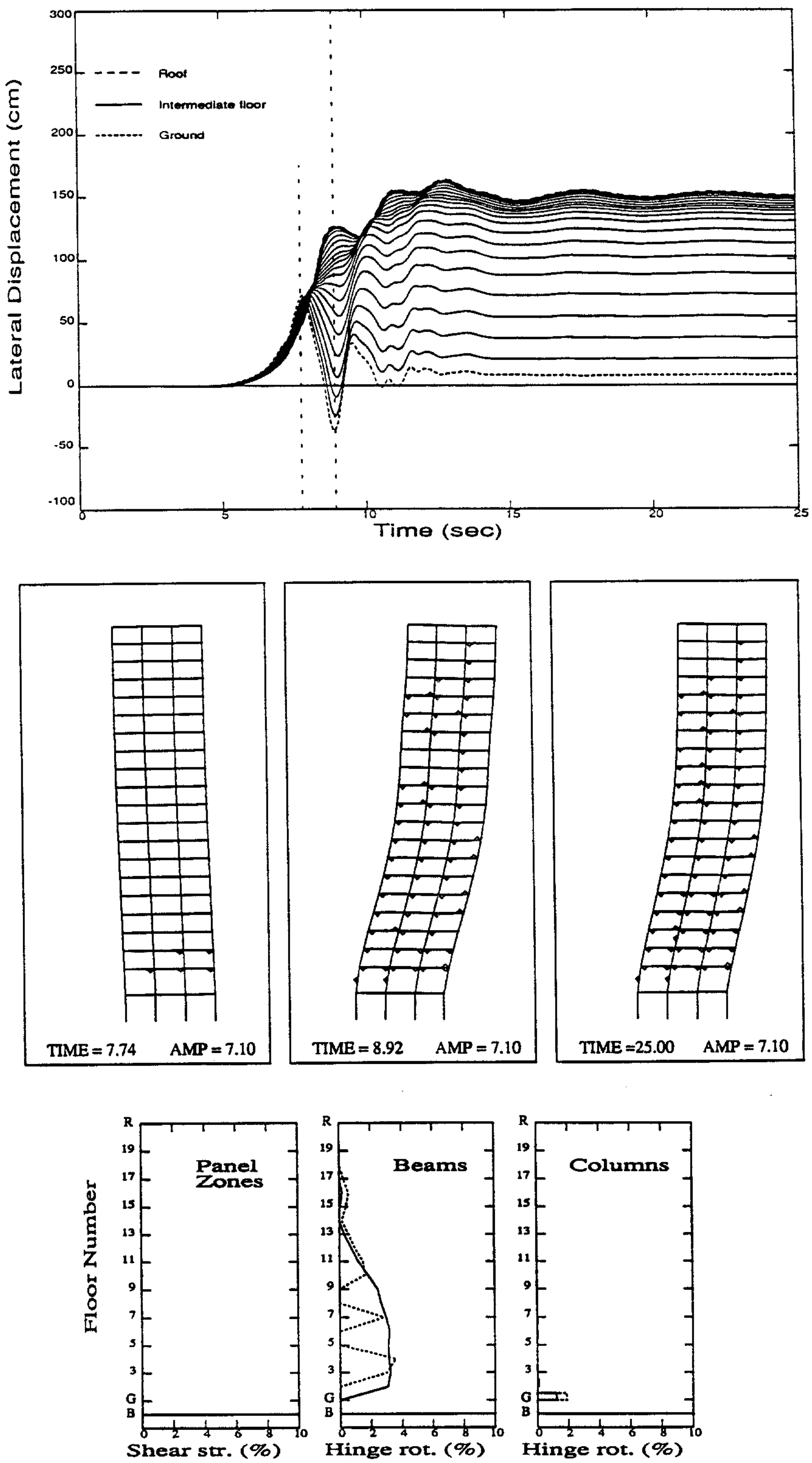

Parameter Study of the Response of Moment-Resisting Steel Frame Buildings to Near-Source Ground Motions

FIGURE 1.50: RESULTS FOR THE 20-STORY BUILDING, CASE I, EP14/H GROUND MOTION.

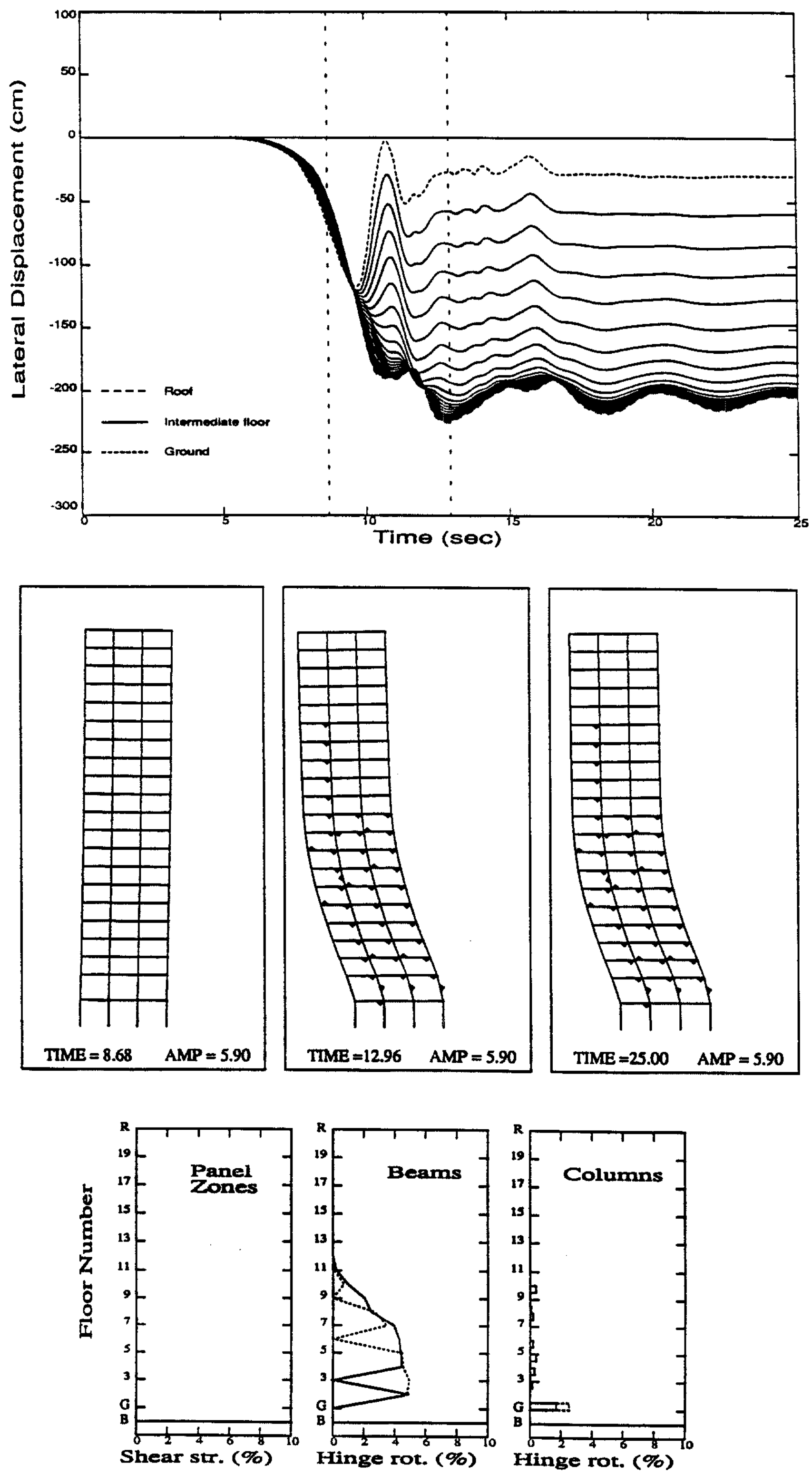

FIGURE 1.51: RESULTS FOR THE 20-STORY BUILDING, CASE I, C05/H GROUND MOTION.

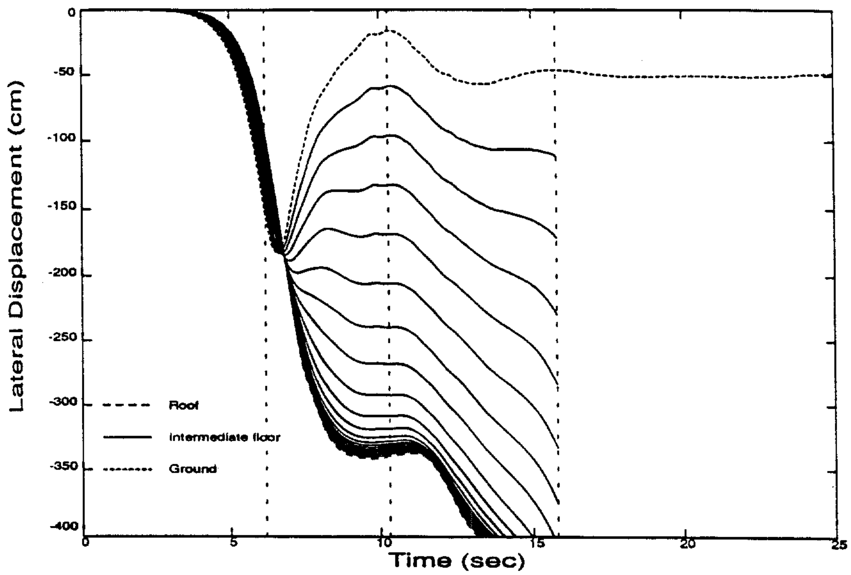

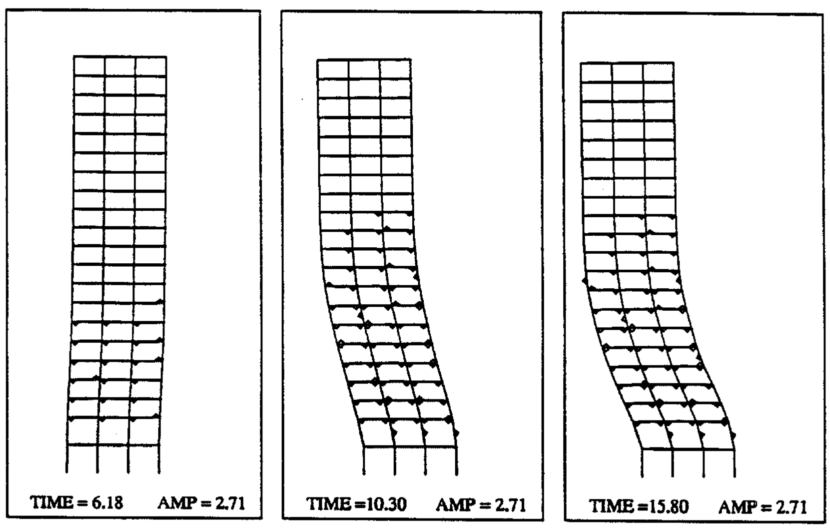

FIGURE 1.52: RESULTS FOR THE 6-STORY BUILDING, CASE BS, SYLM/H GROUND MOTION.

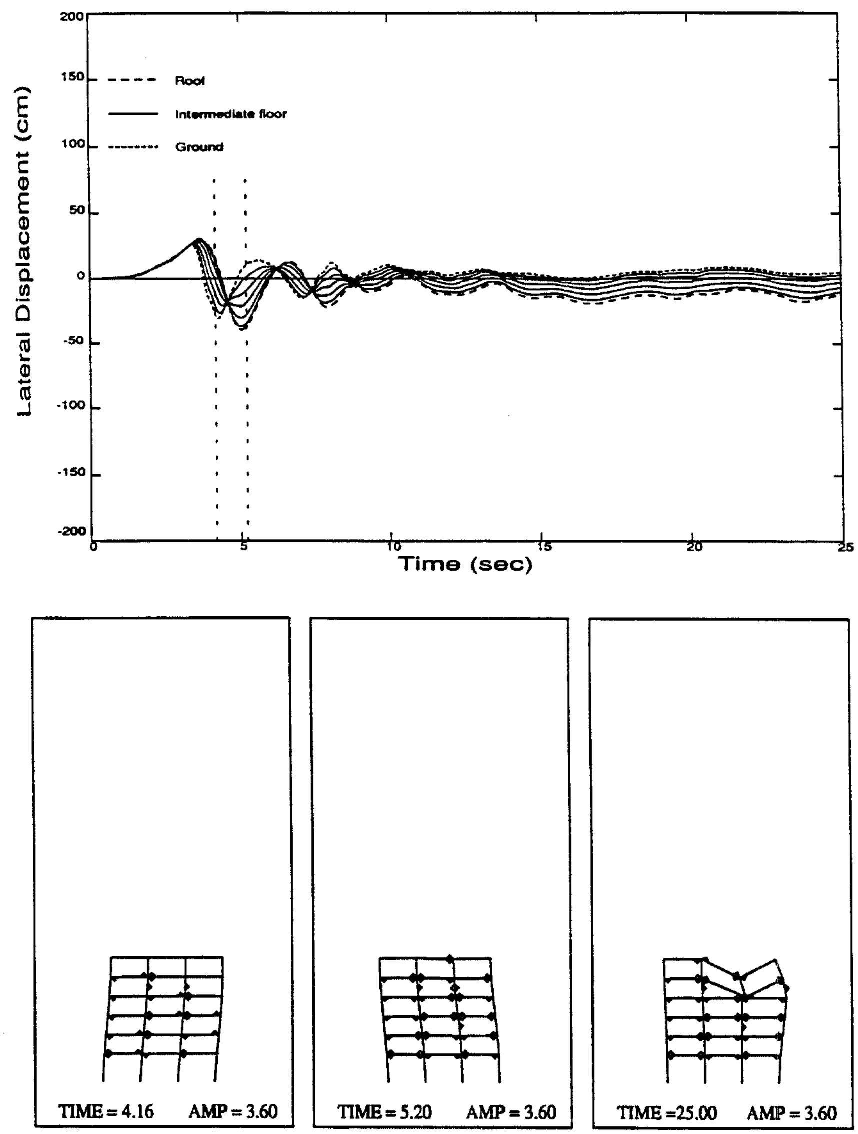

FIGURE 1.53: RESULTS FOR THE 6-STORY BUILDING, CASE BS, NR11/H GROUND MOTION.

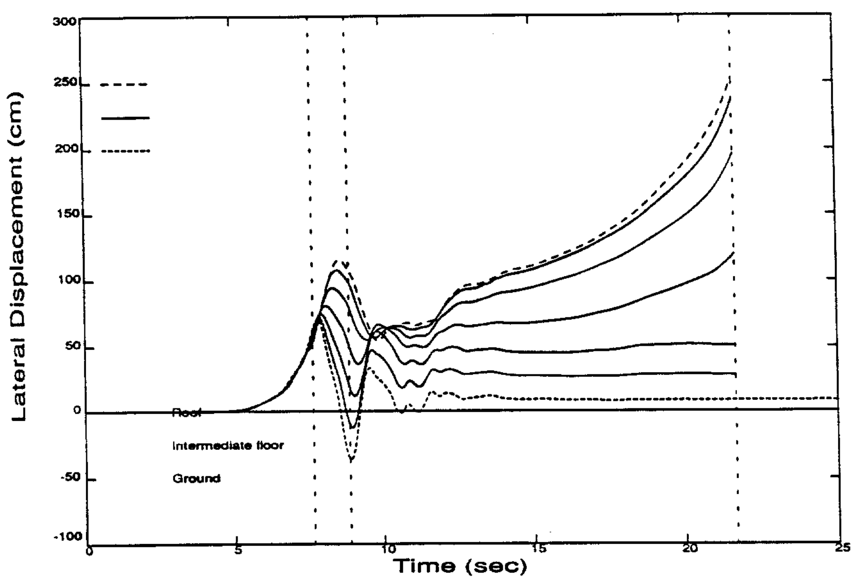

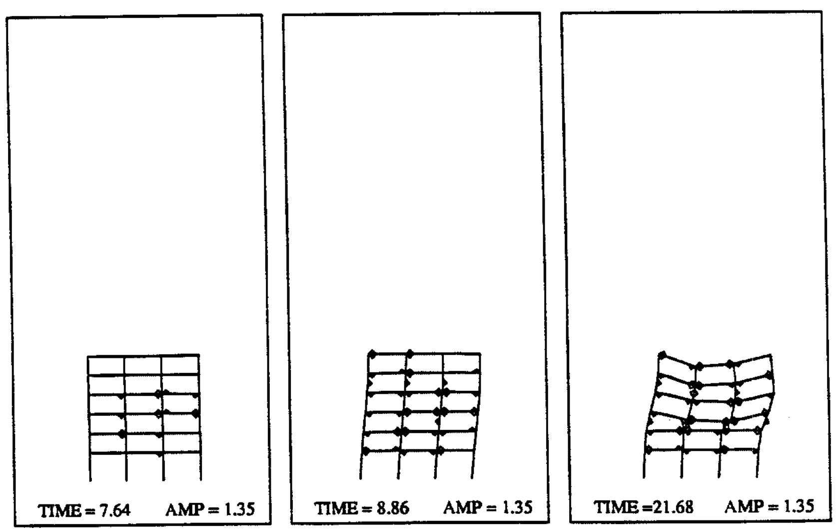

FIGURE 1.54: RESULTS FOR THE 6-STORY BUILDING,
CASE BS, EP17/H GROUND MOTION.

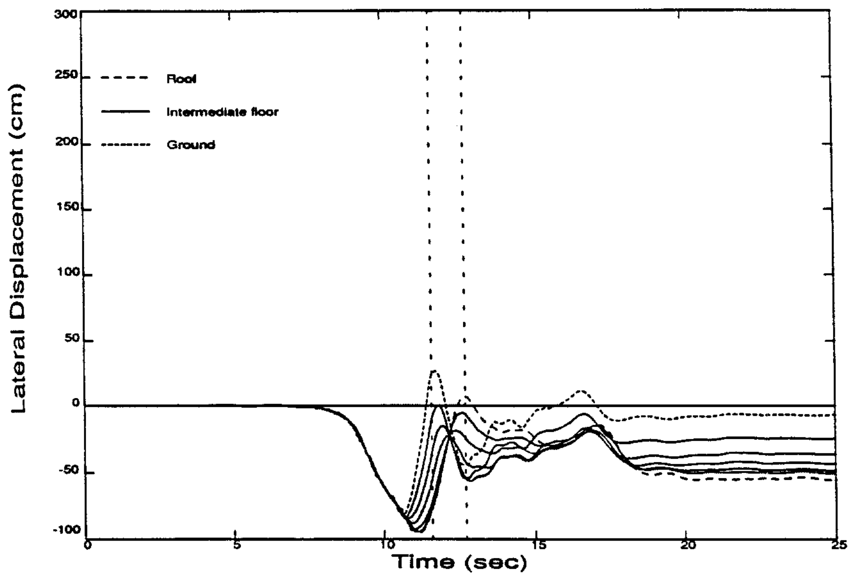

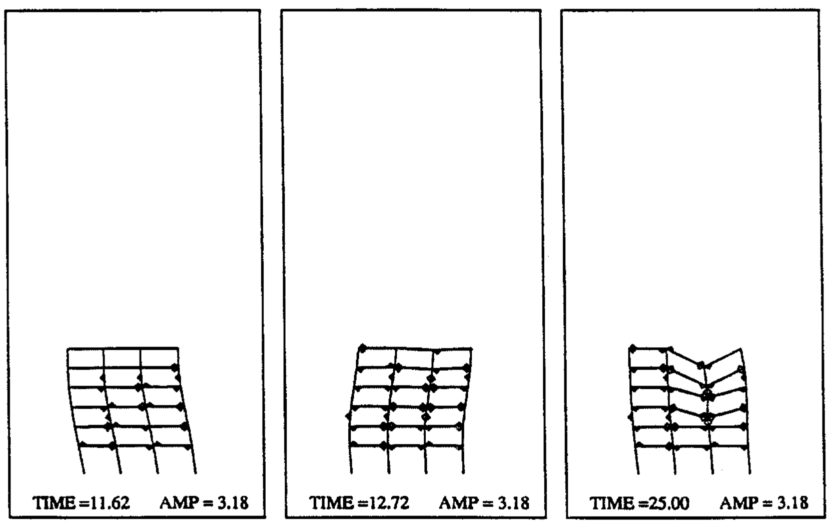

FIGURE 1.55: RESULTS FOR THE 6-STORY BUILDING, CASE BS, C05/H GROUND MOTION.

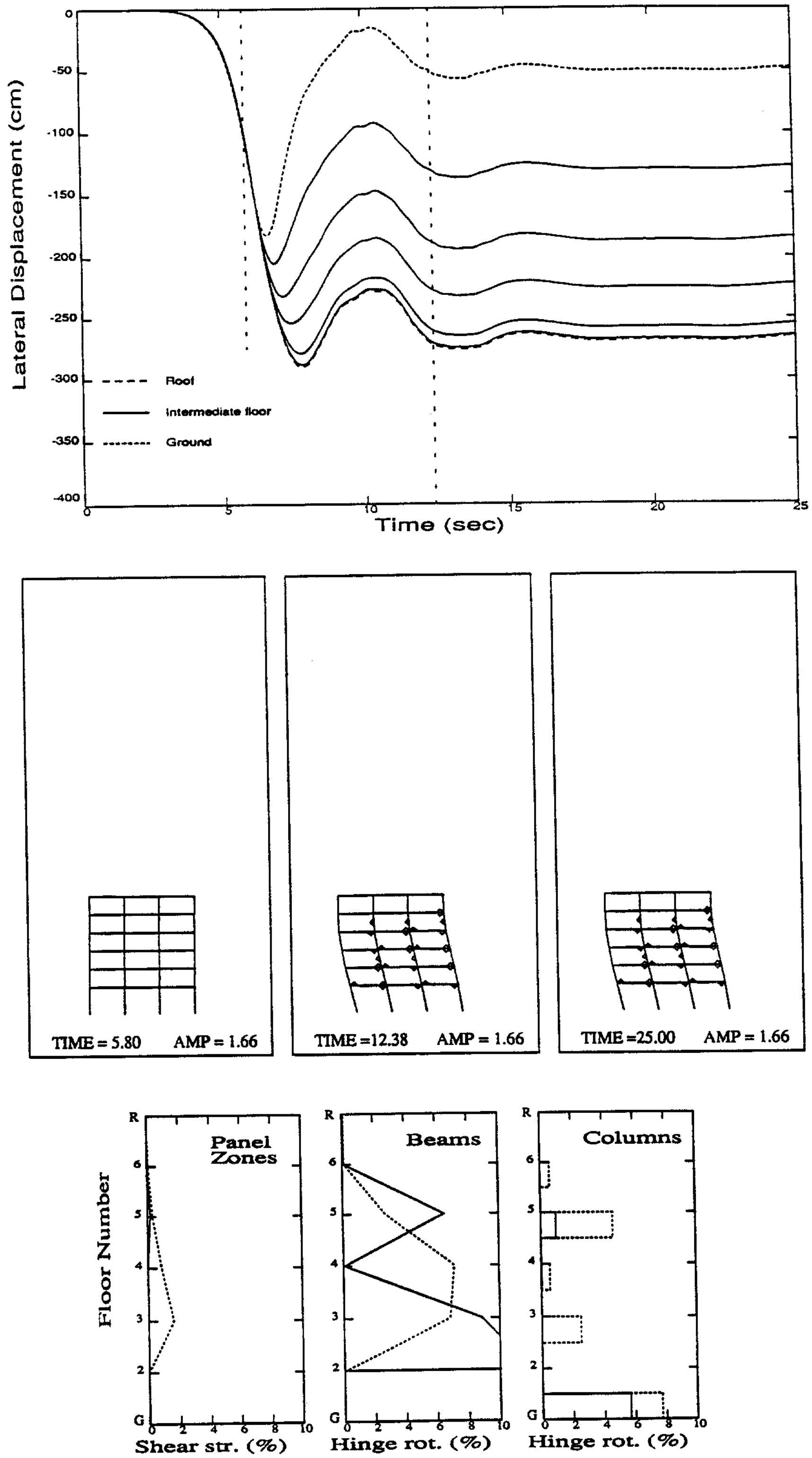

Parameter Study of the Response of Moment-Resisting Steel Frame Buildings to Near-Source Ground Motions

FIGURE 1.56: RESULTS FOR THE 20-STORY BUILDING, CASE BS, SYLM/H GROUND MOTION.

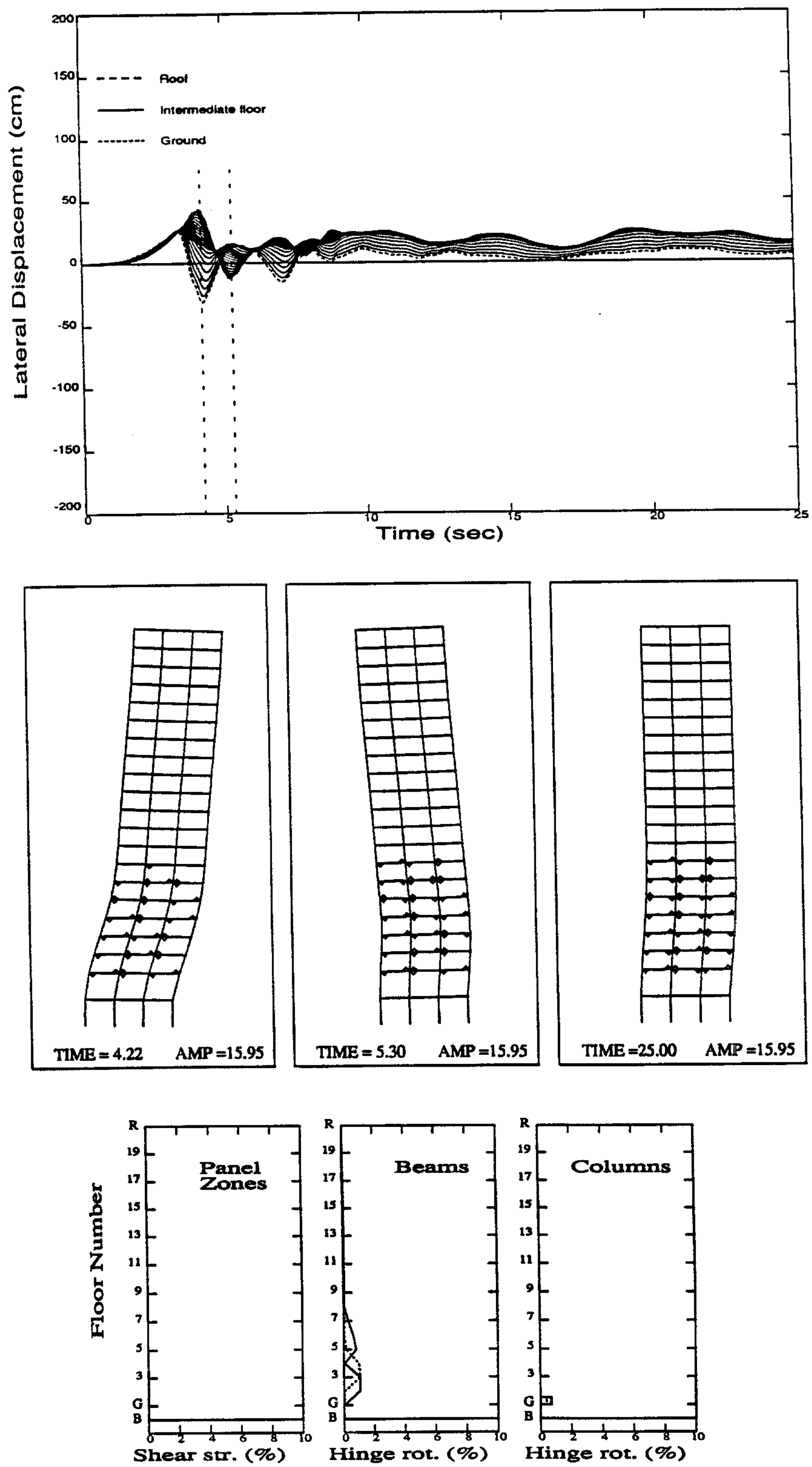

FIGURE 1.57: RESULTS FOR THE 20-STORY BUILDING, CASE BS, NR11/H GROUND MOTION.

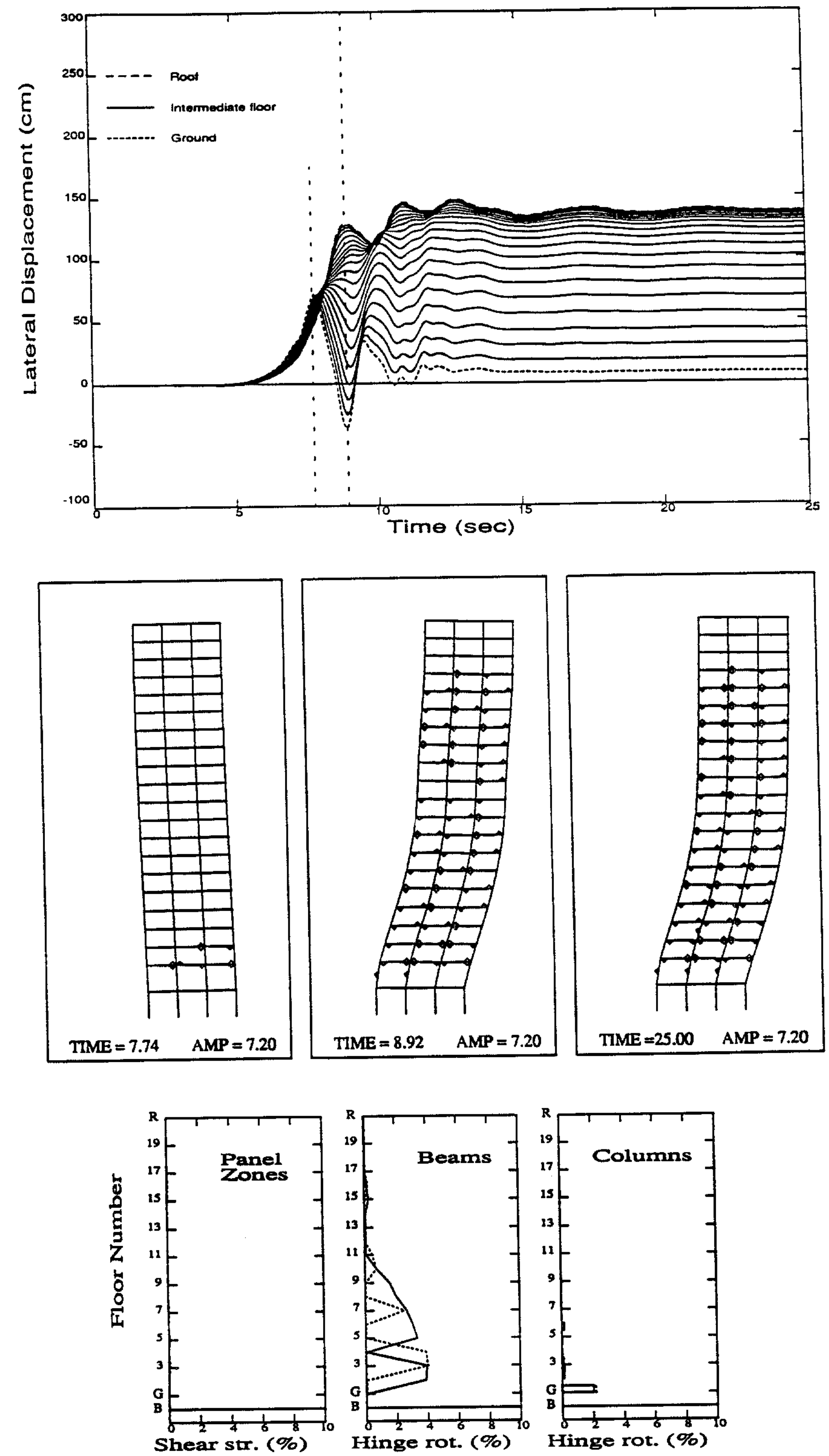

Parameter Study of the Response of Moment-Resisting Steel Frame Buildings to Near-Source Ground Motions

FIGURE 1.58: RESULTS FOR THE 20-STORY BUILDING, CASE BS, EP14/H GROUND MOTION.

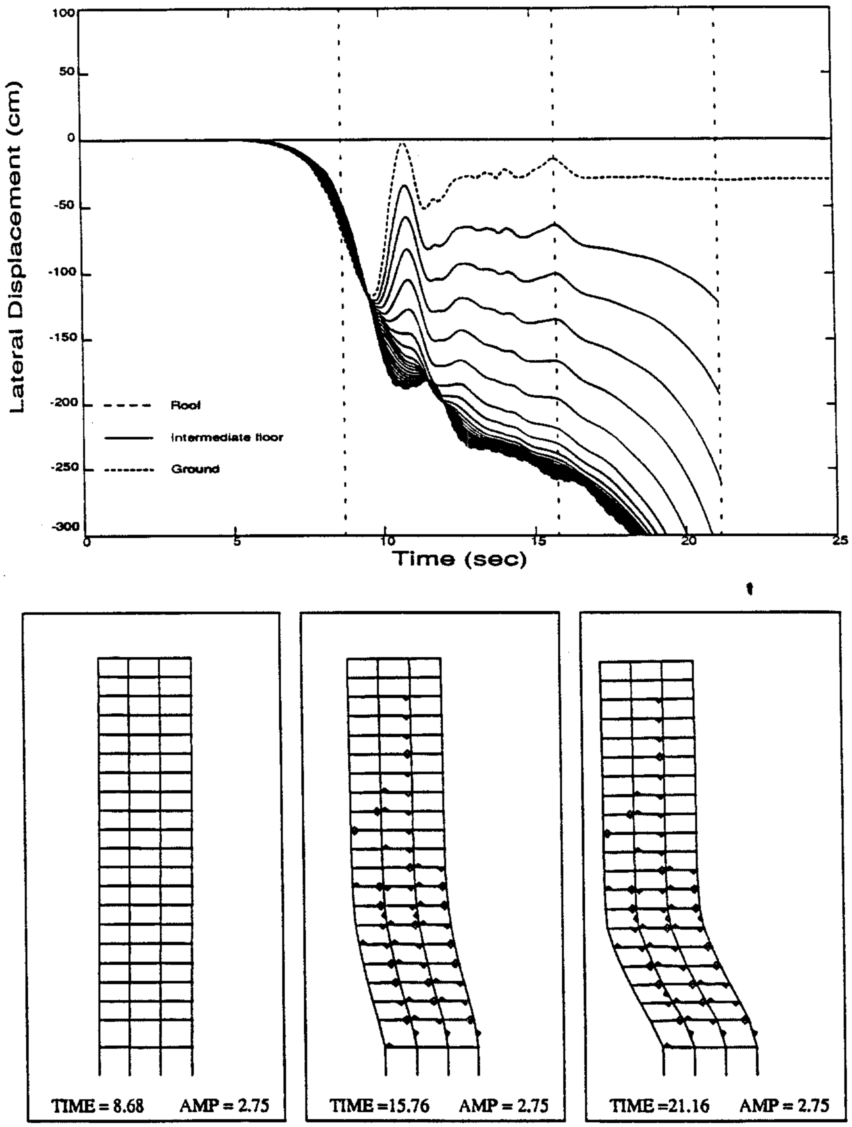

FIGURE 1.59: RESULTS FOR THE 20-STORY BUILDING,
CASE BS, C05/H GROUND MOTION.

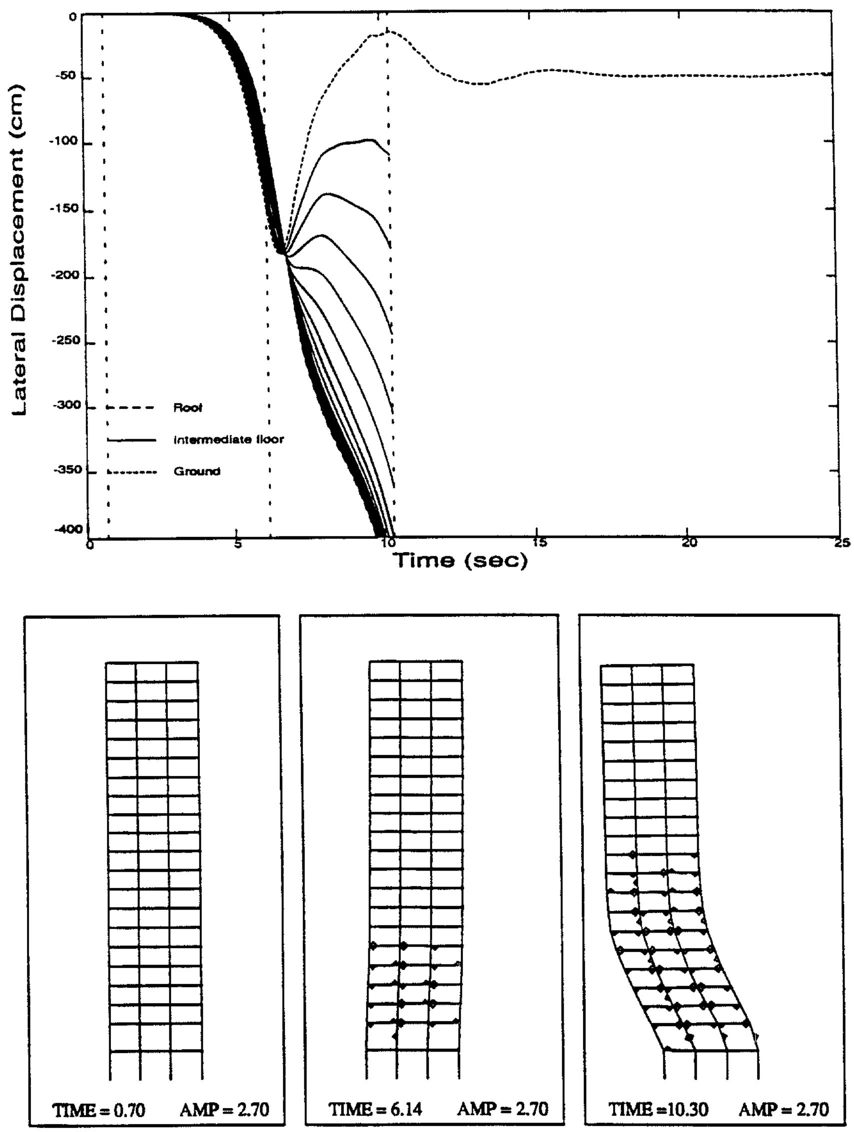

FIGURE 1.60. RESULTS FOR THE 6-STORY BUILDING, CASE I, SYLM/DH GROUND MOTION.

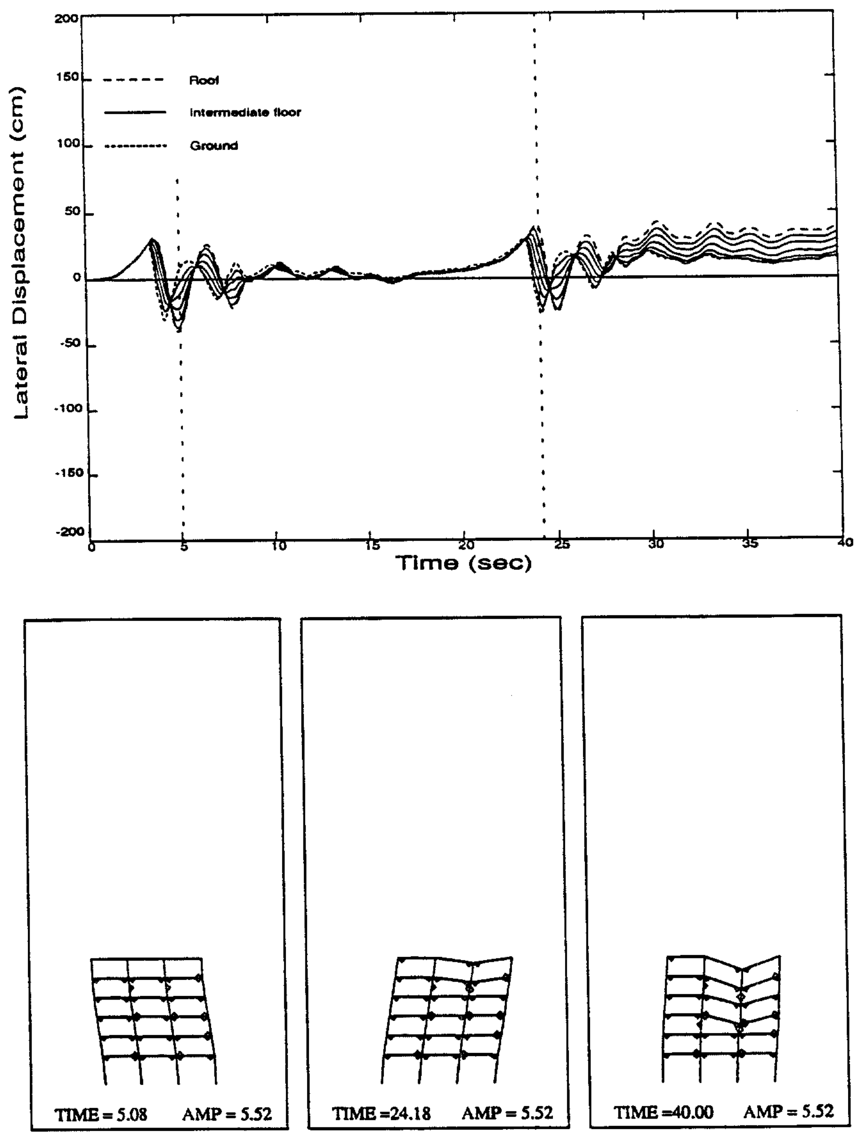

FIGURE 1.61. RESULTS FOR THE 20-STORY BUILDING, CASE I, NR11/DH GROUND MOTION.

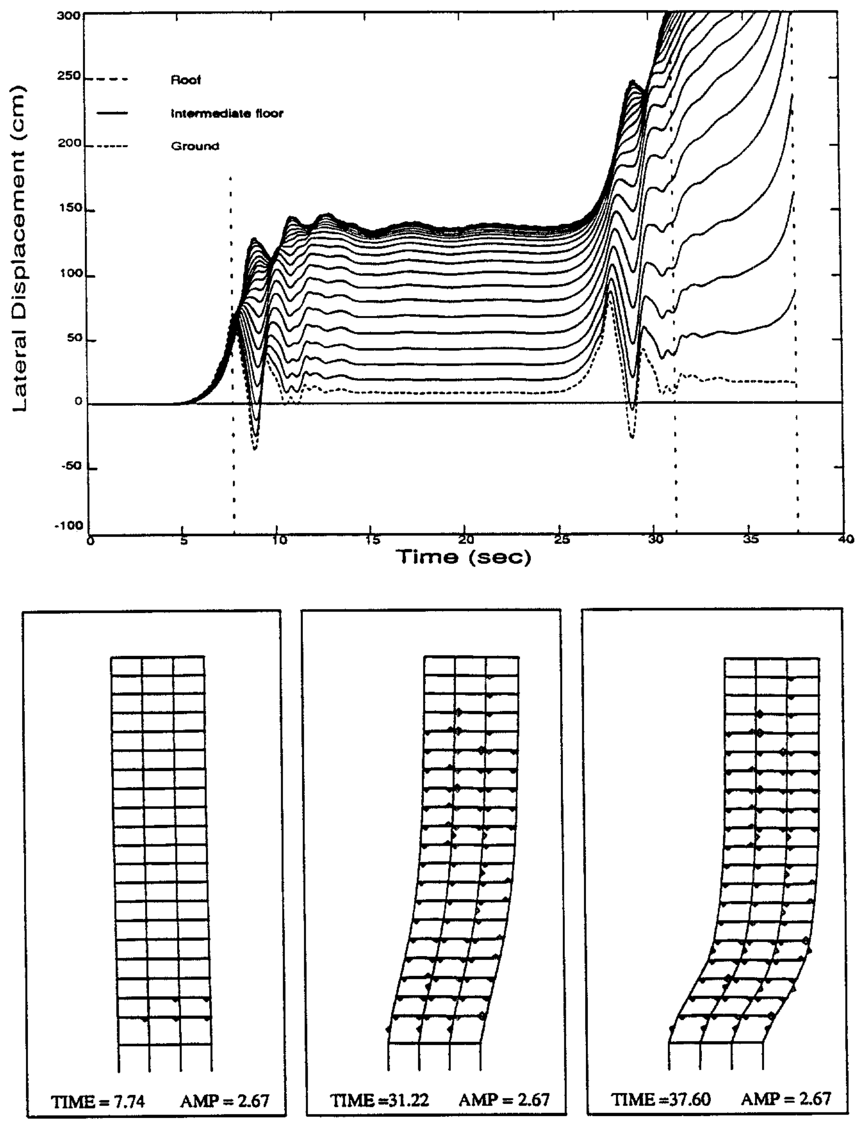

FIGURE 1.62. RESULTS FOR THE 6-STORY BUILDING, CASE P′, SYLM/H GROUND MOTION.

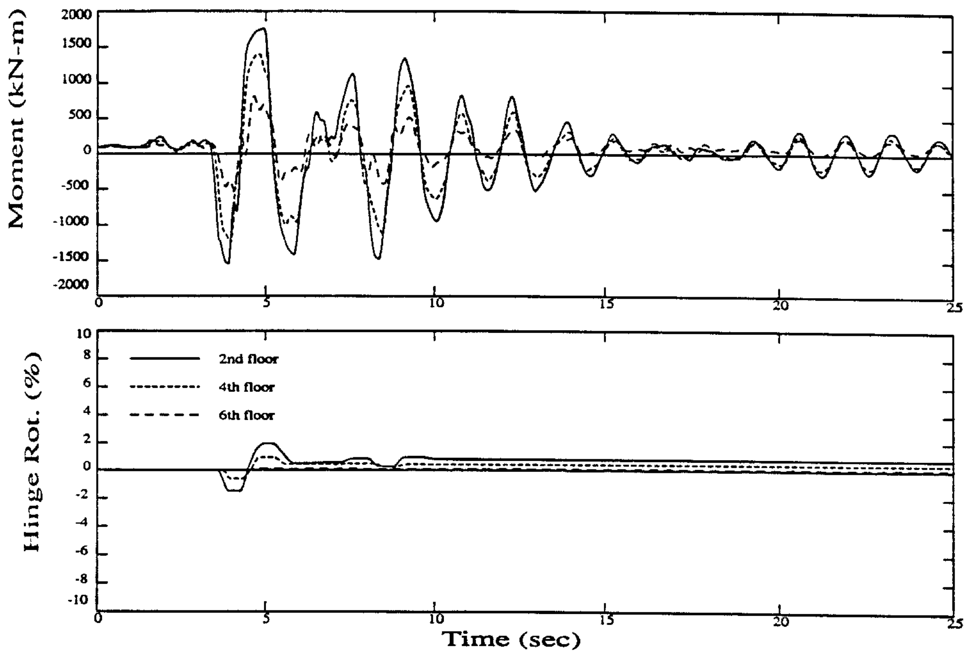

FIGURE 1.63. RESULTS FOR THE 6-STORY BUILDING, CASE P′, SYLM/H+V GROUND MOTION.

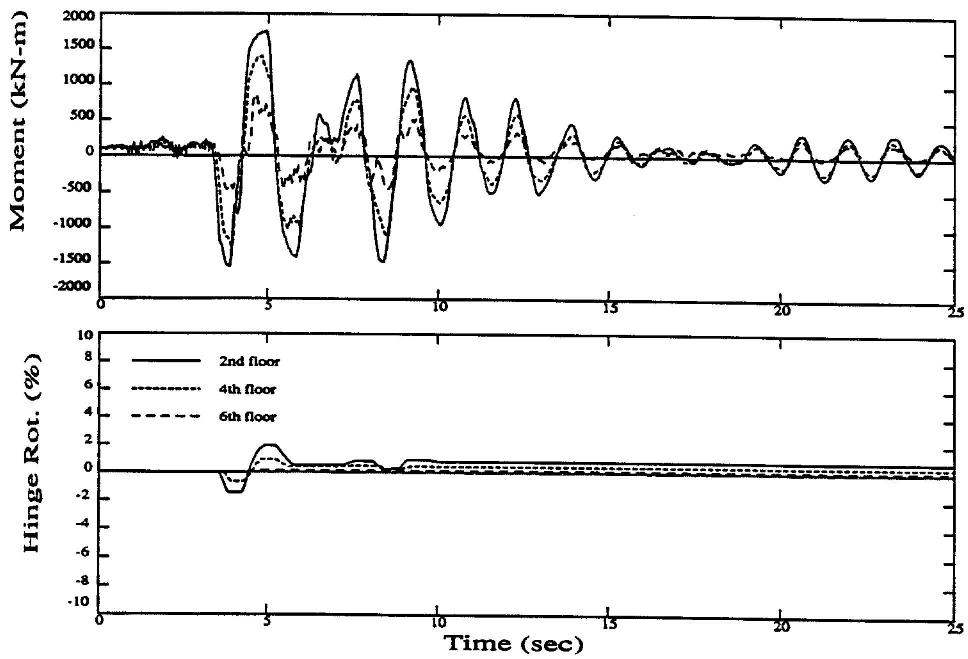

FIGURE 1.64. RESULTS FOR THE 6-STORY BUILDING, CASE P′, EP17/H GROUND MOTION.

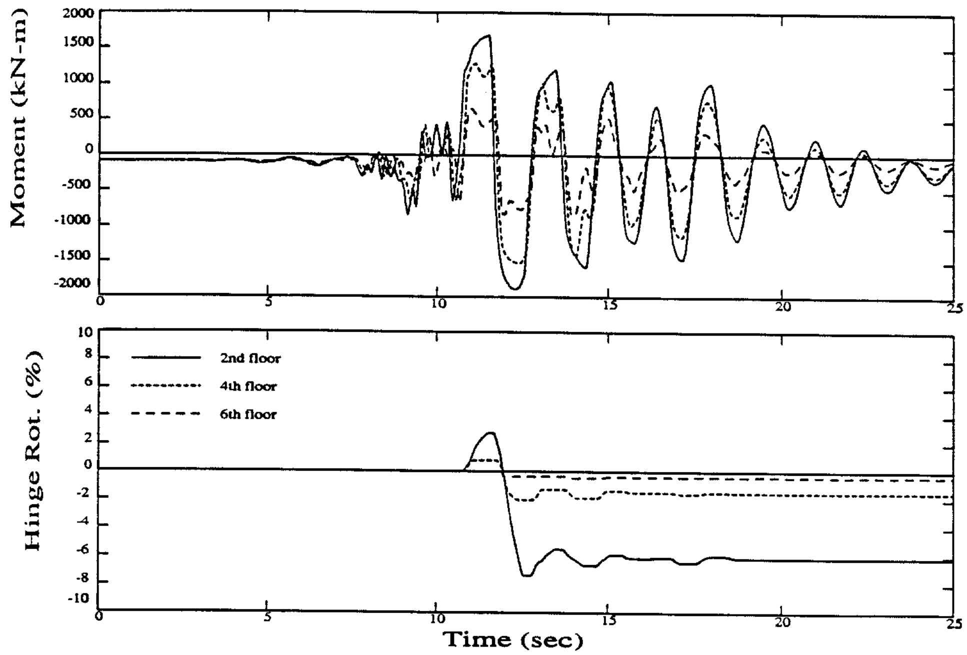

FIGURE 1.65. RESULTS FOR THE 6-STORY BUILDING, CASE P′, EP17/H+V GROUND MOTION.

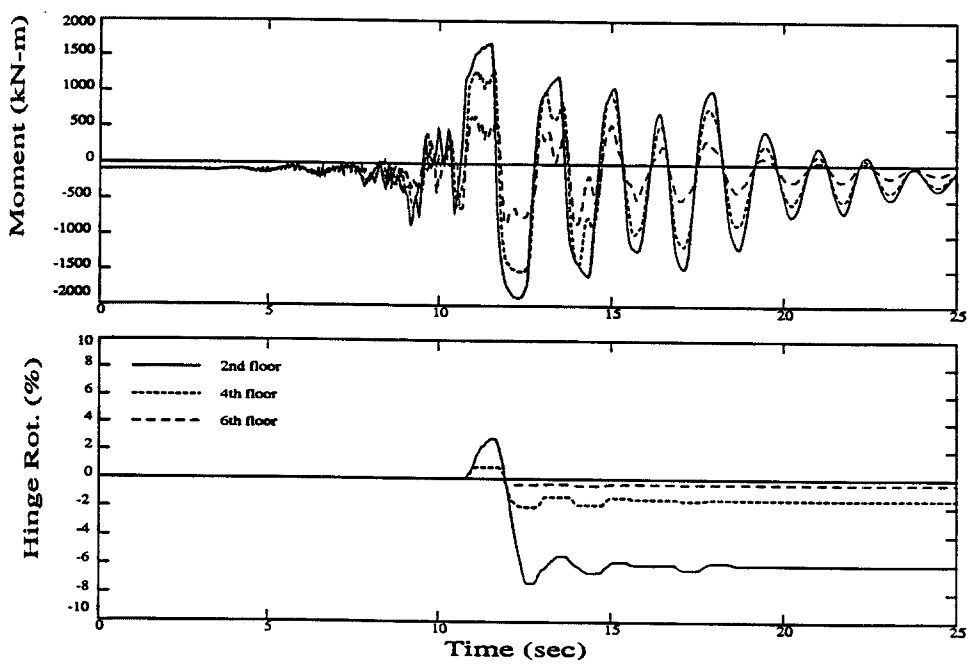

REFERENCES

Anderson, J.C. and V.V. Bertero, 1987. "Uncertainties in Establishing Design Earthquakes," *Journal of Structural Engineering*, ASCE, Vol. 113, No. 8, August, pp. 1709-1724.

Bertero, V.V., S.A. Mahin and R.A. Herrera, 1978. "Aseismic Design Implications of Near-Fault San Fernando Earthquake Records," *International Journal of Earthquake Engineering and Structural Dynamics*, Vol. 6, No. 1, January-February, pp. 31-42.

Challa, V. Murty and J.F. Hall, 1994. "Earthquake Collapse Analysis of Steel Frames," *Earthquake Engineering and Structural Dynamics*, Vol. 23, No. 11, November, pp. 1199-1218.

Heaton, T.H., J.F. Hall, D.J. Wald and M.W. Halling, 1995. "Response of High-Rise and Base-Isolated Buildings to a Hypothetical M_w7.0 Blind Thrust Earthquake," *Science*, Vol. 267, January 13, pp. 206-211.

Roeder, C.W., S.P. Schneider and J.E. Carpenter, 1993. "Seismic Behavior of Moment-Resisting Steel Frames: Analytical Study," *Journal of Structural Engineering*, Vol. 119, No. 6, June, pp. 1866-1884.

Tsai, K.-C. and E.P. Popov, 1988. "Steel Beam-Column Joints in Seismic Moment Resisting Frames," UCB/EERC 88/19, *Earthquake Engineering Research Center*, University of California, November.

ACKNOWLEDGMENTS

Funding for this research was provided by the Federal Emergency Management Agency through the SAC Joint Venture. SAC is a partnership of the Structural Engineers Association of California, the Applied Technology Council, and California Universities for Research in Earthquake Engineering.

APPENDIX: RESPONSE TO REVIEWERS' COMMENTS

1. *You have included the stiffness of the "simple" connected columns in the lateral force analyses as a 1/3 factor for the gamma value. How does this compare with the stiffness that is inherent from these connections, which has been published by Leon? I think that we need to accurately model the contribution of these elements if we are to make statements about life safety issues.*

   Quantifying the contributions of the simple beam-to-column connections in the analysis is an important area where improvement is needed. So far, no comparison to experimental data has been made. In future work, it is planned to model entire simply-connected frames explicitly and correlate the analytical connection model with experimental results. Including these frames will also incorporate the contribution of column bending which may also be significant. (This column contribution is present even if the simple beam-to-column connections transmit zero moment.)

2. *Many of these buildings have basements, which will result in changing the response at the base of the model from a free-field motion due to SSI effects. The reduction can be significant, and may be even greater for large ground motions. Has this effect been considered in the analyses?*

   Proper treatment of earthquake excitation would use free-field motions (those occurring with building absent but excavation and foundation present) as input to the building-foundation-soil system. In the analysis, the effect of the excavation and foundation on the free-field motions has been neglected, which is probably justifiable since the most damaging part of the ground motions are long-period components which have long wavelengths. The foundation-soil system is represented by nonlinear springs at the basement floor level. Horizontal springs at ground level are omitted because they would have little effect due to the high stiffness of the basement story (which results from the assumed presence of concrete walls), and also because of the likely softer characteristics of the backfill. These comments apply only for the 20-story building; the foundation of the 6-story building was taken to be rigid.

3a. *You have included foundation springs in the model to approximate the soil stiffness. I could not determine how the spring stiffness was determined. Changes in this stiffness can significantly alter the structural response.*

   Forces in the horizontal springs were much smaller than those in the vertical springs, and, consequently, results were not sensitive to the properties of the horizontal springs. Therefore, horizontal spring properties were chosen equal to those of the vertical springs. The fundamental period of the building depended greatly on the stiffness of the vertical springs. Rigid springs produce a period of 3.13 seconds while the chosen stiffness of 5254 kN/cm (3000 kips/in) lengthens the period to 3.49 seconds, which is pretty long for a 20-story building. Static vertical deflections under gravity loads (about 2.7 MN, or 600 kips, per column) for the chosen spring stiffness are about 0.5 cm (0.2 in), which seems small, but decreasing the spring stiffness would further lengthen the building period. The vertical spring compressive yield strength of 13.3 MN (3000 kips) provides a factor of safety against bearing failure under gravity loads of 5, and under code wind forces the factor of safety reduces to about 2.3 for the exterior column springs. These springs actually yield for cases *P* and *PS* under the stronger ground motions considered, and the secondary stiffness $\alpha_f = 0.10$ is necessary to prevent excessive vertical displacement in the foundation. The vertical spring tensile yield strength is chosen (arbitrarily) as half the compressive strength because only pile friction and not end-bearing would be effective. Note that none of the numbers chosen are "hard numbers" for an actual foundation design.

3b. *Also, did you include any rotational stiffness to provide fixity at the base? For buildings with basements, this is not as critical due to the backstay effect.*

The vertical springs under each column provide rotation stiffness for the base of the building as a whole.

4. *On page 4, you noted that you assumed that if the column splice capacity was exceeded the compression was completely lost. This would not always be the case, since it would require the columns to completely disengage, with relative movements of more than 1 or 2 inches. In an actual building there are many other mechanisms which would seem to restrain this from happening, floor slabs, adjacent frames, etc. I am not sure that this assumption can be justified.*

Column splice fractures occurred by bending and usually when the story drift exceeded 2 percent. A 2% story drift corresponds to a lateral story offset of about 3 inches which is more than enough to totally offset column flanges at splice fracture locations. The $\gamma = 1/3$ factor is intended to represent additional mechanisms that restrain story drift such as adjacent simply-connected frames. Also note that the results show complete splice fractures occurring only for some analyses of the 6-story building and that all splice fractures for the 20-story building were partial, i.e., involving a single flange (in which case the entire compressive capacity was retained).

5. *On page 6, you assumed that the foundation was rigid. Shouldn't some stiffness be provided to avoid modeling problems?*

A rigid foundation is accomplished by fixing the degrees of freedom at the base of the building by not assigning equation numbers, and this does not introduce any numerical problems.

6. *Also on page 6, whenever you assumed poor column splices, you assumed that 100% were bad. Why not some with a random distribution of bad splices, similar to the flange welds? I know that you can make any number of assumptions, but I am concerned about making*

conclusions based on these analyses without seeing the effects of a smaller number of poor splices.

Splices in interior columns were assumed to be partial penetration welds. This condition was modelled using the full flange areas, but reducing the fracture stress to 2/3 of yield. But there is also a notch present which justifies the 100%-bad assumption. Splices in exterior columns were assumed to be full penetration welds, and, although some designers may have used partial penetration welds there also, the assumption of 100% bad column splices for exterior columns does seem severe. However, in none of the analyses did an exterior column crack all the way through (and thus lose its compressive capacity), and the effect of having a few more exterior column flanges crack at splice locations on the strength and stiffness of the building was probably minor.

7. *The report uses references but does not provide the source and location of the reference. This information needs to be included.*

   References are listed on page 1-76.

8. *The author draws the conclusion that present seismic design forces are too low. This may be correct but it is not logically supported by the paper. The author contends that they are too low because many near field acceleration records produce inelastic story drifts which are much larger than the 2% commonly assumed by structural engineers. This observation is not new. It has been shown in numerous earlier analyses and stated in many papers. A story drift of 6% does not indicate that the existing code is deficient. The present seismic codes are life safety codes and they are deficient only if it can be shown that the structure cannot hold together and avoid collapse at these inelastic deformation levels. The author makes no effort to show this. A large number of steel frames had serious cracking during the Northridge Earthquake, but no lives were lost. No buildings collapsed. With the present life safety seismic design criteria, the design forces and design criteria appear to have performed well. It is quite possible that the life safety criteria should be changed and the forces need to be increased. However, this report does nothing to show this.*

   The author is aware of three previous analyses of modern buildings which show that some recorded near-source ground motions produce large amounts of inelastic deformations, and these reports are listed in the references. The author believes that these papers should have generated serious concern in the engineering community. Now, the Northridge earthquake has provided even more near-source ground motion records that exceed code expectations. Further, recent advances by seismologists in simulating earthquakes offer a more systematic way of quantifying near-source ground motion (and which produce ground motions which can greatly exceed code expectations), and so the time seems ripe for serious study of these effects. The large inter-story drifts (say, above 3%) resulting from building analyses using strong near-source ground motions violate some of the original beliefs on which the life-safety objective of the code is based. This raises an issue about whether the code should be assumed valid until proven to be inadequate (the reviewer's view?), or, since it is now clear that some of the original assumptions about ground motion do not hold, whether the code should be assumed to be inadequate and either revalidated or strengthened (author's view). Of course, we must now also deal with deficiencies in the welded connections of steel buildings which greatly compromise their ductility. This recognition should consider that the Northridge earthquake was only a moderate-size event and that the most damaging ground motions occurred to the north of the fault where there were few buildings, and so this earthquake was not really a "test" of the life-safety objective of the code.

9. *The author presents interesting results related to the probability of failure of welds and the effect of composite floor slabs. He qualifies the conclusions based on the limitations of the model, however I am also concerned that these conclusions may also overstate the case. The probabilities assigned to weld failure were rather arbitrary and extreme.*

   Certainly, the rules used for weld fracture were arbitrary; hopefully, data will soon be forthcoming so that improvements can be made. As for being extreme, it should be considered that the most damaging ground motions occurred where there were few buildings and many of the fractures occurred at sites which really did not shake particularly hard. The ground motions used in the study are pretty severe and place greater demands on the welds than did the Northridge earthquake.

10. *The connection model really does not simulate the couple that can be achieved with a composite slab and its erection plate. As a result, I am concerned that the conclusions concerning the effect of the floor slab are also over stated.*

    The slab model needs improvement and this is planned for future work. The present treatment uses an extra fiber at the top of the beam section to represent the slab. For positive beam moment at the column face (slab in compression), the slab contributes fully to the moment delivered to the column by the beam. (Is this the reviewer's use of the term "couple"?) However, under the opposite moment, the slab may crack and, in this case, does not contribute to the moment delivered to the column. Although slab action as presently modelled is a simplification, the gross effect of an increase in the bending capacity of the beam relative to the column (and which is probably undesirable) is represented, although possibly in too small an amount.

11. *The SAC Program is a very high profile and visible effort, and the authors must be very careful that their conclusions do not overstep the results. Poorly substantiated conclusions in the early work will be difficult to cover over in the future if they are found to be flawed.*

    The author is aware of the sensitive nature of some of the findings of the study, but feels strongly that the combination of bad welds and strong shaking is an important problem. It is possible that some of the simplifications in the analysis may have produced an overstatement of the seriousness of the problem. On the other hand, consideration of such items as all three components of ground shaking, irregular building geometry, long duration of shaking from large earthquakes, etc. can only make the situation worse.

12. *This report does not, as a main objective, attempt to demonstrate predictive analysis capability, but instead uses analysis to show sensitivity to various parameters and make recommendations for further work. Hall's report makes some unique contributing suggestions about how to model damping. He also adds an item to the list of topics for future study that we concur with: "consideration of structural deterioration mechanisms other than weld fracture, such as local flange buckling, should be pursued."*

    No comment necessary.

13. *For the effect of vertical component, it would be also very useful to have a list of axial loads on columns (end columns as well as intermediate columns) for three cases: (1) Gravity only; (2) Horizontal and gravity; and (3) Horizontal and gravity and vertical.*

    The results of **Figures 1.62** (Case P', SYLM/H ground motion), **1.63** (Case P', SYLM/H+V ground motion), **1.64** (Case P', EP17/H ground motion) and **1.65** (Case P', EP17/H+V ground motion) for the 6-story building are extended to include axial load on an interior and exterior column (**Figures 1.66 to 1.69**). Vertical ground motion is seen to have a greater effect on column axial force than on beam bending. The effect may be enough to increase the number of column-splice fractures and is worth investigating.

FIGURE 1.66. ADDITIONAL RESULTS FOR THE 6-STORY BUILDING, CASE P′, SYLM/H GROUND MOTION.

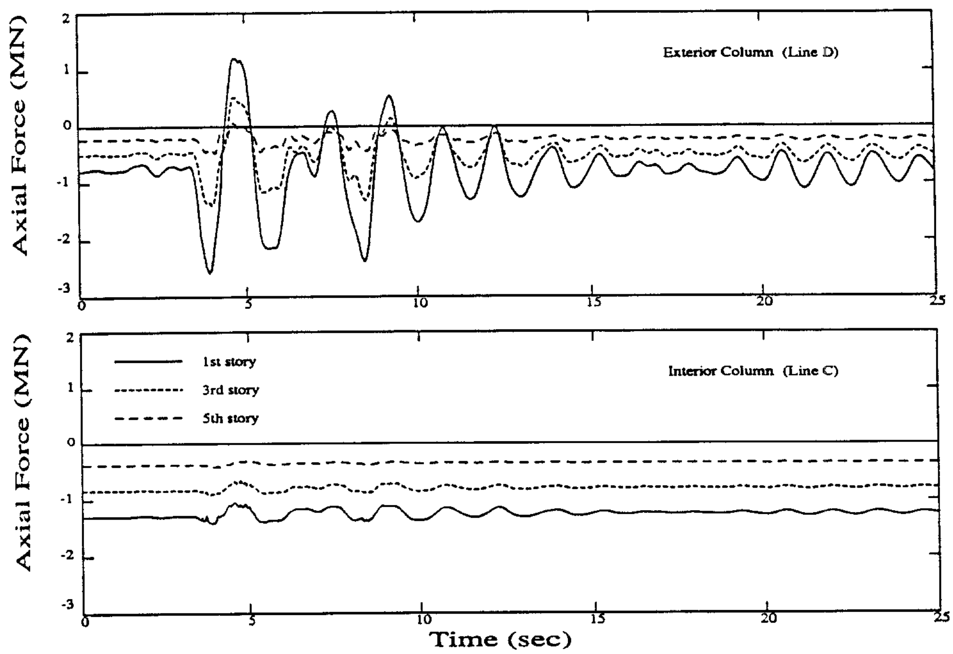

FIGURE 1.67. ADDITIONAL RESULTS FOR THE 6-STORY BUILDING, CASE P′, SYLM/H+V GROUND MOTION.

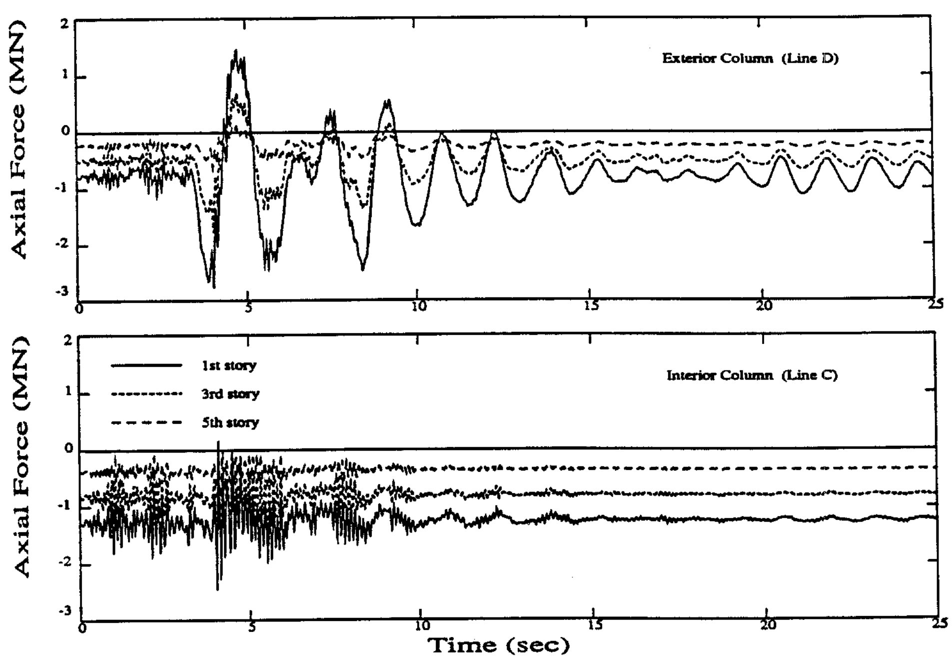

FIGURE 1.68. ADDITIONAL RESULTS FOR THE 6-STORY BUILDING, CASE P′, EP17/H GROUND MOTION.

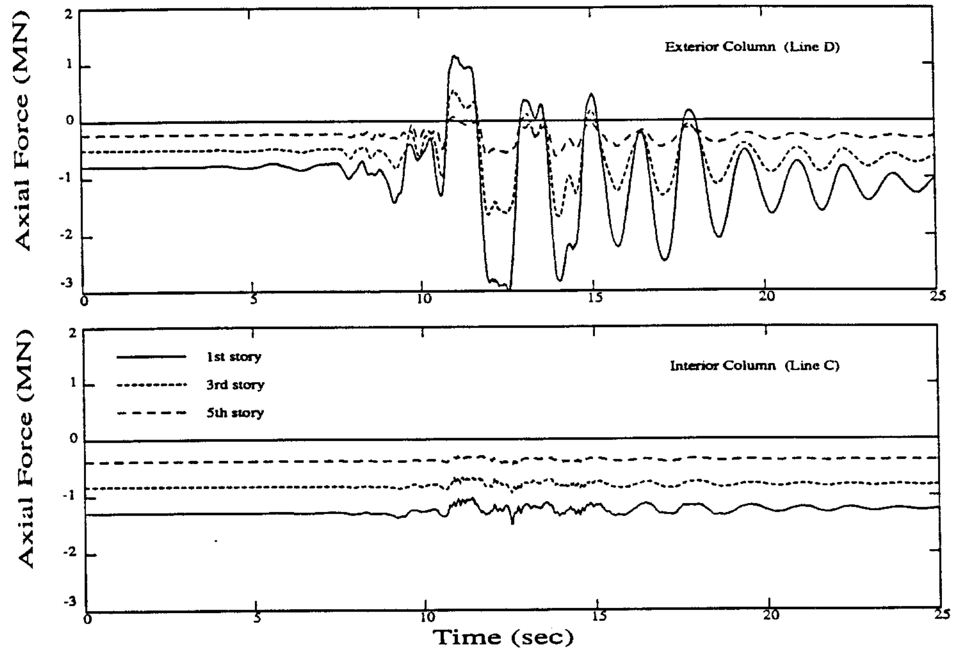

FIGURE 1.69. ADDITIONAL RESULTS FOR THE 6-STORY BUILDING, CASE P′, EP17/H+V GROUND MOTION.